(12) LEVEL III

AD-E430624

AD

TECHNICAL REPORT ARBRL-TR-02300

IMPROVED ANALYTICAL SHAPED CHARGE CODE: BASC

John T. Harrison

March 1981

DTIC ELECTE JUN 16 1981 S D B

AD A100275

US ARMY ARMAMENT RESEARCH AND DEVELOPMENT COMMAND
BALLISTIC RESEARCH LABORATORY
ABERDEEN PROVING GROUND, MARYLAND

81 6 04 035

UNCLASSIFIED

SECURITY CLASSIFICATION OF THIS PAGE (When Data Entered)

REPORT DOCUMENTATION PAGE

READ INSTRUCTIONS BEFORE COMPLETING FORM

1. REPORT NUMBER TECHNICAL REPORT ARBRL-TR-02300	2. GOVT ACCESSION NO. AD-A100275
	3. RECIPIENT'S CATALOG NUMBER
4. TITLE (and Subtitle) IMPROVED ANALYTICAL SHAPED CHARGE CODE: BASC	5. TYPE OF REPORT & PERIOD COVERED Final
	6. PERFORMING ORG. REPORT NUMBER
7. AUTHOR(s) John T. Harrison	8. CONTRACT OR GRANT NUMBER(s)
9. PERFORMING ORGANIZATION NAME AND ADDRESS US Army Ballistic Research Laboratory ATTN: DRDAR-BLT Aberdeen Proving Ground, MD 21005	10. PROGRAM ELEMENT, PROJECT, TASK AREA & WORK UNIT NUMBERS 1L161102AH43
11. CONTROLLING OFFICE NAME AND ADDRESS US Army Armament Research and Development Command US Army Ballistic Research Laboratory (DRDAR-BL) Aberdeen Proving Ground, MD 21005	12. REPORT DATE MARCH 1981
	13. NUMBER OF PAGES 100
14. MONITORING AGENCY NAME & ADDRESS (if different from Controlling Office)	15. SECURITY CLASS. (of this report) UNCLASSIFIED
	15a. DECLASSIFICATION/DOWNGRADING SCHEDULE

16. DISTRIBUTION STATEMENT (of this Report)

Approved for public release, distribution unlimited.

17. DISTRIBUTION STATEMENT (of the abstract entered in Block 20, if different from Report)

18. SUPPLEMENTARY NOTES

19. KEY WORDS (Continue on reverse side if necessary and identify by block number)

Liner acceleration and collapse
Shaped Charge Jet Formation Theory
Shaped Charge Penetration
Explosive metal interaction

20. ABSTRACT (Continue on reverse side if necessary and identify by block number) (ddg)

The work of many researchers has been combined to produce a simplified, analytical, computer code to address the shaped-charge problem. This code named BASC (BRL Analytical Shaped Charge) is programmed in the FORTRAN language. BASC utilizes a modified version of the metal acceleration model of M. Defourneaux of France to account for both the final liner velocity and its acceleration history. The BASC code accurately predicts jet-tip velocity and treats the buildup of the massive lead pellet, for both heavy confined and unconfined charge geometries. Calculation of the massive lead pellet has traditionally

DD FORM 1 JAN 73 1473 EDITION OF 1 NOV 65 IS OBSOLETE

UNCLASSIFIED

SECURITY CLASSIFICATION OF THIS PAGE (When Data Entered)

been difficult and is accomplished in BASC by including time dependent acceleration and material compressibility in the region of the liner near the apex of the conical liner. The BASC code includes the jet formation theory of Pugh, Eichelberger, and Rostoker; the shaped-charge penetration theory of DePersio, Simon and Merendino for penetration-standoff curves; and the piece wise penetration of Defourneaux for hole profiles. BASC enables parametric investigations of shaped charge problems with relatively small amounts of computer time since the code is basically analytic. Results from the BASC code are compared to experiments as well as to more sophicated hydrodynamic computer codes. The report documents BASC, including the equations utilized, necessary empirical relations, FORTRAN listing of the program, selected problem examples and comparison with experiments.

TABLE OF CONTENTS

LIST OF ILLUSTRATIONS

LIST OF THE ILLUSTRATIONS

LIST OF TABLES

I. INTRODUCTION

The Ballistic Research Laboratory (BRL) of the U.S. Army Armament Research and Development Command (ARRADCOM) has a wide interest in the shaped-charge problems, ranging from detailed studies of the flow characteristics of the collapsing liner, to designing practical devices for future warhead applications. For these efforts several experimental and theoretical techniques are employed. Often, it is necessary to determine parametric relationships in the design application. Since it is more feasible to utilize theoretical calculations that are economically sound for parametric studies, the BRL has several finite-difference, hydrodynamic, computer codes that have been applied to shaped-charge problems.[1,2] Although these codes are adaptable to various geometrical considerations, they require operator experience and a seasoned analyst to insure proper application. Further, large, high-speed computers, and long calculational times are necessary. Quite often, it is desirable to have a simplified procedure for addressing parametric design studies quickly and economically. The BRL computer code named BASC (BRL Analytical Shaped Charge)[3] was formulated from analytic expressions to provide such capability. Although several advantages occur with the original BASC approach, several areas of difficulty were experienced, particularly those relating to accurate calculation of jet tip or lead pellet behavior and confined charges. Extensive semi-empirical functions, regarding liner acceleration and confinement effects, have been included to provide more accurate representations. This improved, simplified procedure, hereinafter referred to as the BASC code also, together with additional refinements are presented and discussed in this report.

---

[1] *J. T. Harrison and R. R. Karpp, "Terminal Ballistic Applications of Hydrodynamic Computer Code Calculations," BRLR 1984, April 1977. (AD #A041065)*

[2] *J. T. Harrison, "A Comparison Between the Eulerian, Hydrodynamic Computer Code (BRLSC) and Experimental Collapse of a Shaped Charge Liner," ARBRL-MR-02841, June 1978 (AD A059711)*

[3] *J. Harrison, R. DiPersio, R. Karpp and R. Jameson, "A Simplified Shaped Charge Computer Code: BASC," DEA-AF-F/G-7304 Technical Meeting: Physics of Explosives, Vol II, April-May 1974, Paper 13 presented at the Naval Ordnance Laboratory, Silver Spring, MD.*

The BASC code is an assembly of various theoretical and empirical techniques. Central to the procedure utilized in BASC is the Defourneaux model[4] for final plate velocity resulting from the shock of an adjacent detonating explosive. This assumption is adequate for portions of the liner which are initially removed (remote) from the collapse (jet formation) region or cone axis. In actuality, several shock reverberations are required to achieve a final liner metal velocity. Material near to the apex of the cone can enter the collapse process long before the liner is accelerated fully and, hence, does not achieve its ultimate velocity. This leads to the well known phenomena referred to as "the inverse velocity gradient" which forms the massive jet tip. This phenomena has been observed[5] and calculated earlier.[1,2,6] The author has modified the Defourneaux model to account for the time-dependent acceleration of the liner resulting in a gradual build-up to the ultimate collapse velocity. Since liner elements near the apex region of a cone will not achieve this ultimate velocity, the first element of the jet will move more slowly than the following elements of the jet. The faster elements collide and are compressed into the massive lead pellet. The final jet-tip velocity will become the mass-weighted average of these inverse velocity elements. This is the jet-tip velocity, which will be used in jet penetration theory. BASC uses a combination of the shaped-charge penetration of DiPersio, Simon and Merendino (DSM)[7] and the piece wise penetration of Defourneaux[4]. The DSM model is used to calculate total penetration-standoff curves and the piecewise penetration model is used to calculate whole profiles.

In addition to the inverse velocity gradient, flow into the stagnation region during the collapse process from particles near the apex of a conical liner may be supersonic and fail to form a jet or form a so-called incoherent jet. This is the jet-no-jet criteria. The criteria used in BASC is a modified version of the supersonic limitations of Chou, et. al.[8] The final theoretical technique used in BASC is the

---

[4]*M. Defourneaux, "Hydrodynamic Theory of Shaped Charges and of Jet Penetration," Memorial DeL'art Ille'rie Francasise-T, 44, 1970.*

[5]*R. DiPersio, C. W. Whiteford, and J. Simon, "An Experimental Method of Obtaining Collapse Velocities of the Liner Walls of a Linear Shaped-Charge Liner," BRL-MR-1696, September 1965.(AD #478326)*

[6]*A. Kiwan and H. Wisniewski, "Theory and Computations of Collapse and Jet Velocities of Metallic Shaped Charge Liners," BRLR-1620, November 1972. (AD #907161)*

[7]*R. DiPersio, J. Simon, and A. Merendino, "Penetration of Shaped-Charge Jets Into Metallic Targets," BRLR 1296, September 1965. (AD #476717)*

[8]*P. Chou, J. Carleone, R. Karpp, "Criteria for Jet Formation from Impinging Shells and Plates," J. Appl. Physics, Vol. 47, No. 7, July 1976.*

Pugh, Eichelberger, and Rostoker (PER) theory of jet formation.[9]

This report includes a description of analytical equations, the procedures for their application and a FORTRAN listing of BASC. Experimental results for selected shaped charge problems are presented in a comparison to the calculations. The range of useful applications is discussed as well as the limitations of the approach.

BASC is a "living code" which has provided insights to the jet-formation process and is a very good tool for parametric design for a selected class of problems.

A simplified flow chart and the FORTRAN code listing is presented in Appendices A and B, respectively.

II. GOVERNING EQUATIONS

The initial equation used in the liner acceleration portion of the BASC code determines the angle of liner bending, ϕ, produced by a detonation wave traveling with a velocity, D, and inclined to the liner wall at an angle, i (the angle of incidence). This relationship is illustrated in Figure 1. The author has modified the original platepush relationship of Defourneaux to be

$$\frac{1}{\phi} = \frac{1}{\phi_o} + K\frac{\rho\varepsilon}{eB} , \qquad (1)$$

$$B = 1 + A/\rho_c e_c ,$$

where ρ and ε are the density and thickness of the liner wall, and e is the explosive thickness. Added are ρ_c, e_c, and A which are, respectively, density, thickness, and a constant, which is determined from the experimental data for the confinement casing around the charge[10]. The constant, A, when set to zero, represents an unconfined explosive charge and the Defourneaux relationship, as illustrated in Figure 1. ϕ_o and K are functions of the angle of incidence, i, and

---

[9] *E. M. Pugh, R. J. Eichelberger and N. Rostoker, "Theory of Jet Formation by Charges with Lined Conical Cavities," J. Appl. Physics, Vol. 23, No. 5, May 1952.*

[10] *R. DiPersio, J. Simon, and T. Martin, "A Study of Jets From Scaled Conical Shaped-Charge Liners," BRLMR-1298, August 1960. (AD #246352)*

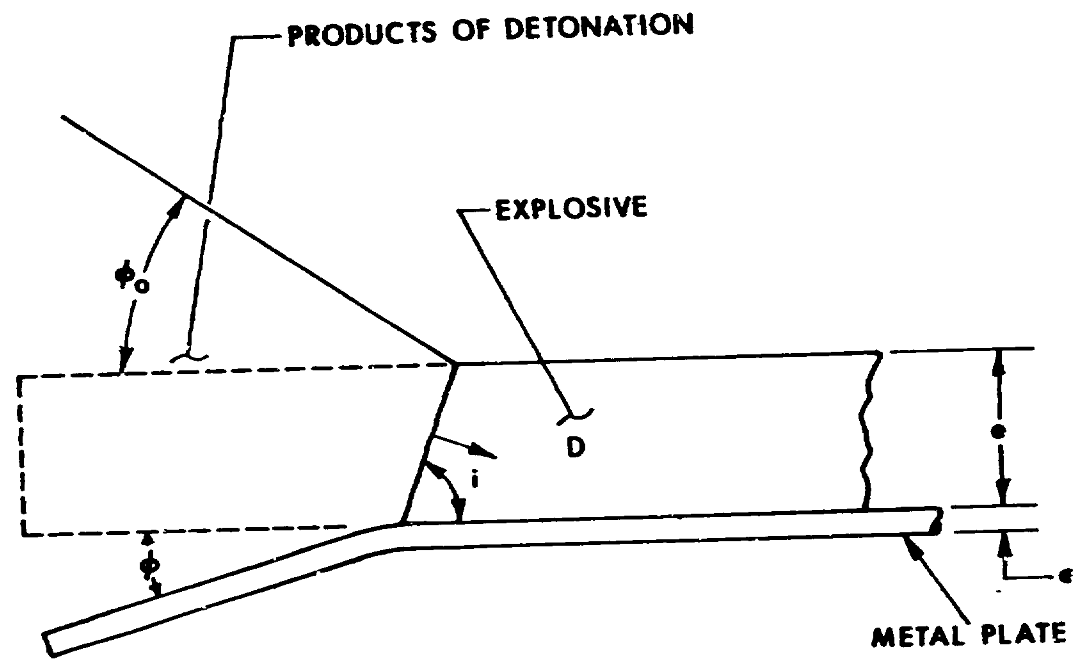

Figure 1. Projection of a Metal Plate by High Explosive

are determined for certain types of explosives.[11] Figure 2 illustrates the functional relationship between ϕ_o, K, and i. K is a constant over the range of i considered for typical shaped-charge designs, i.e. a conical liner contained in a cylinder of explosive. Figure 3 illustrates the linear relationship, Equation 1, that $1/\phi$ has with the ratio of liner mass per unit volume to explosive mass per unit volume, given as

$$\mu = \frac{\rho\ \varepsilon}{\rho_{H.E.} e} ,$$

where $\rho_{H.E.}$ is the density of the explosive. The values of $1/\phi_o$ and K used in Equation 1 are the Y-intercept and the ratio of the slope of the line to the density of explosive respectively. Equation 1 along with the Taylor formula,

$$v_o = 2D \sin \frac{\phi}{2} ,$$

where D is the explosive detonation rate, will result in collapse velocities, v_o, obtained by Gurney.[12] Two types of explosive compositions are shown in Figure 3 (data taken from reference 11) which represent the linear function at a constant grazing (parallel) incidence, i, of the detonation from the normal to the metal surface (see Figure 1).

From the theory of Defourneaux, as the detonation wave sweeps toward the base of a typical shaped charge, ϕ decreases due to the decrease in the explosive thickness, e, shown in Figure 3. This assumption that ϕ decreased monotonically with a decrease in e is justified for most of the liner collapse since there is sufficient time for the liner to undergo several shock reverberations and achieve a bending angle close to its maximum before entering the flow of jet formation. However, the region near the apex of the cone

---

[11] *M. DeFourneaux and L. Jacques, "Explosive Deflection of a Liner as a Diagnostic of Detonation Flows," Proceedings Fifth Symposium (International) on Detonation, ACR-184 Office of Naval Research-Department of Navy, pp. 457-466, Pasadena, California, August 18-21, 1970.*

[12] *R. W. Gurney, "The Initial Velocity of Fragments from Bombs, Shells, and Grenades," BRL Report No. 405, Sept. 1943. (AD #ATI36218)*

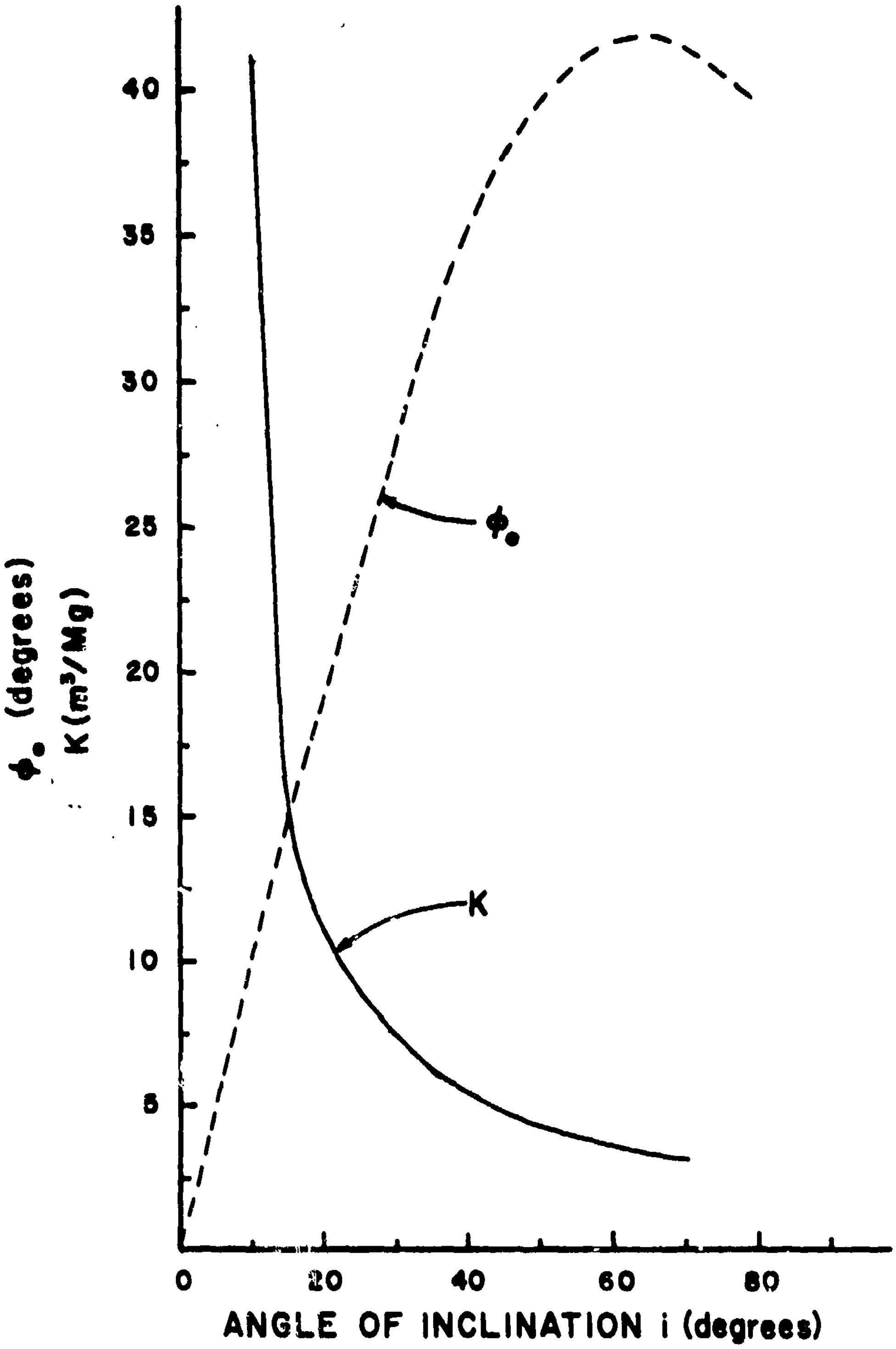

Figure 2. ϕ_0 and K are functions of the detonation wave angle to the liner.

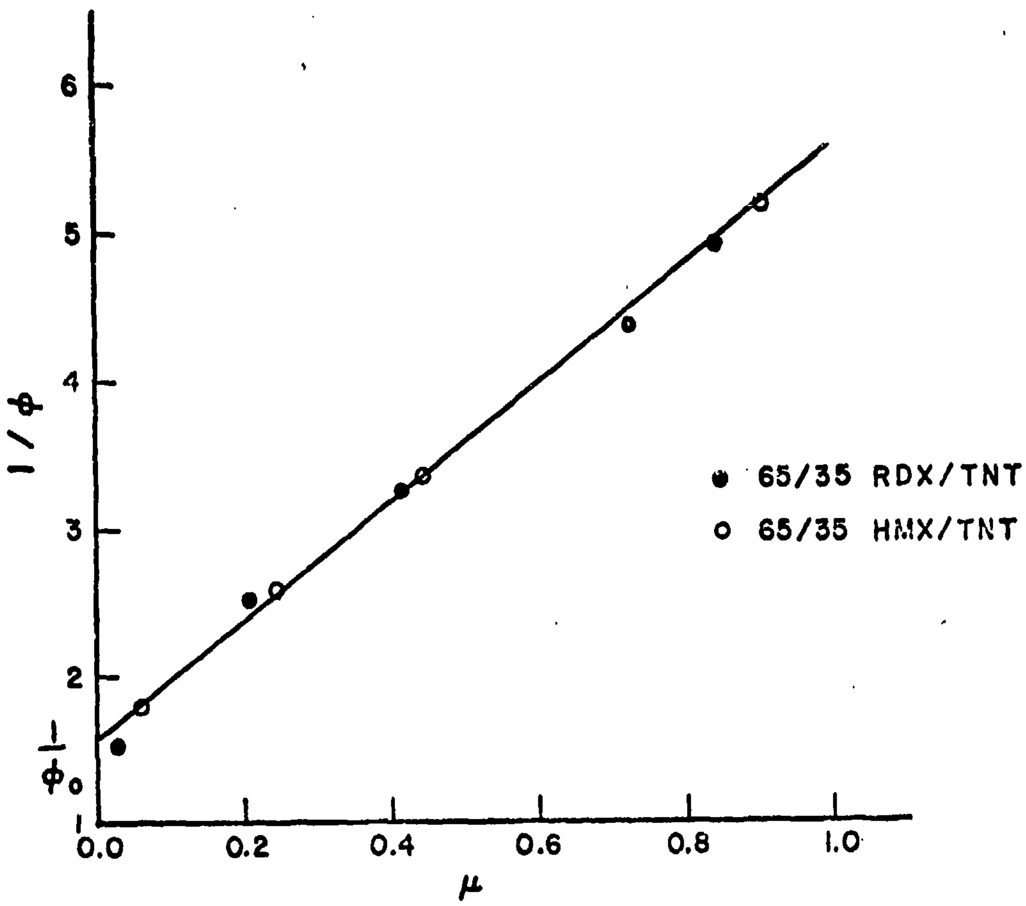

Figure 3. $1/\phi$ vs μ as determined from experiments. Data is taken from Reference 11.

enters the flow shortly after its initial acceleration and hence does not achieve its ultimate bending angle. Therefore, for material close to the liner's apex, ϕ will increase to a maximum. This maximum will be located near liner elements that originate from a position approximately 40% of the liner height measured from the apex of the cone. After this point, ϕ will decrease according to theory. We call this "the inverse collapse process." Associated with this process is the total time that a liner element takes to reach the axis. The equation for the collapse time is

$$\tau = (r \sin i)/(D(\sin(\alpha+\phi)-\sin\alpha)), \tag{2}$$

where several new variables are introduced. r is the instantaneous distance of a liner element from the axis before its collapse. α is the half angle of the cone of a conical liner or, in the general case, the instantaneous angle with the axis made by a tangent line to the liner. τ will be affected by the inverse collapse process. Material close to the liner apex enters the flow of jet formation sooner than would be predicted by the collapse of Defourneaux.[4]

In order to calculate the inverse collapse process, a new equation for the bending angle, ϕ and an iterative scheme were added to the code. The new equation for ϕ is

$$\phi_N = \phi \; e \sqrt{\frac{b}{\tau}} \; , \tag{3}$$

where $$b = C_1 \left[\frac{k\rho\varepsilon}{eB}\right] ,$$

C_1, is a constant determined from shape-charge collapse data.[13] The iterative scheme, between Equations (2) and (3), continues until the criteria of ϕ_N approaching ϕ within an epsilon is satisfied.

Having determined ϕ and τ, we can proceed with the collapse process.

[13] *F.E. Allison and R. Vitali, "An Application of Jet Formation Theory to the 105-mm Shaped-Charge," BRLR-1165, March 1962. (AD #277458)*

The velocity of collapse of the liner walls, v_o, toward the charge axis to form the jet is given by

$$v_o=2D(\sin(\phi/2))/(\sin i) \qquad (4)$$

The apparent explosive detonation velocity, with respect to liner wall is given by

$$Da=D/\sin i \qquad (5)$$

The substitution of Equation 5 into Equation 4 yields

$$v_o=2Da\ \mathrm{Sin}(\phi/2)\ . \qquad (6)$$

This is the so-called Taylor formula utilized in the code. The angle between the collapse direction and the charge axis is given by

$$\gamma = (\pi/2) - (\alpha + (\phi/2)). \qquad (7)$$

The liner element first hits the axis at a distance, $\overline{sp}$, from the liner apex, given by

$$\overline{sp} = (z \sin\phi) / (\cos\alpha(\sin(\alpha+\phi) - \sin\alpha)), \qquad (8)$$

where z is the axial component of the liner element position before its collapse.

While the liner is collapsing, the angle formed by a tangent to the collapsed portion on the axis and the axis itself (called the collapse angle) is computed from

$$\tan(\beta-\alpha) = \frac{\Delta z[\sin(\alpha+\phi) - \sin\alpha]\tan\phi + r\Delta\phi\cos\alpha}{\Delta z[\sin(\alpha+\phi) - \sin\alpha] - r\Delta\phi\cos\alpha\tan\phi}\ , \qquad (9)$$

where Δz is the axial increment chosen in the computational scheme, and $\Delta\phi$ is the incremental change in ϕ between adjacent liner elements. The cartesian coordinates of a liner element (which originates at position z,r) during collapse are given by the pair of equations:

$$\begin{aligned} x(z,t) &= z + v_o n\Delta t \sin(\alpha + (\phi/2)) \\ y(z,t) &= r - v_o n\Delta t \cos(\alpha + (\phi/2)), \end{aligned} \qquad (10)$$

where Δt is the time interval taken by the detonation wave between successive liner elements and n is a positive integer. These equations apply in the time interval given by

$$0 < n\Delta t \leq \tau .$$

Figure 4 is an illustration of the relationship of the variables employed in the BASC code of a generalized axisymmetric collapse of a typical shaped charge. Shown on Figure 5 are drawings giving a detailed description of the collapse process. Figure 5A shows the velocity vectors of an element at point, P, on the collapsing liner. The element is projected toward the axis of symmetry with a collapse velocity, v_o, and a bending angle, ϕ. When the detonation wave with velocity, D, has progressed a distance, P', (i.e. from point P to point Q) during the time interval, τ, then the element initally at point P will collide with the cone axis, producing the geometrical relations at the collision or stagnation point, $\overline{sp}$, shown in Figure 5B. This relationship at the stagnation point is with respect to a coordinate system moving at the stagnation point velocity, $v_{\overline{sp}}$. The velocity of the liner wall flowing into the stagnation point is v_f and the angle between it and the cone axis is the collapse angle, β. Figure 5C shows a cross-section of the collapsing liner depicting the variables employed. Applying Bernoulli's equations at the stagnation point, we find that the flow velocity, v_f, separates into two equal but directionally opposite velocities. One is called the jet velocity, v_j, and the other is called the slug velocity, v_N. This relationship is shown on Figure 6. Resolving the flow velocity, v_f, at the stagnation point in the laboratory coordinate system (Figure 6A), the following set of equations are obtained:

$$v_j = v_f + v_{\overline{sp}} , \tag{11}$$

$$v_N = v_{\overline{sp}} - v_f . \tag{12}$$

In accordance with the laws of conservation of mass and momentum, when the liner material reaches the cone axis after its collapse, it proceeds either as a fast-moving jet or as the more massive but slower-moving slug (Figure 6A). The jet velocity equation that results is

$$v_j = v_o \cos(\alpha + (\phi/2) - (\beta/2))/\sin(\beta/2) , \tag{13}$$

and the equation for the slug velocity is

$$v_N = v_o \sin(\alpha + (\phi/2) - (\beta/2))/\cos(\beta/2) . \tag{14}$$

The relative distribution of mass (Figure 6B) that results in jet and

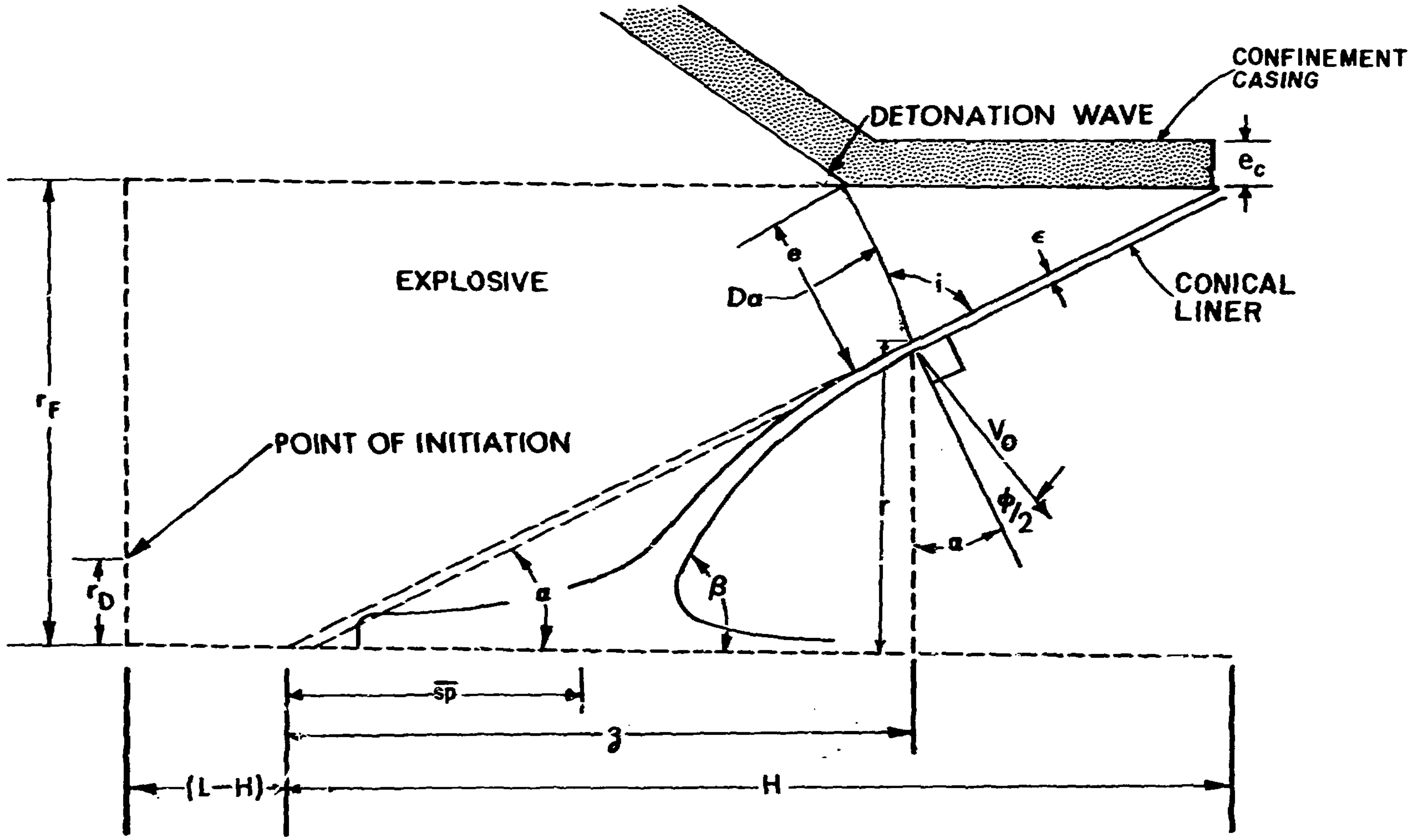

Figure 4. Line drawing illustrating the quantities employed in the BASC code of a generalized axisymmetric collapse of a shaped-charge.

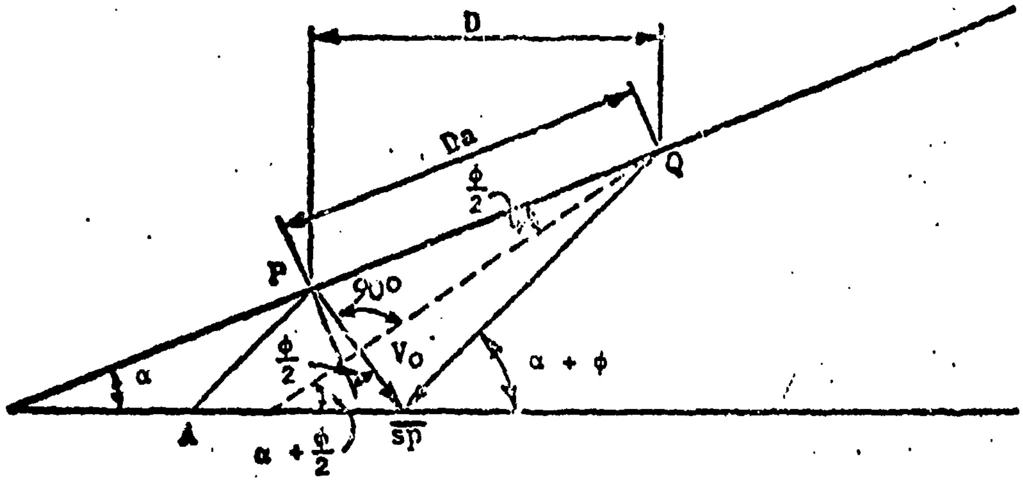

A. Velocity vectors of an element of the collapsing liner.

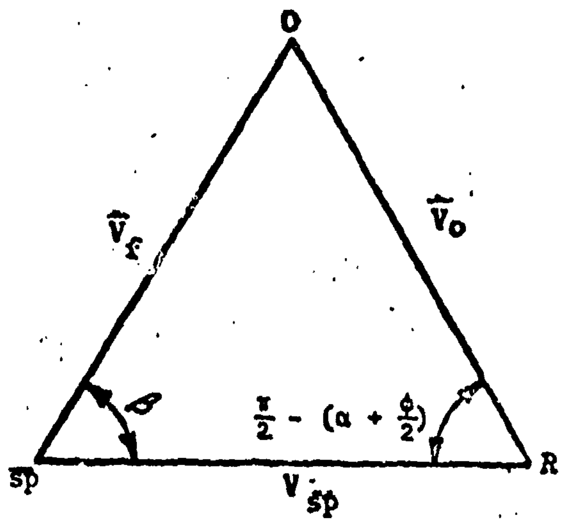

B. Geometrical relations at the stagnation point.

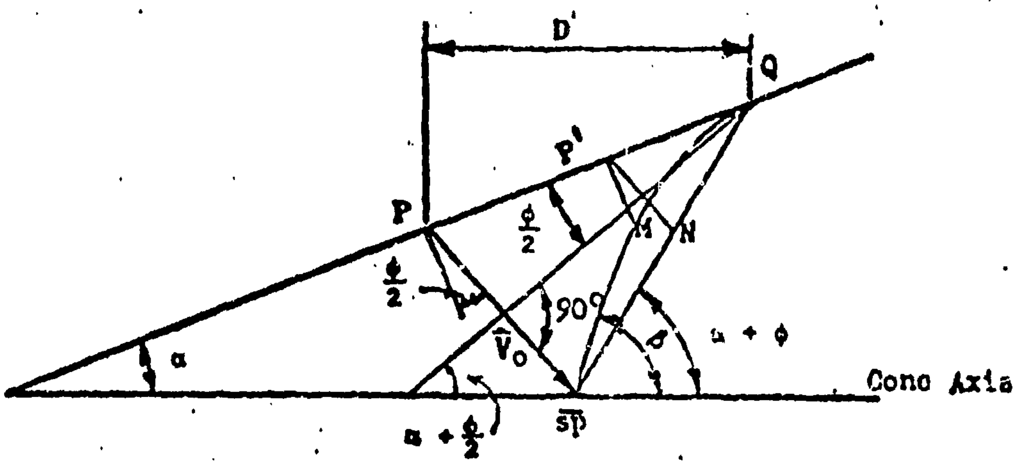

C. Cross-section of collapsing liner.

Figure 5. Illustration of the relationship between variables and the collapse process.

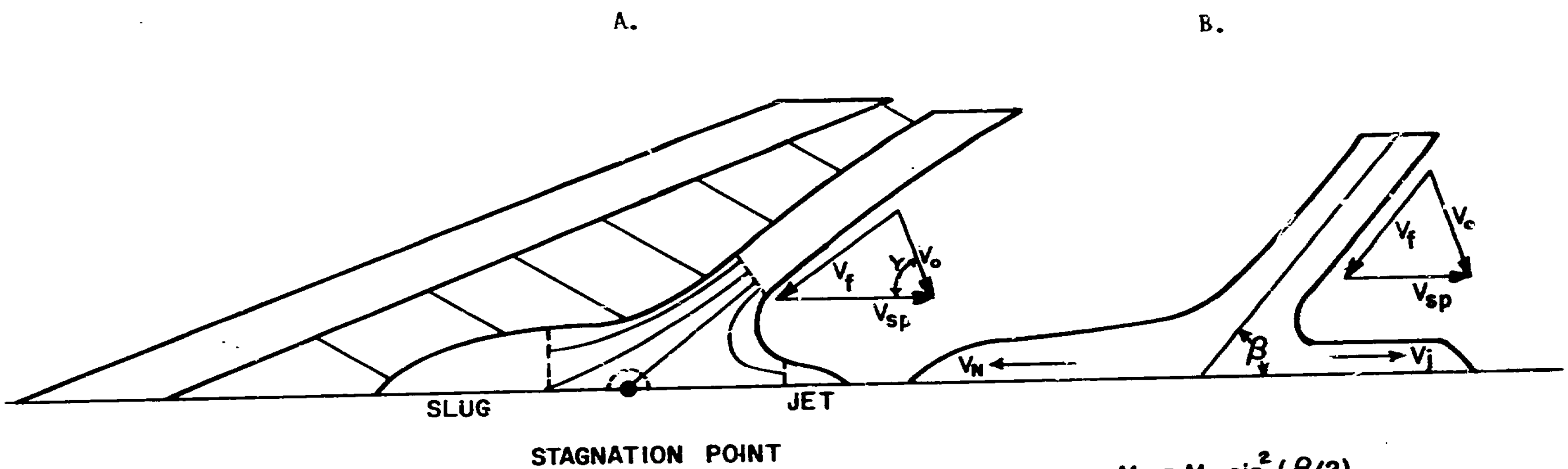

$$V_j = V_f + V_{\overline{sp}}$$

$$V_N = V_{\overline{sp}} - V_f$$

$$M_i = M_L \sin^2(\beta/2)$$

Figure 6. Illustration of the resolved variables in the laboratory coordinate system.

slug material are calculated, respectively, by

$$\frac{dm_j}{dm_L} = \sin^2(\beta/2)$$

and (15)

$$\frac{dm_N}{dm_L} = \cos^2(\beta/2) \ .$$

Also, the relative distribution of the kinetic energy for the jet and slug, respectively, are

$$\frac{dE_j}{dE_L} = \cos^2(\alpha + (\phi/2) - (\beta/2))$$

and (16)

$$\frac{dE_N}{dE_L} = \sin^2(\alpha + (\phi/2) - (\beta/2)) \ .$$

The variables dm_L and dE_L are the incremental change in the liner's mass and kinetic energy, respectively.

The impinging flow velocity, v_f, has been considered by shaped-charge researchers such as Walsh, et. al.[14]; Cowan, et. al.[15]; and Chou, et. al.[8] to be critical in the jet-formation theory. As illustrated in Figure 7, when v_f is less than the material sound speed, c, the jet formed is coherent or a good jet (Figure 7A). Even when v_f is slightly greater than c, this too forms a coherent jet (Figure 7B). But, when v_f is sufficiently greater than c, the jet will be incoherent or bifurcated. We call it a no-jet condition (Figure 7C). From equations 11 and 12, solving for v_f yields

$$v_f = .5(v_j - v_N) \ . \tag{17}$$

We then use the following relationship as the jet limiting criteria for a coherent jet:

$$M_R = v_f/c < 1.23 \ . \tag{18}$$

[14] *J.M. Walsh, R.G. Shreffler, and F.J. Willig, "Limiting Velocity Conditions for Jet Formation in High Velocity Collisions," Journal of Applied Physics, Vol. 24, No. 3, pp. 349-359, March 1957.*

[15] *G.R. Cowan and A.H. Holtzman, "Flow Configurations in Colliding Plates: Explosive Bonding," Journal of Applied Physics, Vol. 34, No. 4, pp. 928-939, April 1963.*

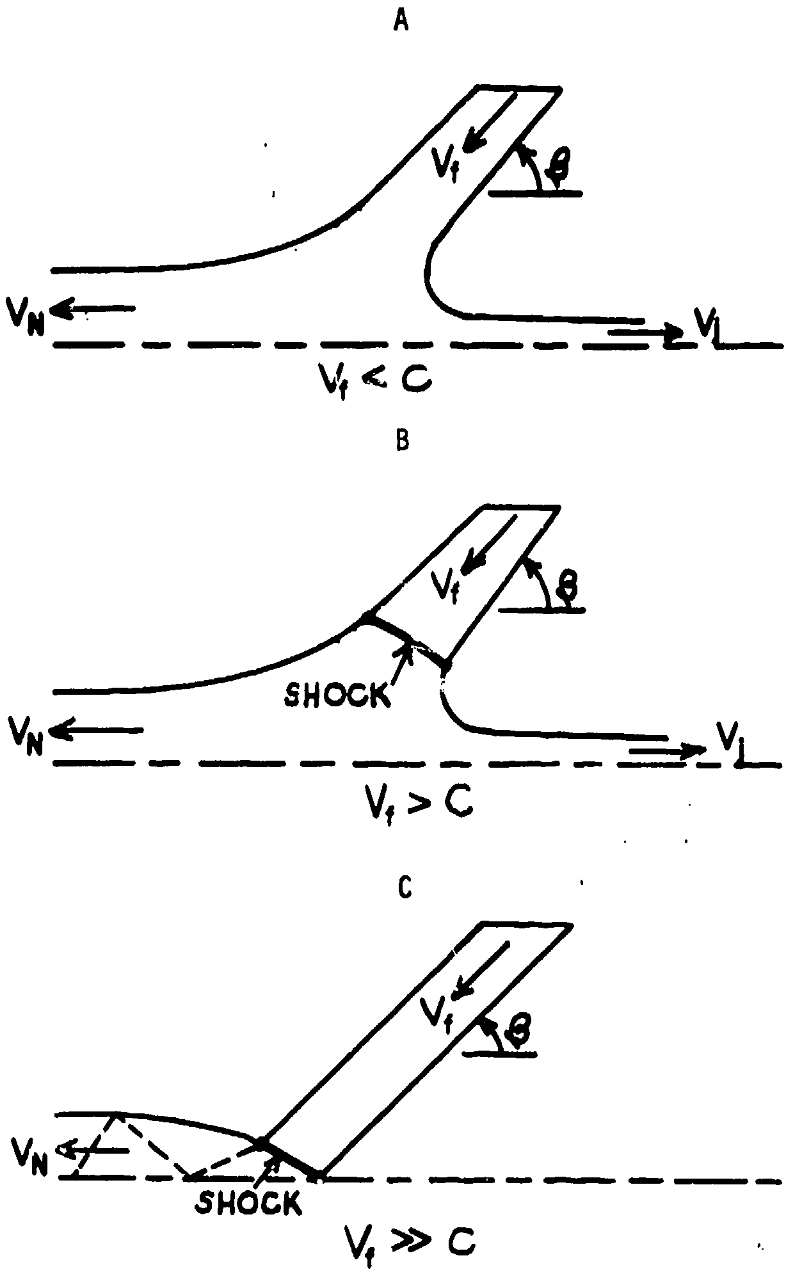

Figure 7. Illustration of the variables employed in the BASC code to limit jet formation. The jet limiting criteria for a coherent jet (A and B) is $M_R = \nu_f/c < 1.23$.

The threshold factor for a coherent jet, $M_R=1.23$, is determined by comparing radiographic, jet-particle data measured[16] from experiments[17] with BASC results. The threshold factor holds for several materials considered in BASC calculations.

In order to determine the jet-tip velocity and the mass of the lead pellet to be used in the shaped-charge penetration theory, the inverse velocity gradient has to be equilibrated and the jet mass in this region to be compressed into a single zonal element, LP. This zone will then contain the so-called steady-state, lead pellet. The equilibrated jet-tip velocity, v_{jo}, is obtained by the following process:

$$v_j^{i+1} = \frac{v_j^{i+1} \left[\frac{dm_j}{dm_L}\right]^{i+1} dm_L^{i+1} + v_j^{i} \left[\frac{dm_j}{dm_L}\right]^{i} dm_L^{i}}{\left[\frac{dm_j}{dm_L}\right]^{i+1} dm_L^{i+1} + \left[\frac{dm_j}{dm_L}\right]^{i} dm_L^{i}}$$

for $v_j^{i+1} > v_j^{i}$ and $1 \leq i \leq LP$, where i is the i^{th} zonal element. The equilibrated jet-tip velocity is

$$v_{jo} = v_j^{LP} \tag{18}$$

The steady-state, lead pellet mass is

$$dm_{jo} = \sum_{i=1}^{LP} \left[\frac{dm_j}{dm_L}\right]^{i} dm_L^{i} \quad . \tag{19}$$

In the theory of shaped-charge jet penetration into a target used in BASC, an important parameter is the time that a given liner element, which enters into the jet, arrives at the bottom of the target hole when penetration is in progress. Time is usually started from the moment the detonation wave reaches the apex of the liner. A time parameter, θ, is defined by

$$\theta = t_z + \tau \quad , \tag{20}$$

---

16 *Private Communication from J. Blische at BRL.*

17 *R. DiPersio, W.H. Jones, A.B. Merendino, and J. Simon, "Characteristics of Jets from Small Caliber Shaped Charges with Copper and Aluminum Liners," BRLMR No. 1866, September 1967. (AD #823839)*

where t_z is the time at which the detonation wave reaches the liner element at an initial axial distance, z, from the apex and τ is the time taken by this element to collapse onto the charge axis. The sum of standoff distance from the liner base to the initial surface of the target, h, and the liner height, H, defines Z_o:

$$Z_o = h+H. \tag{21}$$

The time for the tip of the jet to reach the target surface is

$$T_o = Z_o/v_{jo} \tag{22}$$

It is assumed that the jet tip originates from the zonal element, LP, and contains the highest velocity of the jet, v_{jo}. An element from the liner between LP and base results in a jet velocity, v_j, which is less than v_{jo} and is a function of its initial axial distance, z. A parameter, μ is defined by

$$\mu = v_{jo}/v_j \tag{23}$$

The time for the portion of jet formed from a given element of the liner to reach the bottom of the target hole is

$$T = \mu^{(1+k)} [T_o + (1+k) \sum_o^i \mu^{-k}(\Delta f)_i] \tag{24}$$

where $(\Delta f)_i = f_i - f_{i-1}$ and denotes the i^{th} zonal element. In this equation, $k = \sqrt{\rho_j/\rho_c}$, where ρ_j is the jet density (assumed equal to the liner density), and ρ_c is the target density. f is a time parameter given by

$$f = ((\theta/\mu) - (\overline{sp}/v_{jo})) \quad , \tag{25}$$

where $\overline{sp}$ was previously defined by Equation 8, and v_{jo}, θ, and μ were defined by Equations 18, 20, and 23. The value of μ to be used outside the bracket in Equation 24 is that which applies to the original elemental liner position. Δf is the difference in f values between adjacent elemental positions, and the summation applies to all adjacent elemental positions up to the point in question on the liner.

While the jet is still continuous in nature, it stretches due to its velocity gradient and, therefore, decreases in diameter with increase in time. The equation for calculating the jet radius, r_j, is

$$r_j^2 = - \frac{2 r \varepsilon D \sin^2 (\beta/2)}{\frac{\Delta Z}{\Delta t_z}\Big|_T \sin i} \tag{26}$$

In this equation, r is the initial radial position of the liner element from the charge axis, ε is the liner thickness at this position, and β is the collapse angle that is formed when this element reaches the charge axis. The factor, $\frac{\Delta Z}{\Delta t_z}\Big|_T$, is given by

$$\frac{\Delta Z}{\Delta t_z}\Big|_T = (T-t_z)\frac{\Delta v_j}{\Delta t_z} - v_j + \frac{\Delta(z-r\cot(\beta/2))}{\Delta t_z} \tag{27}$$

In this equation, t_z is defined following Equation 20 and Δt is the incremental time interval between arrival of the detonation wave between successive liner elements (a constant). The value computed by Equation 27 is a function of time, T, which starts at zero when the detonation wave first reaches the liner apex. It is a negative value which increases in absolute value as T increases. Therefore, it can be seen from Equation 26 that the jet radius, which originates from material at any point on the liner, decreases with an increase in T. The minus sign in Equation 26 is necessary to make r_j^2 a positive quantity.

When the jet cannot sustain any further stretching, it breaks up into individual axial particles. It is assumed that this occurs throughout the whole jet at the same time. The breakup time for the jet is designated as T_1 and, at present, must be obtained from experimental observations.[1] At times greater than the jet breakup time, the individual jet particles do not stretch in length or decrease in diameter. The constant jet particle radius that one obtains for material originating from a given element of the liner is calculated by Equation 26 in which the factor $\frac{\Delta Z}{\Delta t_z}\Big|_T$ is calculated at the breakup time, T_1 in Equation 27. However, radii of different particles are different due to the variability of the initial liner element position in Equations 26 and 27.

The equations that are used for jet penetration theory are dependent upon the standoff distance between the charge and the target. If the target is placed close enough to the charge so that the jet tip reaches the target before the time of jet breakup, one set of equations are used. On the other hand, if the jet particulates before reaching the target surface, a different set of equations must be used. In the former case, even though the jet

starts penetrating in the continuous state, it becomes discontinuous before the end of penetration and different equations are required after time T_1. The variables and the two states of penetration are illustrated in Figure 8.

The jet penetrates the target in both the continuous and discontinuous state whenever the following criteria is satisfied:

$$Z_o < v_{jo} T_1 \quad . \tag{28}$$

The depth of penetration into the target, p, for any T, such that $T_o \leq T \leq T_1$,

$$p = Z_o \left[\left(\frac{T}{T_o}\right)^{(k/(k+1))} - 1 \right] \quad , \tag{29}$$

where all factors have been previously defined. For times greater than T, the equation used is

$$p = Z_o \left[(k+1) \left(\frac{T_1}{T_o}\right)^{(k/(k+1))} \frac{T}{T_1 + kT_1} - 1 \right] \quad . \tag{30}$$

The total penetration depth into the target is calculated by

$$P_T = (k+1)(v_{jo}T_1)^{\frac{k}{k+1}} Z_o^{\frac{1}{k+1}} - \sqrt{k(k+1)U^{min} T_1 (v_{jo}T_1)^{\frac{k}{k+1}} Z_o^{\frac{1}{k+1}}} - Z_o \quad . \tag{31}$$

The only hitherto undefined term in Equation 31 is the factor U^{min}. This is called the minimum penetration velocity. According to theory, the velocity of penetration into the target monotonically decreases with increase in penetration depth until it reaches the value U^{min}. When U^{min} is reached, penetration stops and all remaining jet material just piles up at the bottom of the target hole. U^{min} is an empirical constant whose value depends upon the target material and its hardness. It is invariant with standoff distance. With a given charge, target, and standoff distance, the computer calculates the constant total penetration depth from Equation 31. This value is used by the computer as a signal to stop calculating p in Equation 30 and also to determine the time at the end of the penetration process. The radius of the hole in the target before the time of jet breakup is given by

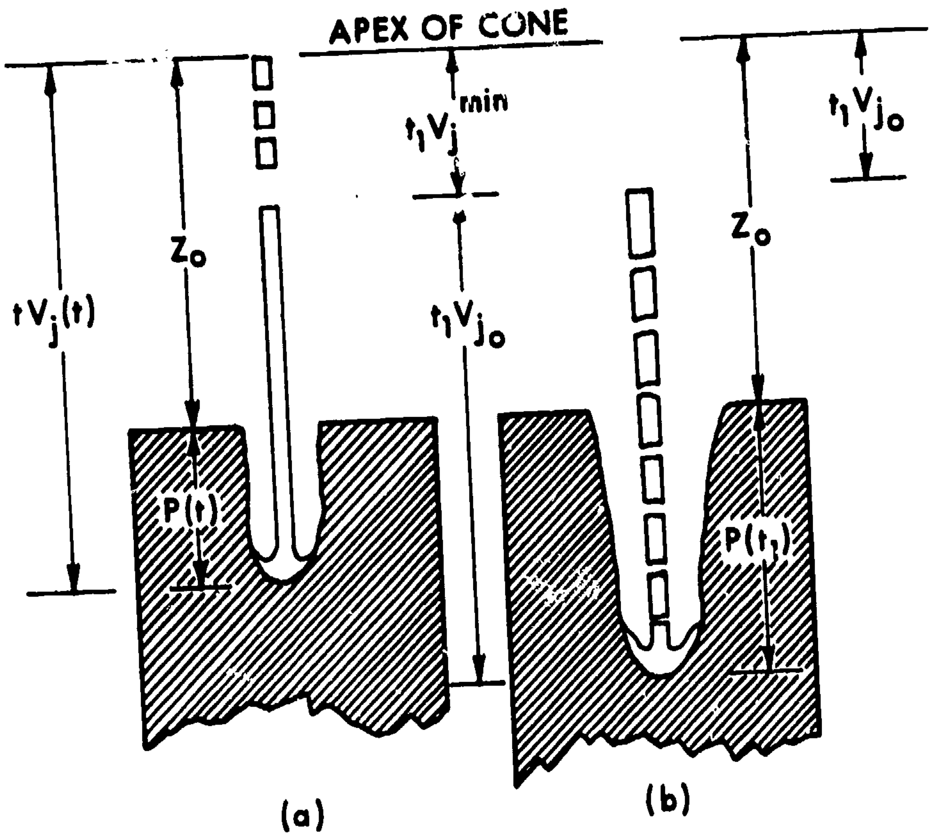

Figure 8. Schematic cross section of a shaped-charged jet penetrating a target in two states:

(a) Continuous and discontinuous,

(b) Discontinuous.

$$r_c = \sqrt{\frac{\rho_j}{2kc_k}} \sqrt{\frac{T_1}{T_o}} \left(\frac{Z_o}{Z_o+p}\right)^{\frac{3+k}{2k}} v_{jo}\, r_j \quad . \tag{32}$$

This equation contains one last empirical constant of the target, c_k. This is the jet kinetic energy needed to produce a unit of hole volume in the target. Its value depends upon the target used and its hardness. The value of r_j in Equation 32 is obtained by Equations 26 and 27. After the breakup time, T_1, the hole radius is obtained by

$$r_c = \sqrt{\frac{\rho_j}{2kc_k}} \; \frac{1}{k} \left[(k+1) \left(\frac{Z_o}{v_{jo}T_1}\right)^{\frac{1}{k+1}} - \frac{Z_o+p}{v_{jo}T_1}\right] v_{jo}\, r_j \, , \tag{33}$$

where r_j is now obtained by Equations 26 and 27 with the restriction that the factor $\frac{\Delta Z}{\Delta t_z}\Big|_T$ must be evaluated at $T = T_1$. The hole profile, as computed by Equation 33, is terminated when the penetration depth, p, reaches the value P_T as calculated by Equation 31.

The last set of penetration equations is used when the standoff distance between charge and target is so large that the following condition is satisfied:

$$Z_o > v_{jo}\, T_1 \quad . \tag{34}$$

In this case, all penetration is accomplished by the jet while it is particulated in nature. The equation for penetration depth is then

$$p = v_{jo}\, (T-T_o)\, T_1 \; / \; (T_1 + (T/k)) \tag{35}$$

where the time factor, T, varies between the time of first target impact, T_o, and the time of last jet penetration, T_p. The total penetration depth is given by

$$P_T = [v_{jo}\, T_1 - \sqrt{U^{min}\, 1_i\, (v_{jo}\, T_1 + (Z_o/k)]k} \quad . \tag{36}$$

The radius of the hole produced in the target as a function of its depth is given by

$$r_c = v_{jo}\, r_j\, (1-(p/k\, v_{jo}\, T_1))\, \sqrt{\rho_j/2k\, c_k} \quad , \tag{37}$$

where the jet radius, r_j, is obtained by Equations 26 and 27 with the restriction that the factor $\left.\frac{\Delta Z}{\Delta t_z}\right|_T$ is evaluated at $T = T_1$.

The variation of total penetration depth with standoff distance is computed by means of Equations 31 and 36. The factor Z_o is the only variable in these equations. Equation 31 is used first until Z_o increases to the value $v_{jo}\, T_1$, then Equation 36 is used.

III. CALCULATIONAL SCHEME

The BASC code enables one to perform parametric studies for designing warheads. The variables employed in the code of the generalized, axisymmetric collapse of a shaped charge were illustrated previously in Figure 4. The parameters which can vary include the following:

α	(ALPHA)	The half angle of the liner (degrees)
K	(CON)	The empirical constant for the detonation products. Value known for Composition B explosive.
ε	(EPS)	The thickness of the liner (cm)
ρ_j	(RHOJ)	The density of the liner (gm/cm^3)
ρ_c	(RHOC)	The density of the target (gm/cm^3)
r_F	(RF)	Radius of the base of [illegible] charge (cm).
H	(H)	Height of the liner (cm). If H is zero, H will be calculated by $H = \frac{r_F}{\tan\alpha}$.

D	(D)	Detonation velocity (cm/μs)
SO	(SO)	Standoff distance between base of liner and target, (cm)
C_K	(CK)	Constant for determining hole volume
T_1	(T1)	Jet breakup time (μs)
U^{MIN}	(UMIN)	Velocity cutoff for the penetration of jet into a target (cm/μs)
L	(DPOINT)	Initially the total length of the charge (cm) but is converted to be the initiation point of the explosive (i.e. DPOINT = L-H).
RDPT	(RDPT)	Radius above axis where explosive is initiated (cm).
JOHN	(JOHNI)	If JOHNI greater than zero, ϕ_o will vary; if not, ϕ_o will be a calculated constant.
N	(N)	The number of zones into which the grid is subdivided. If N is zero, default is seventy zones.

The code will set up the grid based upon Figure 4 and the equation for increment in Z is

$$DZ = H/N \tag{38}$$

and from this the time increment is

$$DTZ = DZ/D \quad . \tag{39}$$

Therefore, at each increment in Z we have also the corresponding time increment.

The code then marches sequentually through the governing equations (1-19), calculating and storing jet formation information to be printed and plotted at the end of the iteration. Those variables include:

i	I	i^{th} zone
α	ALPHA(I)	Tangent angle of liner wall to the axis (degrees)
z	Z(I)	z distance from apex to base of liner

t_z	TZ(I)	Time at the i^{th} zone
γ	GAMMA(I)	Angle (degrees)
E	E(I)	Thickness of explosive above i^{th} zone
ϕ	PHI(I)	Angle (degrees)
β	BETA(I)	Angle (degrees)
$\Delta\phi$	DPHI(I)	Increment of angle ϕ
$\frac{1}{\phi}$	RPHI(I)	Reciprocal of angle ϕ
V_o	V(I)	Collapse velocity (cm/μs)
r	R(I)	Radius of the i^{th} zone (cm)
τ	TAU(I)	Time to collapse i^{th} zone (μs)
$\overline{sp}$	C(I)	Distance from the apex of the liner where i^{th} zone will hit the axis (cm)
v_j	VJ(I)	Velocity of the jet in (cm/us)
v_N	VN(I)	Velocity of the slug in (cm/μs)
$\frac{dm_j}{dm_L}$	DMJ(I)	Relative mass of the jet, dimensionless
$\frac{dm_N}{dm_L}$	DMN(I)	Relative mass of the slug, dimensionless
$\frac{dE_j}{dE_L}$	DEJ(I)	Relative energy of the jet, dimensionless
$\frac{dE_N}{dE_L}$	DEN(I)	Relative energy of the slug, dimensionless
v_f	RV(I)	Relative velocity between the jet and slug

In the penetration portion of BASC, the constants listed below must be calculated:

$$VJO = \text{jet tip velocity from Equation 18} \quad (40)$$

$$ZO = H + SO \quad (41)$$

$$TO = \frac{ZO}{VJO} \quad (42)$$

$$AKAY = \sqrt{\frac{\rho_j}{\rho_c}} \quad (43)$$

PT = Total penetration (cm) from Equation 31 or 36 (44)

The next set of outputs are for the penetration of the jet into the target. The code also marches through the governing Equations 20-37, calculating and storing penetration information to be printed and plotted at the end of the iteration. The variables calculated and stored are listed below:

i	I	i^{th} zone
μ	AMU(I)	Relative velocity between the jet tip velocity and jet velocity of the i^{th} zone
θ	THETA(I)	Time parameter in microseconds
f	F(I)	Time parameter in microseconds
Δf	DF(I)	Time increment of f in microseconds.
T	T(I)	Time that the i^{th} element reaches the bottom of the target hole in microseconds.
Δt	DT(I)	Time increment of T
r	RSQ(I)	is $\sqrt{r_j^2}$ which is the radius of the i^{th} element of the jet.
A	A(I)	is equal to $z - r \cot \beta/2$.
ΔA	DELA(I)	is the increment of A(I).
Δv_j	DVJ(I)	is the increment of jet velocity.

$\frac{\Delta z}{\Delta t}\Big\vert_z$	DZODT(I)	Equation 27 in governing equations
r_c	RC(I)	Radius of the hole in target of the i^{th} zone in centimeters
p	p(I)	Depth of penetration in centimeters

After these parameters have been printed and plotted, the code then returns to start and begins another case. This is continued until the end of file (i.e. next problem) is encountered causing the run to terminate.

IV. COMPARISON OF BASC CODE RESULTS

The performance of the BASC code is best illustrated by presenting results of a calculation and comparing these results, where possible, with experimental data or with results from other numerical techniques. The first set of comparisons will be with experimental results from the following:

a. 105-mm, unconfined, 42°, copper-lined shaped charge with a Composition B explosive fill tested by Allison and Vitali[13].

b. A study of jets from scaled, 42°, copper-lined, conical shaped charges filled with Composition B explosive (test by DiPersio, et. al.[10]).

c. 3.2-inch, BRL precision, shaped charge with a copper liner 42° apex angle, and Composition B explosive fill, having its jet characteristics measured[16] from radiographic data recorded at the BRL.

d. A study of jet characteristics from small-caliber shaped charges with copper and aluminum liners and variation in apex angle from 20° to 90°. All charges were filled with Composition B explosive. The tests conducted at the BRL by DiPersio, et. al.[17]

The second set of comparisons will be another numerical technique. The other technique is the two-dimensional, hydrodynamic computer program based upon the Eulerian numerical scheme called the BRLSC (Ballistic Research Laboratory Shaped Charge) code.[18] The BRLSC

[18] *M.L. Gittings, "BRLSC: An Advanced Eulerian Code for Predicting Shaped Charges," Vol. I, BRL CR 279, Prepared by System, Science and Software, December 1975.* (AD #A023962)

code is a **modified** version of the HELP (Hydrodynamic Elastic-Plastic) code[19] developed by System, Science and Software.

Figure 9 and 10 are experimental comparisons for the 105-mm, unconfined, shaped charge. Collapse velocity, v_o, and jet velocity, v_j as a function of the relative distance from the apex of the cone are shown on Figure 9. The dashed line is the jet velocity after jet compression and illustrates exact agreement with both the jet tip velocity and position on the axis between BASC and experiment. This illustrates that jet tip is compressed into one element at a position which is approximately 40% of the distance from the apex of the cone. The collapse velocity is slightly higher than that calculated by Allison and Vitali, but the overall agreement is good. Figure 10 shows a comparison of the predictions of jet mass versus cone mass between the BASC code and Allison and Vitali. Those two predictions are in slight disagreement with one another because Allison and Vitali were unable to recover 100% of all the slug material. They used essentially the same theory as the BASC code to predict jet mass, and all of the material is required to accurately predict the true conservation laws.

Figure 11 is the second experimental comparison of the scaled, shaped charge with a heavy confinement casing. This figure shows collapse velocity, v_o, and jet velocity, v_j, as a function of the relative distance from the apex of the cone. The dashed line is the compressed jet velocity distribution. This again illustrates exact agreement for both jet tip velocity and its position on the axis between BASC and experiment. The open squares at approximately the 48% position from the apex of the cone shows the spread in the experimental data from the experimental scaled rounds. The BASC code results are identical for the same scaled rounds (see Reference 10). Shown at the base of the cone, for values greater than 80% of the distance from the apex of the cone, is a change in the slope of the jet velocity curve. This is due to gas leakage or breaking of the confinement casing. This phenomenon is modeled in BASC as a gradual change in the confinement factor, A in Equation 1, until it reaches zero, i.e. unconfined. This comparison shows very good agreement with the experimental results.

Table I is a tabulation of a comparison between measured, radiographic experimental data and BASC code results from the 3.2-inch, BRL, precision shaped charge. The jet tip velocity and mass at jet particle number one are in agreement, but the accumulated total jet mass from jet particle number one to jet particle number

---

[19] L.J. Hageman and J.M. Walsh, *"HELP, A Multi-Material Eulerian Program For Compressible Fluid and Elastic-Plastic Flows in Two Space Dimensions and Time," BRL CR 39, Prepared by System, Science and Software, May 1971. (AD Nos. 726459 and 726460)*

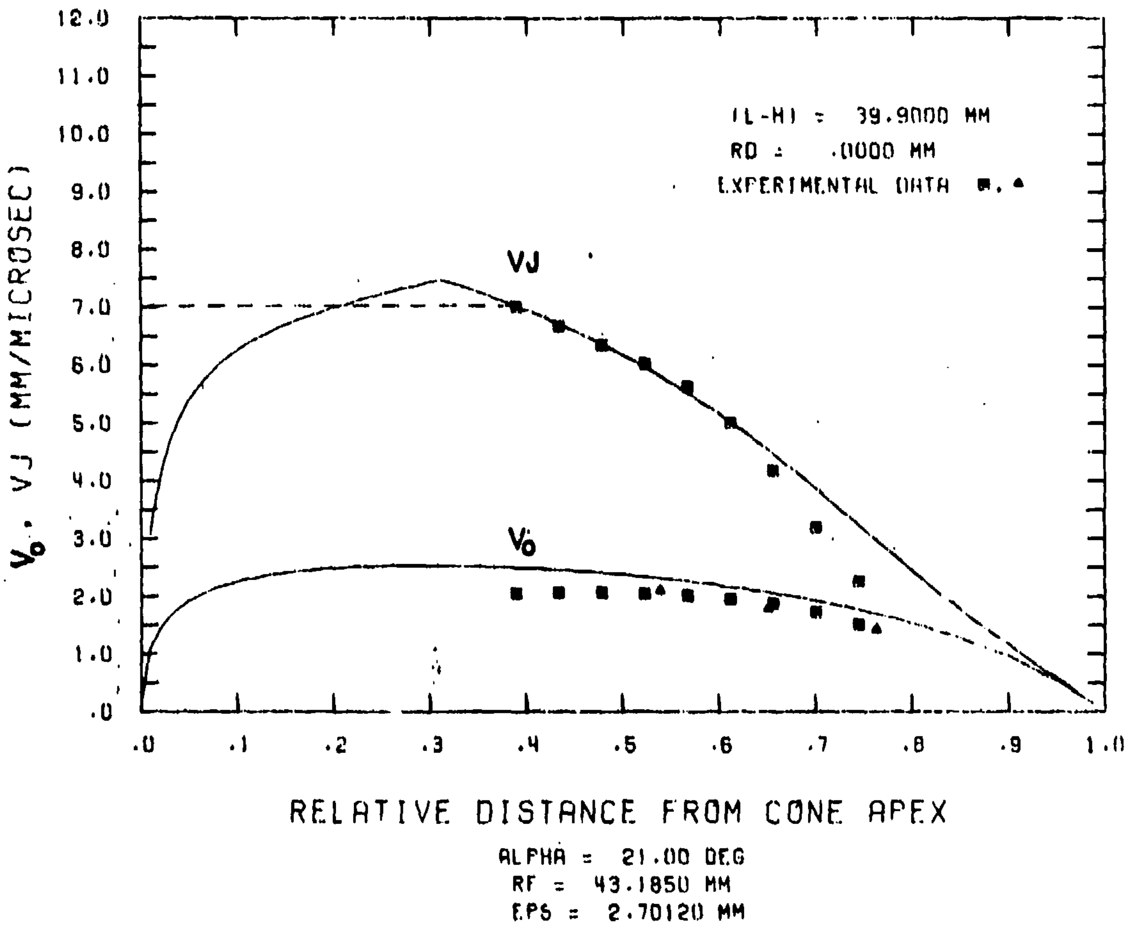

Figure 9. Comparison between experimental and BASC Code results of jet and collapse velocities from the 105-mm, unconfined, shaped charge.

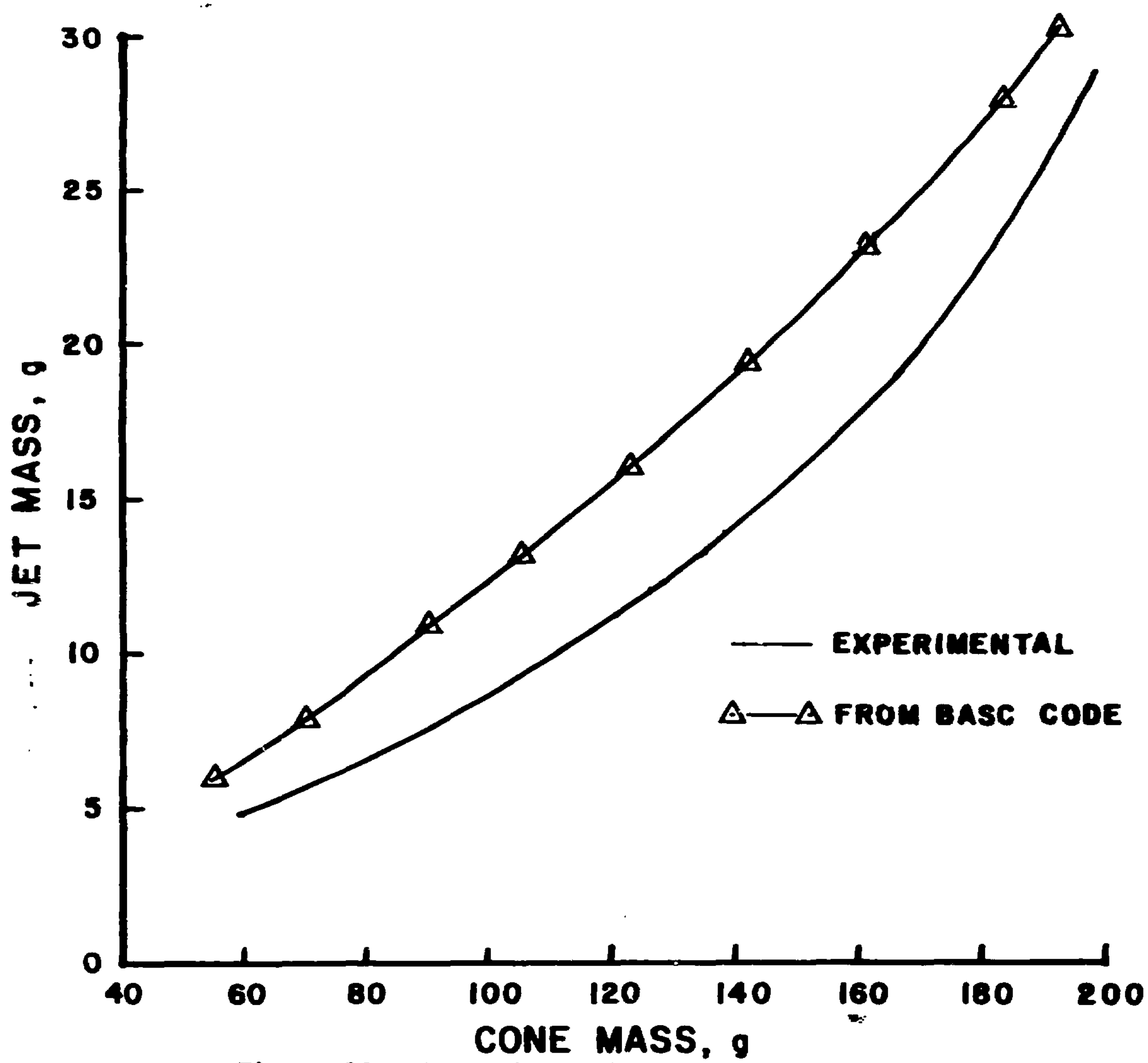

Figure 10. Comparison of calculations of jet mass vs cone mass between BASC code and experimental results from the 105-mm, unconfined, shaped-charge (Reference 13).

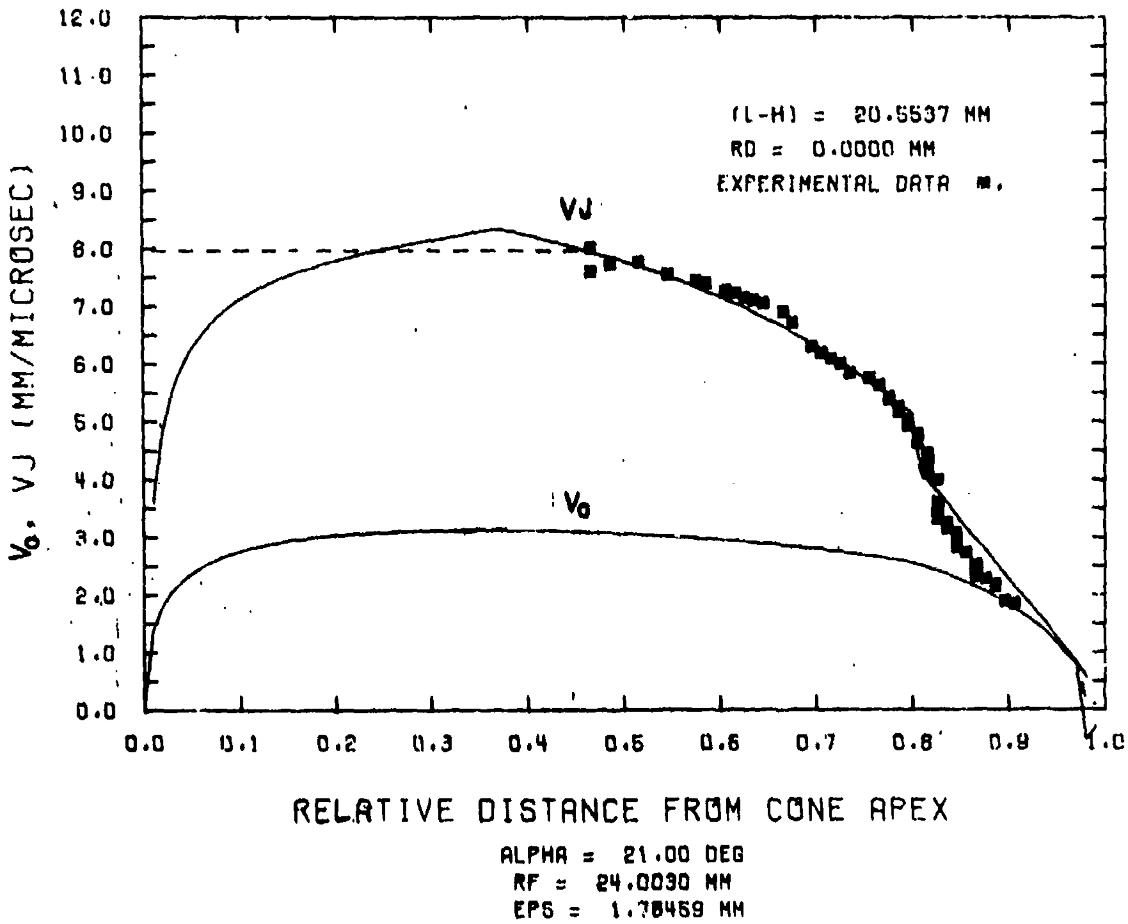

Figure 11. Comparison between BASC code and experimental results for scaled, heavily-confined, shaped charges (Reference 10). Jet and collapse velocities vs % of the distance from the apex of the cones are shown. Solid lines are BASC code results. The dashed line is the final, computed, compressed jet velocity profile. The jet tip for both experimental and BASC results is shown compressed into a position 48% from the apex of the cone.

forty-three is 10 grams heavier in the BASC code results. Also, the code results show 46% more total accumulated kinetic energy from the first forty-three jet particles than that obtained from experiment. Overall, this comparison is reasonable considering the material loss from such physical effects as erosion and possible errors in the data reduction measurements and calculations of the experimental results.

Table I. BASC Calculations and Measured, Experimental Radiographic Data[16] of Jet Velocity, Mass, and Kinetic Energy for the 3.2-in. (81.3-mm), BRL, Precision, Shaped Charge

Jet Particle No.	Velocity (km/s) Measured	Velocity (km/s) BASC	Accumulated Mass (g) Measured	Accumulated Mass (g) BASC	Kinetic Energy (kJ) Measured	Kinetic Energy (kJ) BASC
1	7.74	7.74	3.7	4.3	110.	128.
43	2.90	2.98	22.6	32.6	348.	507.

The last experimental comparison will be the characteristics of jets from small caliber shaped charges with copper and aluminum liners. In this study, only the liner designs referred to as 1½-inch (38.1-mm) liner base diameter charges in Reference 17 will be considered. The apex angle will include 20°, 40°, 60° and 90° cones for both the copper and aluminum liners. These are all confined with a steel casing around the charge. The pertinent dimensions for the shaped-charge designs considered can be found in Reference 17 on pages 9 and 10. The results from the BASC code calculations and the experiments are summarized on Table II. All of the results of the BASC code are within a 5% error boundary except the liner type with a 90° apex angle and aluminum cone which is 10%. The results of the calculations are slightly higher than the experiments for all of the aluminum liner types.

Table II. Summary of Results From the Small-Caliber, Shaped-Charge Study for the 38.1-mm (1½-in.), Base Diameter Design

Liner Type	Jet Tip Velocity, V_{jo} (km/s) Experiment	Jet Tip Velocity, V_{jo} (km/s) Predicted (BASC)
20° apex angle, Cu Cone	9.9	9.80
40° apex angle, Cu Cone	8.2	8.00
60° apex angle, Cu Cone	6.7	6.64
90° apex angle, Cu Cone	5.5	5.48

Liner Type	Experiment	Predicted (BASC)
20° apex angle, Al Cone	11.2	11.80
40° apex angle, Al Cone	9.3	9.75
60° apex angle, Al Cone	8.1	8.54
90° apex angle, Al Cone	6.8	7.50

The final two sets of comparisons involve the two numerical techniques: BASC and BRLSC. First, Figure 12, is a comparison of the calculated flow field for the 105-mm, unconfined shaped charge reported[2] for the BRLSC code and the BASC code at 25 μsec after initiation of the explosive. The radius of the jet and slug are in excellant agreement, but the tip of the jet is slightly behind in the BASC calculation. This is due to the fact that the BASC code takes very large time steps which will not allow the inverse velocity gradient to be equilibrated at this snap shot in time. The second set of comparisons between BASC and BRLSC codes is shown on Table III. The results shown are from an improved version of the BRLSC Code.[20] Table III is a tabulation of six calculated results from BASC and BRLSC as well as four experimental results, which can be used as a guide in this comparison. All of the calculations and experiments in this study involved identical copper liners (21°, 81.3-mm base diameter, 1.9-mm thickness). Calculations 1 through 4 employed TNT, Comp B, Octol and PBX, respectively as explosive filler.

Table III. Computational Matrix and Summary of Results

Calculation Number	HE Fill	Confinement	Total Jet Mass (g)		Jet Kinetic Energy (kJ)	
			BRLSC	BASC	BRLSC	BASC
1	TNT	Light	19.66	28.42	196.	385.
2	Comp B	Light	22.56	30.73	287.	507.
3	Octol	Light	27.40	32.03	349.	570.
4	PBX	Light	27.97	33.49	381.	614.
5	Comp B	Heavy	33.63	60.41	475.	1262.
6	Octol	Heavy	35.17	60.16	360.	1406.

[20] *R.T. Sedgwick, L.J. Walsh and M.S. Chawla, "Effects of High Explosive Parameters and Degree of Confinement on Jets from Lined Shaped Charges," BRL CR 245, Prepared by System, Science and Software, July 1975. (AD #B006987L)*

Calculation Number	Predicted Final Jet Tip Velocity (km/s)		Measured Jet Tip Velocity (km/s)
	BRLSC	BASC	
1	5.95	6.79	6.8
2	7.15	7.74	7.7
3	7.40	8.17	8.1
4	7.80	8.44	8.3
5	7.44	8.86	---
6	7.78	9.36	---

In these four calculations, the charge was confined in an aluminum casing (treated as being unconfined in the BASC code). Calculations 5 and 6 employed Comp B and Octol as explosive fills which were confined in a steel casing with a thickness of 10mm. The calculational matrix is shown in Table III with the degree of confinement provided by the aluminum and steel casing is referred to as light and heavy, respectively. The summary of the results of both codes (BASC and BRLSC) as well as the results of the jet tip velocities measured from experiments[21] are also shown in Table III. The quantities summarized represent the total jet which is composed of jet material having a velocity greater than or equal to a velocity of 2.8 km/s. The results indicate the ratio of predicted total jet mass of BRLSC code to the BASC code is approximately 65% for all calculations.

The comparison of jet tip velocity data is illustrated on Figure 13. The theoretically predicted values for calculations 1 through 4 from both the BASC and BRLSC codes are compared with the experimental determined jet tip velocity data. Figure 13 is a plot of calculated jet velocites versus the measured jet tip velocities. The open triangles are the final jet tip velocities as predicted by the BRLSC code[20] and the open squares are those predicted by the BASC code. There is very good agreement between the BASC code and the observed results for those rounds considered and the BRLSC code's agreement is less than 10% except for TNT which is 12.5%.

In summary, we have demonstrated in these comparisons the predictive ability of the BASC code. In addition, several of its salient features has been shown. These features include the predictive characteristics of BASC with respect to variations in casing confinement, variations in cone apex angle, variations in liner density and thickness, variations in explosive fill, and the effects of scaling. We have, also, demonstrated its predictive ability with respect to other sophisticated numerical schemes.

---

[21]*J. Simon, "The Effect of Explosive Detonation Characteristics on Shaped-Charge Performance," BRLMR-2414, August 1979.* (AD #B000337L)

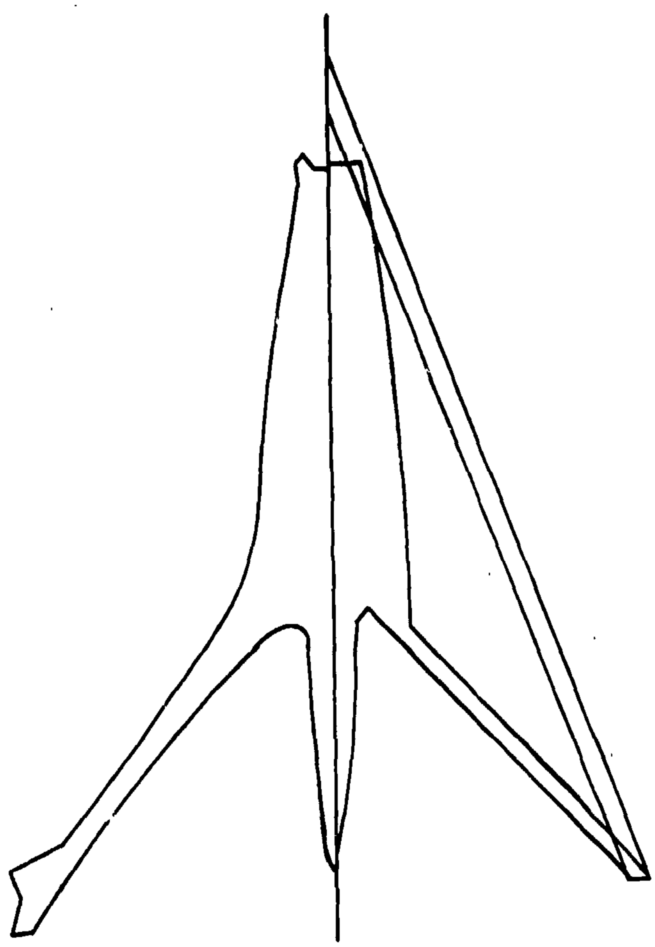

Figure 12. Comparison of calculations of the flow field between BASC code and a 2-D, Hydrodynamic Code (BRLSC) (Reference 2). These calculations are of the 105-mm, unconfined, shaped-charge shown at the time approximately 25μs after the initiation of the explosive. The BRLSC Code results are to the left of the axis of symmetry and the BASC code results are to the right.

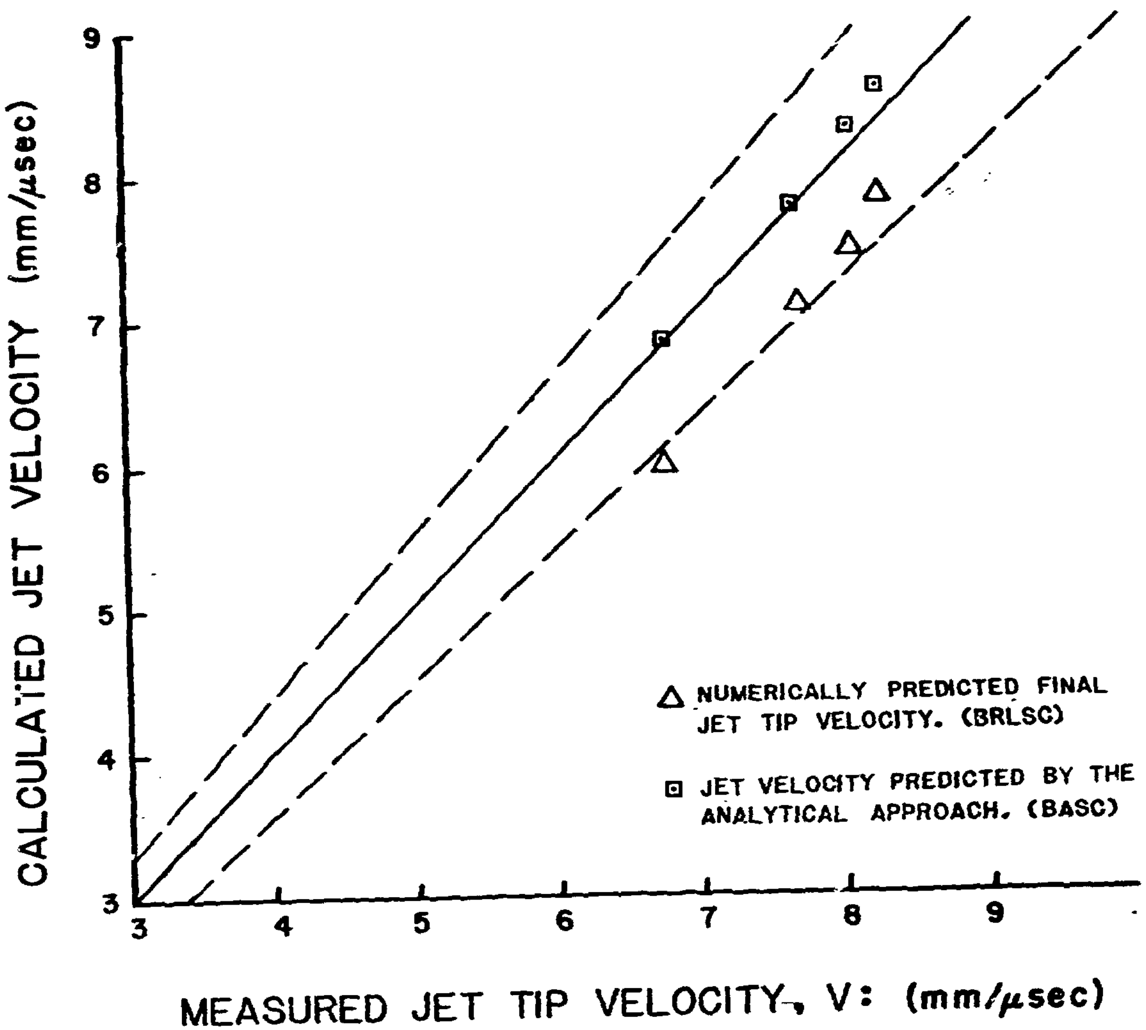

Figure 13. Comparison of Calculated and Measured Jet Tip Velocities from Shaped-Charge Designs 1 through 4, Shown on Table III.

Based upon these comparisons, it is concluded that, for many conical shaped-charge designs, the BASC code is a useful, predictive model for jet characteristics. Since it requires only fractions of a minute to do several shaped-charge design calculations on most computing systems (large or small), this calculational scheme is an economical approach for warhead design and analysis.

V. LIMITATIONS OF BASC

The current version of BASC requires several empirically determined constants. The collapse model requires the determination of ϕ_o and k; their relationship to the angle of incidence, i; the constant A for a confined casing; and finally, C1, a constant calibrated to the 105-mm, unconfined, shaped charge for the time of collapse near the apex of the cone. Penetration requires a cutoff velocity, Umin, and a breakup time, T_1.

Breakup time, as used in the theory of DiPersio, et. al.[7], is a quantity determined from a radiograph of the jet. It is treated as a constant, but only approximates that value for conical liners with uniform wall thicknesses. Work by Simon[21] shows that breakup time for a given geometry remains a constant over changes in the Chapman-Jouguet pressure of 186-380 kbars. The codes, as used, requires a predetermined value for T_1 for a given shaped-charge geometry. The value of T, scales with cone diameter. All of these limitations stem from the empirical nature of the equations of the code.

Geometrical considerations for conical collapse may or may not be a limitation to the BASC code. Research will have to be conducted in order to determine this fact. Since the initial cone half-angle varies as a function of distance along the axis, z, and since each zonal element has no interaction with other elements, all geometrical considerations should be solvable.

Current limitations will be corrected by future changes to the code. These changes are explained in the next section.

VI. FUTURE MODIFICATIONS

There are several tasks intended to improve BASC. The major areas of research are the following: (1) modeling the jet formation for

several different materials and geometrical consideration, (2) modeling the viscous effects, as suggested by Walters,[22] in a nature compatible with BASC, (3) modeling the breakup of the jet with reference to a maximum strain to break, (4) modeling the threshold for a jet-no-jet criteria for many more materials.

As explained earlier, elements in the apex region of a conical liner reach the jet formation region before these elements are accelerated to their maximum attainable velocity. To account for this characteristic of conical, liner apex flow, which is so important in determining exact jet-tip velocities, transient acceleration is being modeled by an empirical constant determined from normalized, copper liner data[13]. This constant accounts for the number of shock reverberations that occur in the copper liner before it enters the flow of jet formation. We can improve upon this constant by obtaining experimental collapse data for a number of different materials.

Research conducted by Simon indicates that the breakup of the shaped-charge jet may be related to a maximum strain, which is a function of strain rate. These observations were made for copper liners with many different explosive fillers ranging from TNT (C-J pressure 186 kbars) to a high HMX explosive (C-J pressure 380 kbars), but with only one charge and liner geometry. Work is continuing by Chou, et. al.,[23,24] to define the critical condition for breakup models based on these results and will be added to the code where piecewise strains and strain rates will be calculated. We will continue to calculate penetration velocity, U, and will terminate penetration according to a minimum value of U as demonstrated by DiPersio, et. al.; but we will explore the use of $v_{J_{min}}$ as the penetration cut-off criteria. Finite-difference codes may be applied either directly or in a simplified form to generate a library of parameters by computational experiments. This will assist in the research of some of these critical parameters utilized in the BASC code.

As certain elements of the shaped-charge collapse problem are accurately modelled, that section of the BASC code will be modified. The code is considered a "living" code, constantly being updated but applied within its limitations at all stages of its development.

---

[22] *W. Walters, "Influence of Material Viscosity on the Theory of Shaped-Charge Penetration," ARBRL-MR-02941, August 1979. (AD #B041486L)*

[23] *P.C. Chou and J. Carleone, "Calculations of Shaped-Charge Jet Strain, Radius and Breakup Time," BRLCR-246, July 1976. (AD #B007240L)*

[24] *J. Carleone, P.C. Chou, and R. Ciccarelli, "Shaped-Charge Jet Stability and Penetration Calculations," BRLCR-351, September 1977. (AD #A050117)*

VII. SUMMARY

BASC is a simple, well-documented, shaped-charge code that may be applied to many problems to predict trends and gross effects. Difficulties in predicting the jet-tip characteristics still exist for some materials, but future modifications should correct this deficiency. The code is so structured that it can grow and become more widely applicable as modeling improvements are available.

ACKNOWLEDGEMENT

The author is grateful to Robert DiPersio, now retired, and Robert R. Karpp, now of Los Alamos Scientific Laboratory, for their many contributions in the formulation of the BASC code.

The author is grateful to Mary Scarborough of the BRL for her artistic work in the preparation of the illustrations used in this report.

REFERENCES

1. J.T. Harrison and R.R. Karpp, "Terminal Ballistic Applications of Hydrodynamic Computer Code Calculations," BRLR 1984, April 1977. (AD #A041065)
2. J.T. Harrison, "A Comparison between the Eulerian, Hydrodynamic Computer Code (BRLSC) and Experimental Collapse of a Shaped Charge Liner," ARBRL-MR-02841, June 1978. (AD A059711)
3. J. Harrison, R. DiPersio, R. Karpp and R. Jameson, "A Simplified Shaped Charge Computer Code: BASC," DEA-AF-F/G-7304 Technical Meeting: Physics of Explosives, Vol II, April-May 1974, Paper 13 presented at the Naval Ordnance Laboratory, Silver Spring, MD.
4. M. Defourneaux, "Hydrodynamic Theory of Shaped Charges and of Jet Penetration," Memorial DeL'art Ille'rie Francasise-T, 44, 1970.
5. R. DiPersio, C.W. Whiteford, and J. Simon, "An Experimental Method of Obtaining Collapse Velocities of the Liner Walls of a Linear Shaped-Charge Liner," BRL-MR-1696, September 1965. (AD #478326)
6. A. Kiwan and H. Wisniewski, "Theory and Computations of Collapse and Jet Velocities of Metallic Shaped Charge Liners," BRLR-1620, November 1972. (AD #907161)
7. R. DiPersio, J. Simon, and A. Merendino, "Penetration of Shaped-Charge Jets into Metallic Targets," BRLR 1296, September 1965. (AD #476717)
8. P. Chou, J. Carleone, R. Karpp, "Criteria for Jet Formation from Impinging Shells and Plates," J. Appl. Physics, Vol. 47, No. 7, July 1976.
9. E.M. Pugh, R.J. Eichelberger and N. Rostoker, "Theory of Jet Formation by Charges with Lined Conical Cavities," J. Appl. Physics, Vol. 23, No. 5, May 1952.
10. R. DiPersio, J. Simon, and T. Martin, "A Study of Jets From Scaled Conical Shaped-Charge Liners," BRLMR-1298, August 1960. (AD #246352)
11. M. Defourneaux and L. Jacques, "Explosive Deflection of a Liner as a Diagnostic of Detonation Flows," Proceedings Fifth Symposium (International) on Detonation, ACR-184 Office of Naval Research-Department of Navy, pp. 457-466, Pasadena, California, August 18-21, 1970.

REFERENCES (Cont'd)

12. R.W. Gurney, "The Initial Velocity of Fragments from Bombs, Shells, and Grenades," BRL Report No. 405, Sept. 1943. (AD #ATI36218)

13. F.E. Allison and R. Vitali, "An Application of Jet Formation Theory to the 105-mm Shaped Charge," BRLR-1165, March 1962. (AD #277458)

14. J.M. Walsh, R.G. Shreffler, and F.J. Willig, "Limiting Velocity Conditions for Jet Formation in High Velocity Collisions," Journal of Applied Physics, Vol. 24, No. 3, pp. 349-359, March 1957.

15. G.R. Cowan and A.H. Holtzman, "Flow Configurations in Colliding Plates: Explosive Bonding," Journal of Applied Physics, Vol. 34, No. 4, pp. 928-939, April 1963.

16. Private Communication from J. Blische at BRL.

17. R. DiPersio, W.H. Jones, A.B. Merendino, and J. Simon, "Characteristics of Jets from Small Caliber Shaped Charges with Copper and Aluminum Liners," BRLMR No. 1866, September 1967. (AD #823839)

18. M.L. Gittings, "BRLSC: An Advanced Eulerian Code for Predicting Shaped Charges," Vol. I, BRL CR 279, Prepared by System, Science and Software, December 1975. (AD #A023962)

19. L.J. Hageman and J.M. Walsh, "HELP, A Multi-Material Eulerian Program For Compressible Fluid and Elastic-Plastic Flows in Two Space Dimensions and Time," BRL CR 39, Prepared by System, Science and Software, May 1971. (AD Nos. 726459 and 726460)

20. R.T. Sedgwick, L.J. Walsh and M.S. Chawla, "Effects of High Explosive Parameters and Degree of Confinement on Jets from Lined Shaped Charges," BRL CR 245, Prepared by System, Science and Software, July 1975. (AD #B006987L)

21. J. Simon, "The Effect of Explosive Detonation Characteristics on Shaped Charge Performance," BRLMR-2414, September 1974. (AD #B000337L)

22. W. Walters, "Influence of Material Viscosity on the Theory of Shaped-Charge Penetration," ARBRL-MR-02941, August 1979. (AD #B041485L)

23. P.C. Chou and J. Carleone, "Calculations of Shaped-Charge Jet Strain, Radius and Breakup Time," BRLCR-246, July 1975. (AD #B007240L)

24. J. Carleone, P.C. Chou, and R. Ciccarelli, "Shaped-Charge Jet Stability and Penetration Calculations," BRLCR-351, September 1977. (AD #A050117)

APPENDIX A

FLOWCHART OF COMPUTER PROGRAM

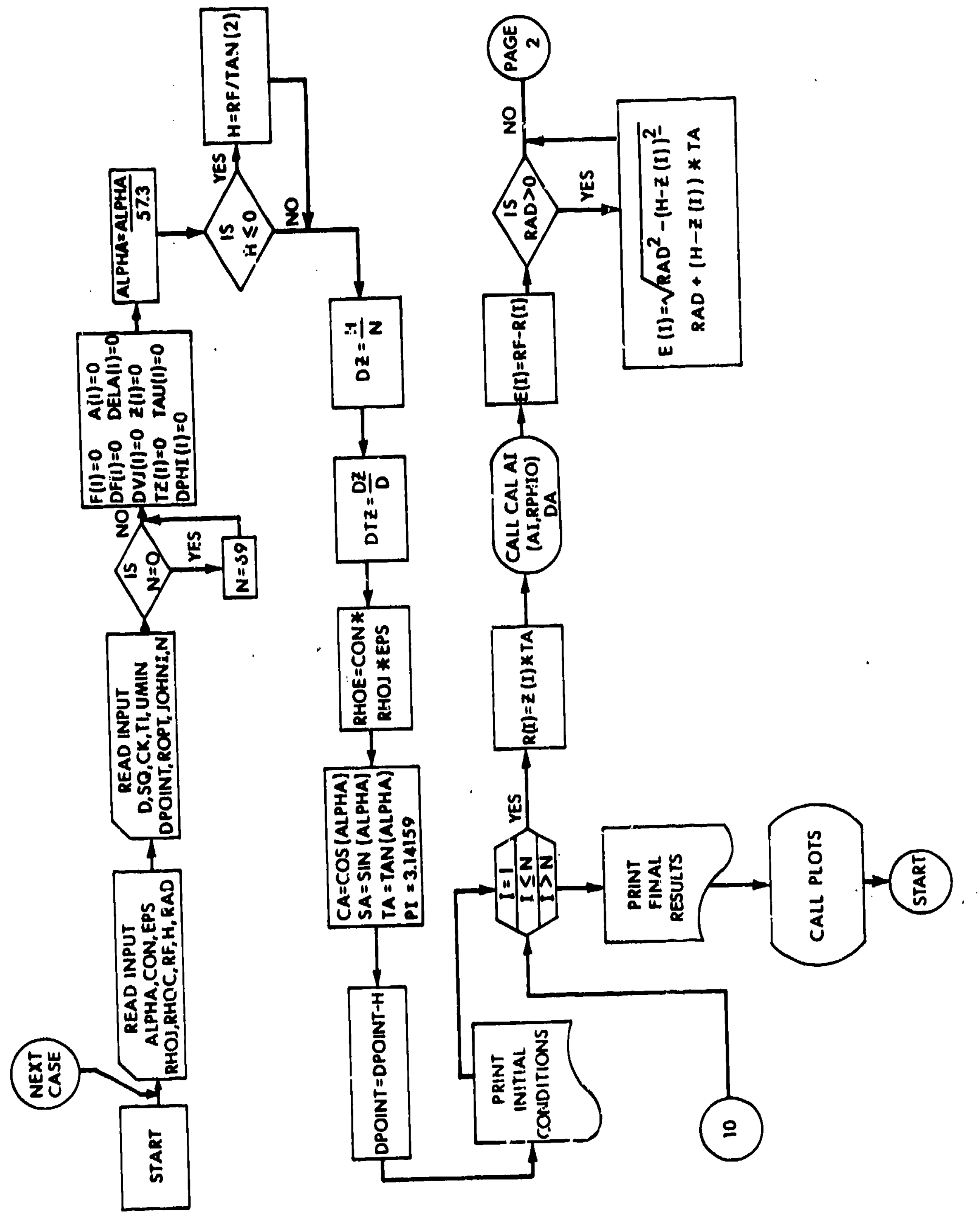
START
NEXT CASE
READ INPUT ALPHA,CON,EPS RHOJ,RHOC,RF,H,RAD
READ INPUT D,SQ,CK,TI,UMIN DPOINT,ROPT,JOHNI,N
IS N=O
YES
N=39
NO
F(I)=0 A(I)=0
DF(I)=0 DELA(I)=0
DVJ(I)=0 Z(I)=0
TZ(I)=0 TAU(I)=0
DPHI(I)=0
ALPHA=ALPHA/57.3
IS H≤0
YES
H=RF/TAN(2)
NO
DZ=H/N
DTZ=DZ/D
RHOE=CON* RHOJ*EPS
CA=COS(ALPHA)
SA=SIN(ALPHA)
TA=TAN(ALPHA)
PI =3.14159
DPOINT=DPOINT-H
PRINT INITIAL CONDITIONS
I=1 I≤N I>N
YES
R(I)=Z(I)*TA
CALL CAL AI (AI,RPHIO) DA
E(I)=RF-R(I)
IS RAD>0
YES
E(I)=√(RAD²-(H-Z(I))²) RAD+(H-Z(I))*TA
NO
PAGE 2
PRINT FINAL RESULTS
CALL PLOTS
START
10

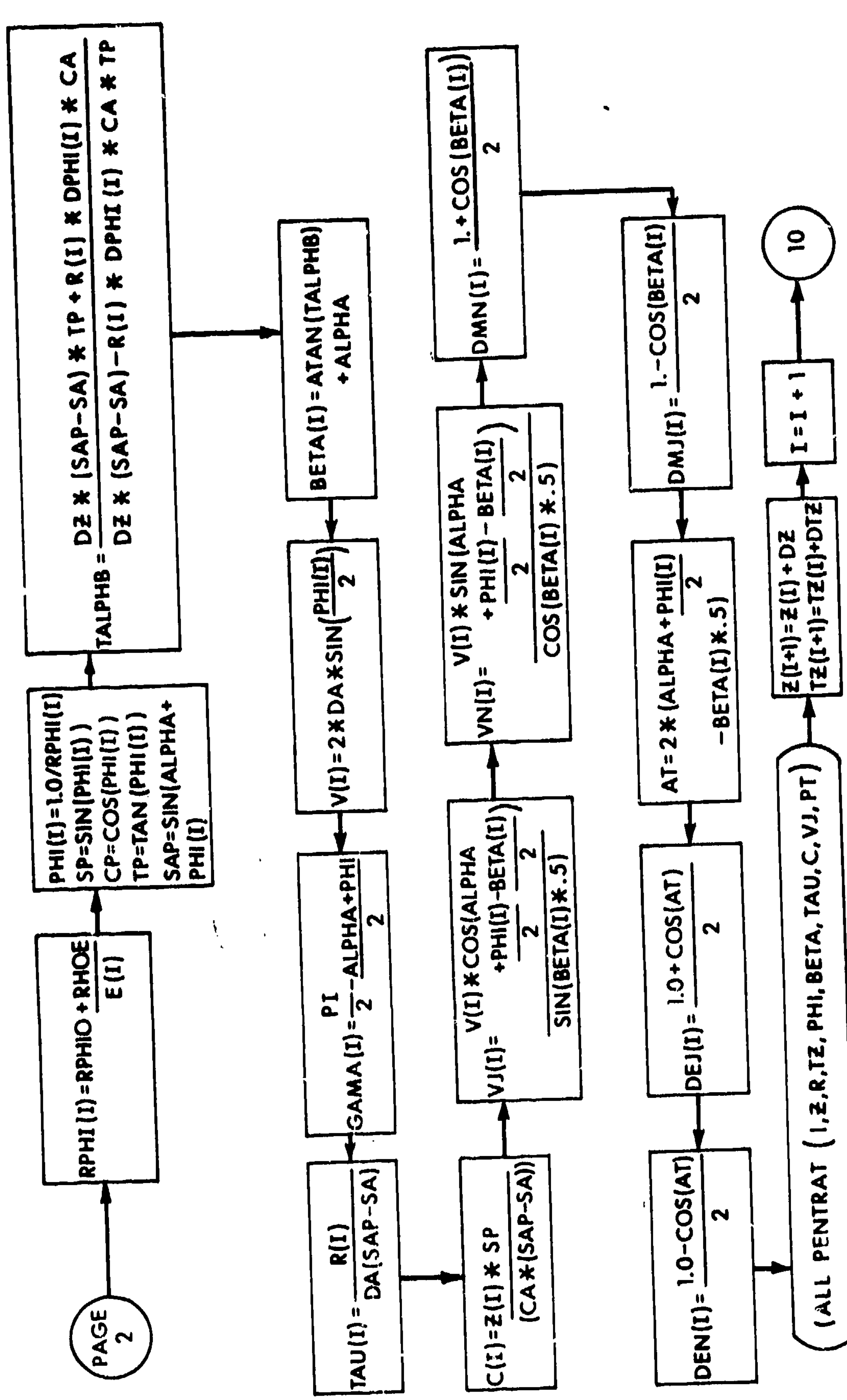
PAGE 2
RPHI(I)=RPHIO+RHOE/E(I)
PHI(I)=1.0/RPHI(I)
SP=SIN(PHI(I))
CP=COS(PHI(I))
TP=TAN(PHI(I))
SAP=SIN(ALPHA+PHI(I)
TALPHB = DZ * (SAP−SA) * TP + R(I) * DPHI(I) * CA / DZ * (SAP−SA) − R(I) * DPHI(I) * CA * TP
BETA(I)=ATAN(TALPHB) +ALPHA
TAU(I)= R(I) / DA(SAP−SA)
GAMA(I)= PI/2 − ALPHA+PHI/2
V(I)=2*DA*SIN(PHI(I)/2)
C(I)=Z(I) * SP / (CA*(SAP−SA))
VJ(I)= V(I)*COS(ALPHA +PHI(I)/2 −BETA(I)/2) / SIN(BETA(I)*.5)
VN(I)= V(I) * SIN(ALPHA +PHI(I)/2 − BETA(I)/2) / COS(BETA(I)*.5)
DMN(I)= 1.+COS(BETA(I)) / 2
DEN(I)= 1.0−COS(AT) / 2
DEJ(I)= 1.0+COS(AT) / 2
AT=2*(ALPHA+PHI(I)/2 −BETA(I)*.5)
DMJ(I)= 1.−COS(BETA(I)) / 2
(ALL PENTRAT (I,Z,R,TZ,PHI,BETA,TAU,C,VJ,PT)
Z(I+1)=Z(I)+DZ
TZ(I+1)=TZ(I)+DTZ
I=I+1
10

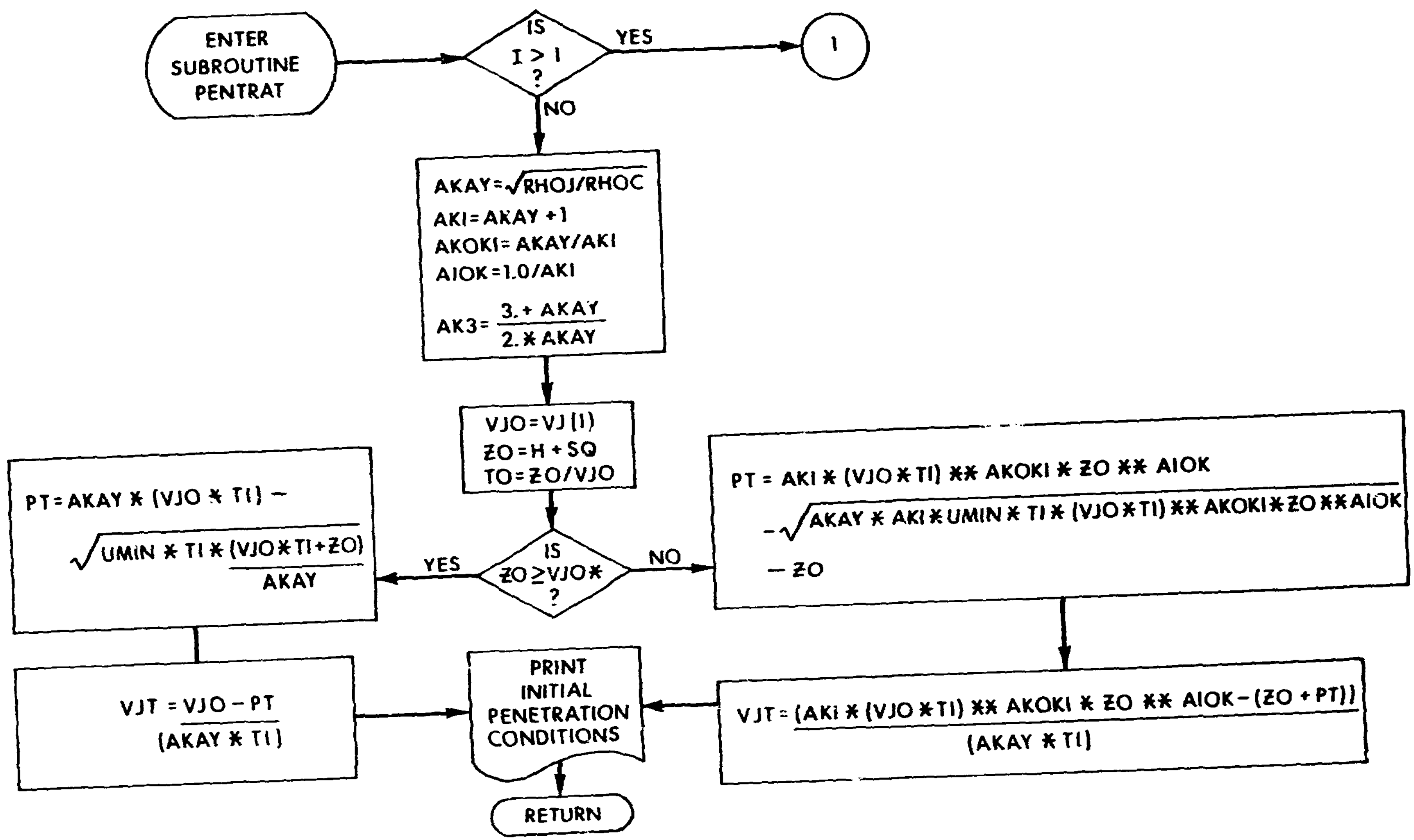
ENTER SUBROUTINE PENTRAT
IS I > 1 ?
YES
1
NO
AKAY=√RHOJ/RHOC
AKI=AKAY +1
AKOKI=AKAY/AKI
AIOK=1.0/AKI
AK3= 3.+AKAY / 2.*AKAY
VJO=VJ(I)
ZO=H+SQ
TO=ZO/VJO
IS ZO≥VJO* ?
YES
NO
PT=AKAY*(VJO*TI) − √UMIN*TI*(VJO*TI+ZO) / AKAY
PT = AKI*(VJO*TI)**AKOKI*ZO**AIOK − √AKAY*AKI*UMIN*TI*(VJO*TI)**AKOKI*ZO**AIOK − ZO
VJT = VJO − PT / (AKAY*TI)
VJT = (AKI*(VJO*TI)**AKOKI*ZO**AIOK−(ZO+PT)) / (AKAY*TI)
PRINT INITIAL PENETRATION CONDITIONS
RETURN

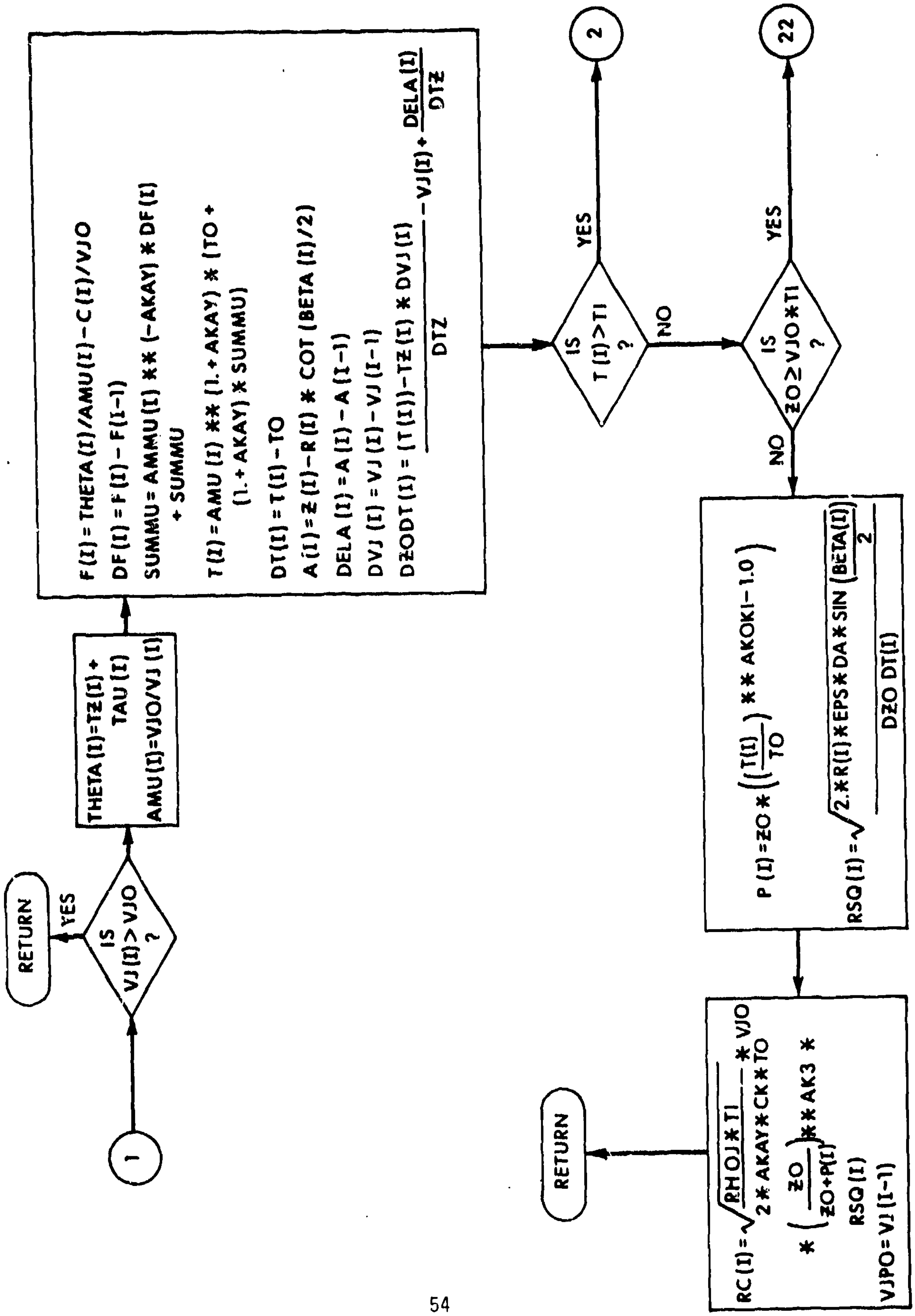
1
IS VJ(I) > VJO ?
YES
RETURN
THETA(I)=TZ(I)+TAU(I)
AMU(I)=VJO/VJ(I)
F(I) = THETA(I)/AMU(I) − C(I)/VJO
DF(I) = F(I) − F(I−1)
SUMMU = AMMU(I) ** (−AKAY) * DF(I) + SUMMU
T(I) = AMU(I) ** (1.+AKAY) * (TO + (1.+AKAY) * SUMMU)
DT(I) = T(I) − TO
A(I) = Z(I) − R(I) * COT (BETA(I)/2)
DELA(I) = A(I) − A(I−1)
DVJ(I) = VJ(I) − VJ(I−1)
DZODT(I) = (T(I)) − TZ(I) * DVJ(I) / DTZ − VJ(I) + DELA(I)/DTZ
IS T(I) > TI ?
YES
2
NO
IS ZO ≥ VJO*TI ?
YES
22
NO
P(I) = ZO * ((T(I)/TO) ** AKOKI − 1.0)
RSQ(I) = √(2.*R(I)*EPS*DA*SIN(BETA(I)/2)) / DZODT(I)
RC(I) = √(RHOJ*TI / 2*AKAY*CK*TO) * VJO * (ZO/ZO+P(I)) ** AK3 * RSQ(I)
VJPO = VJ(I−1)
RETURN

22

$$P(I) = \frac{VJO * (T(I) - TO * TI}{\dfrac{TI + T(I)}{AKAY}}$$

$$VJP = \frac{VJO * \left(TI + \dfrac{TO}{AKAY}\right)}{\dfrac{TI + T(i)}{AKAY}}$$

$$DVJP = VJP - VJPO$$

$$VJPO = VJP$$

$$DZODT(I) = \left(TI - T(I)\right) * DVJP - VJP + DELA(I)$$

$$RSQ(I) = \sqrt{\frac{2. * R(I) * EPS * DA * SIN\left(\dfrac{BETA(I)}{2}\right) ** 2}{DZODT(I)}}$$

$$RC(I) = \sqrt{\frac{RHOJ}{2. * AKAY * CK}} * RSQ(I) * VJO$$

RETURN

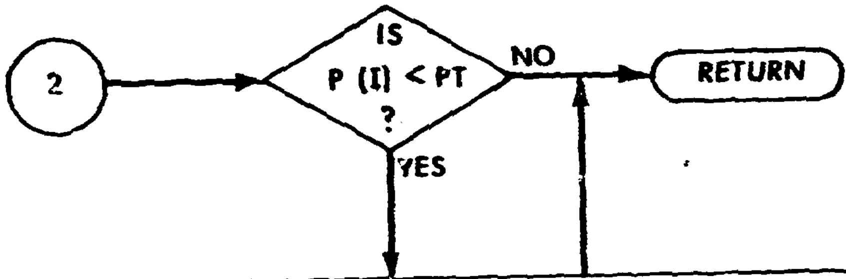

$$P(I) = \left(\frac{AKI * \left(\frac{TI}{TO}\right) ** AKOKI * T(I)}{T(I) + AKAY * TI} - 1.0 \right) * ZO$$

$$RSQ(I) = \sqrt{\frac{2. * R(I) * EPS * DA * SIN\left(\frac{BETA}{2}\right) ** 2}{DZODT(I)}}$$

$$RC(I) = \sqrt{\frac{RHOJ}{2 * AKAY * CK}} * \frac{VJO}{AKAY} * (AKI * \left(\frac{ZO}{VJO * TI}\right) ** AIOK - \frac{(ZO + P(I))}{VJO * TI}) * RSQ(I)$$

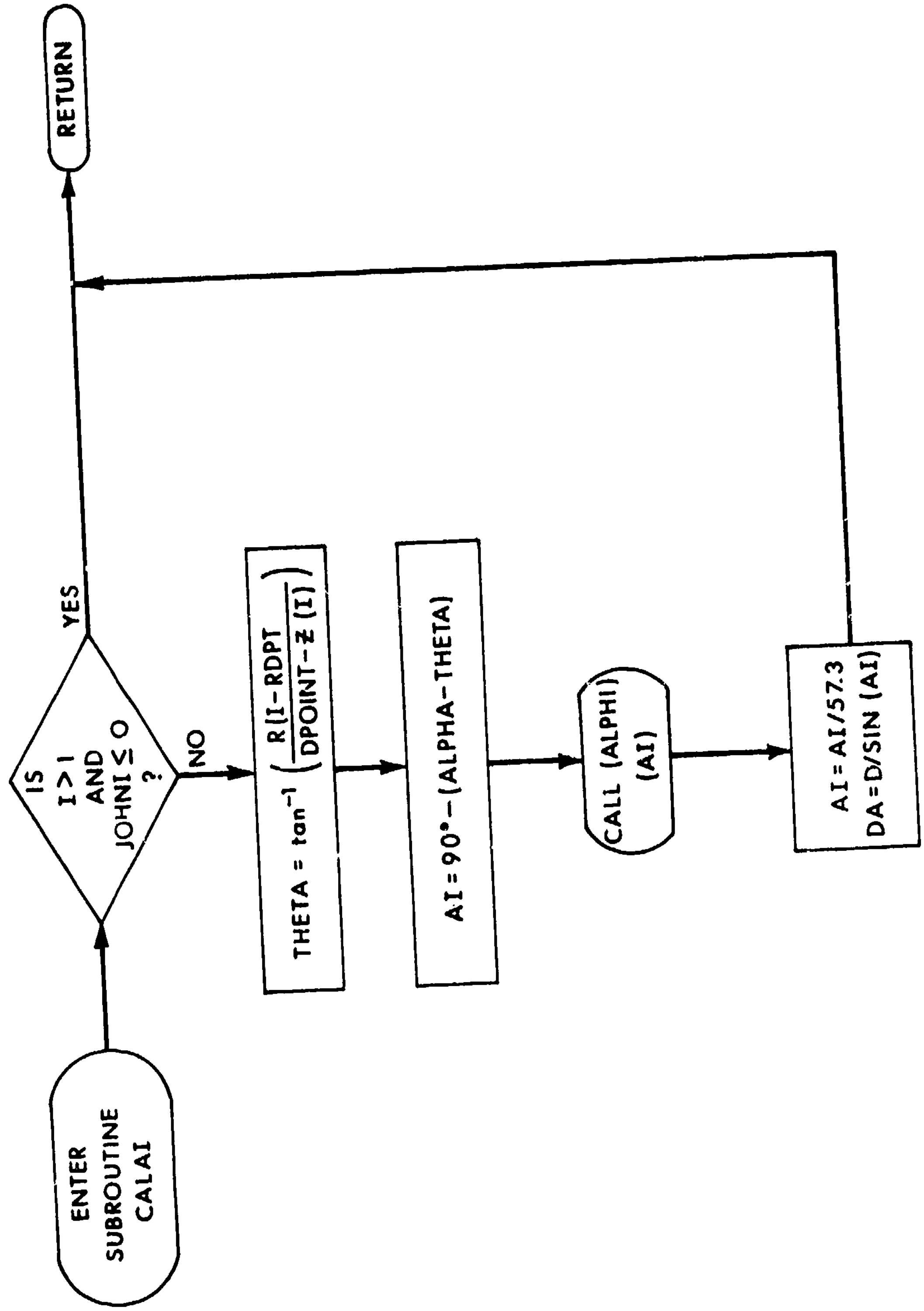
ENTER SUBROUTINE CALAI
IS I > 1 AND JOHNI ≤ O ?
YES
NO
RETURN
THETA = $\tan^{-1}\left(\frac{R(I-RDPT}{DPOINT-Z(I)}\right)$
AI = 90° − (ALPHA − THETA)
CALL (ALPHI) (AI)
AI = AI/57.3
DA = D/SIN (AI)

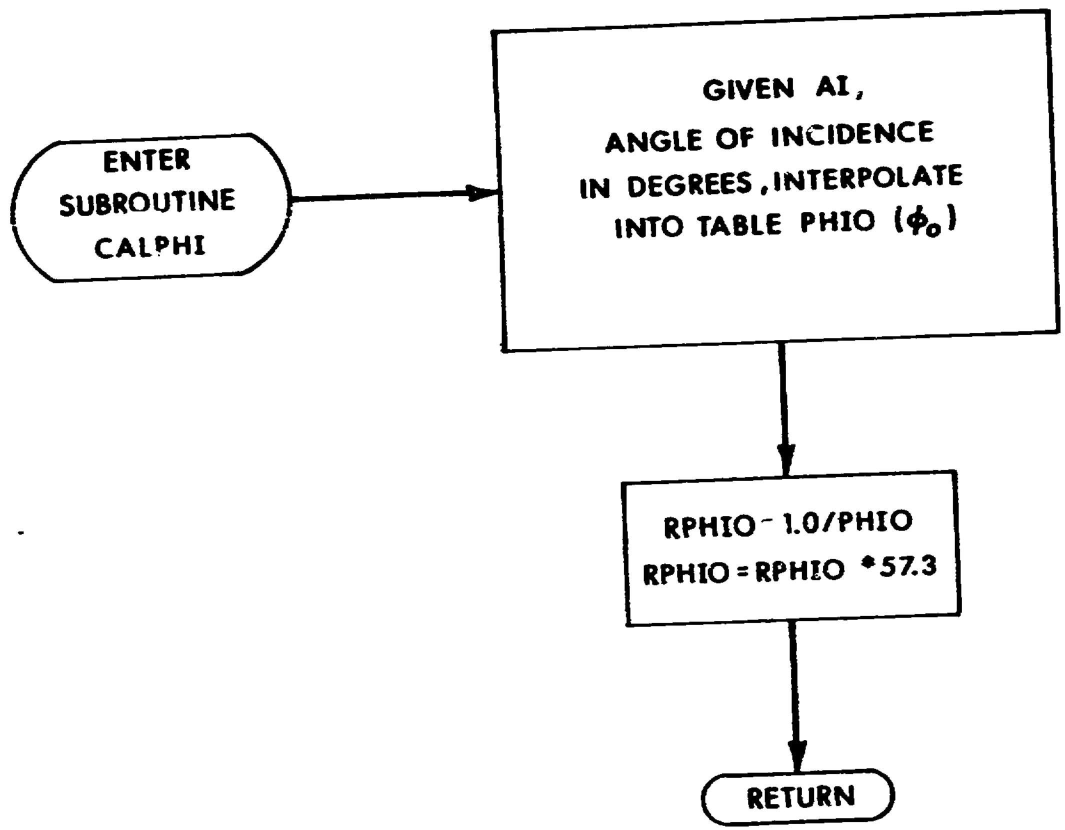
ENTER
SUBROUTINE
CALPHI
GIVEN AI,
ANGLE OF INCIDENCE
IN DEGREES, INTERPOLATE
INTO TABLE PHIO (ϕ_o)
RPHIO = 1.0/PHIO
RPHIO = RPHIO * 57.3
RETURN

APPENDIX B

FORTRAN IV

COMPUTER PROGRAM LISTING, SAMPLE INPUT AND OUTPUT

```
      PROGRAM RASC(INPUT,OUTPUT,TAPE5=INPUT,TAPE6=OUTPUT)
C     BRL ANALYTICAL SHAPED CHARGE (RASC)  CODE
C
C
C     PROGRAMMED BY JOHN T. HARRISON
C
C
C                       BRL ANALYTICAL SHAPED CHARGE CODE
C
C                       WRITTEN IN STANDARD FORTRAN IV
C     SEMI-EMPIRICAL CODE BASED ON THE FORMULA-
C
C                  1/PHI=1/PHI0+K*RHOJ*EPS/E
C
C
C     UNITS FOR THIS CODE ARE CENTAMETERS,GRAMS,AND MICROSECENDS.
C
C     THE CODE WILL CALCULATE COLLAPSE VELOCITY OF THE LINER AND
C          VELOCITIES,MASSES,AND ENERGIES OF BOTH THE JET AND SLUG.
C
C     THIS CODE WILL PREDICT PENETRATION AND HOLE PROFILE AND GIVE
C        PENETRATION-STANDOFF CURVES AND TABLES.
C
C                    LIST OF VARIABLES
C
C     ALRAD   =  ALPHA IN RADIANS
C     CON     =  DETONATION PRODUCTS CONSTANT (K).
C     DZ      =  DELTA Z DISTANCE ALONG THE LENGTH OF THE LINER
C     DT7     =  TIME THE DETONATION WAVE ARRIVES AT EACH Z POINT
C     AI      =  ANGLE OF INCIDENCE
C     Z(I)    =  DISTANCE ALONE LINER
C     TZ(I)   =  TIME AT EACH POINT ON LINER
C     GAMA(I)=  ANGLE BETWEEN AXIS AND COLLAPSE DIRECTION.
C     BETA(I)=  COLLAPSE ANGLE
C     V(I)    =  COLLAPSE VELOCITY
C     TAU(I)  =  TIME FOR EACH ELIMENT TO REACH THE AXIS
C     PHI(I)  =  ANGLE OF LINER BENDING.
C     PHI0    =  ANGLE OF EXPLOSIVE BENDING.
C     RPHI0   =   1/PHI0
C     RPHI    =  1/PHI
C     C(I)    =  POINT ON THE AXIS WHERE EACH PARTICLE WILL HIT
C     VJ(I)   = VELOCITY OF THE JET
C     VN(I)   =  VELOCITY OF THE SLUG
C     C0      =  SOUND SPEED OF LINER MATERIAL( COPPER C0=.395 CM/MSEC)
C     RV(I)   =  FLOW VELOCITY (VF). DIRECTED INTO STAGNATION POINT.
C     DEJ(I)  =  DELTA ENERGY IN EACH JET SEGMENT
C     DEN(I)  =  DELTA ENERGY IN EACH SLUG SEGMENT
C     R(I)    =  RADIUS OF THE CONE AT EACH DELTA Z DISTANCE
C     DA      = APARENT DETONATION RATE.
C     DML(I)  = DELTA MASS OF THE LINER
C     E(I)    =  AMOUNT OF EXPLOSIVE ABOVE EACH POSITION ON THE LINER
C     DPOINT =  INITIALLY IS THE TOTAL HEIGHT OF THE CHARGE. THEN BE-
C               COMES THE INITIATION POINT ON THE Z DIRECTION.
C     NRAD    =  RADIUS OF CURVATURE OF THE CONFINMENT.
C              IF NRAD=0.-THEN THERE WILL BE A LINEAR THICKNESS OF EXPLO
C
C                   INPUT PARAMETERS
```

```
C
C
C     CARD NUMBER 1
C
C
C     IJOHN  = 1, A PARAMETRIC STUDY,  2, A NEW CASE.
C
C     HEAD   =  A HEADING CARD.
C
C
C     CARD NUMBER 2
C
C     ALPHA  =  HALF ANGLE OF THE CONE IN DEGREES.
C     EPS    =  THICKNESS OF THE LINER,(0 IF UNKNOWN OR VARIABLE)
C     RHOJ   =  DENSITY OF THE LINER
C     RF     =  FINAL RADIUS OF THE CONE
C     H      =  HEIGHT OF THE CONE. IF H=0., THEN H WILL BE COMPUTED.
C     COF    = CONFINEMENT FACTOR(0 FOR UNCONFINED, IF CONFINED = THICKN
C     RHOCON = DENSITY OF THE CONFINEMENT
C     NPLT   = NUMBER OF PLOTS, 0=SKIP, 1=ALL, 2=VEL. + PENETRATION
C     NPOS   = NUMBER OF (R,Z) POSITIONS TO BE READ IN.
C              IF NPOS IS 0 DO NOT READ IN (R,Z) COORIDNATES.
C     CARD NUMBER 3
C
C     RHOC   =  DENSITY OF THE TARGET
C     SO     =  STAND OFF DISTANCE
C              IF SO= 0. PENATRATION STANDOFF CURVES WILL BE PLOTTED.
C     CK     =  CONSTANT FOR DETERMINING HOLE VOLUME
C               IF (CK =0.)  CK WILL BE CALCULATED AND UMIN WILL THEN
C               BECOME THE BHN TO BE READ IN.
C     UMIN   =  VELOCITY MIN. USED IN THE PENETRATION THEORY
C               IF(CK =0.) UMIN WILL BE THE BHN.
C     T1     =  BREAKUP TIME OF THE JET
C               IF( T1 = 0.) T1 WILL BE CALCULATED.
C     DPOINT = INITALLY IS THE TOTAL HEIGHT OF THE CHARGE
C     RDPT = RADIUS ABOVE AXIS WHERE EXPLOSIVE IS INITIATED.
C     NEXPL  = EQUATION OF STATE NUMBER FOR THE EXPLOSIVE.
C              NEXPL       EXPLOSIVE       DENSITY       DETONATION RATE
C               1             COMP B          1.72                 .8
C               2             OCTOL           1.82                 .85
C               3             LX              1.84                 .877
C     N      =  THE NUMBER OF ZONES Z-AXIS IS TO SUBDIVIDED. IF N=0 THE
C                   DEFAULT VALUE IS N=69.
C
C
      DIMENSION EXPLO(6), RHOHE(6), DV(6)
      DIMENSION RI(100),IMAT(100)
      DIMENSION EPSI(100), DAI(100)
      DIMENSION RP(300),PLOT(3)
      DIMENSION PSO(50), PPT(50)
      DIMENSION CONF(4)
      DIMENSION UJK(200), DMJK(200)
      DIMENSION HEAD(6)
      DIMENSION DML(100), RV(100), DEL(100)
      DIMENSION Z(100), TZ(100), TAU(100), E(100), PHI(100), DPHI(100),
     1  BETA(100), GAMA(100), R(100), C(100), VJ(100), VN(100), DMJ(100)
     2  , DMN(100), DEJ(100), DEN(100), RPHI(100), V(100)
```

```
C                                                                       MAIN114
C       COMMON                                                          MAIN115
C                                                                       MAIN116
        COMMON ALRAD, EPS, RHOJ, RHOC, RF, RPHI0, DTZ, SO, CK, DA, H, D,  MAIN117
      1  PT, DEGTOR                                                     MAIN118
        COMMON AMU(100), THETA(100), F(100), DF(100), T(100), DT(100),  MAIN119
      1  G(100), P(100), A(100), DELA(100), DVJ(100), DZODT(100),       MAIN120
      2  RSQ(100), RC(100), T1, UMIN                                    MAIN121
        COMMON /LPLOT/ Z, TZ, TAU, E, PHI, DPHI, BETA, GAMA, R, C, VJ, VN,MAIN122
      1  DMJ, DMN, DEJ, DEN, RPHI, V                                    MAIN123
C                                                                       MAIN124
        DATA HEAD(8) /1H>/                                              MAIN125D
        DATA CONF(1), CONF(2) /10HUNCONFINED, 1H>/                      MAIN126D
        DATA CONF(3), CONF(4) /10HCONFINED  , 1H>/                      MAIN127D
        DATA PLOT(1),PLOT(2),PLOT(3)/4HSKIP,3HALL,9HVEL + FEN/          MAIN129D
        DATA EXPLO(1) /6HCOMP B/ , EXPLO(2) /5HOCTOL/                   MAIN128D
        DATA EXPLO(3) /4H TNT/,EXPLO(4)/8HPBX-9404/,EXPLO(5)/4HLX14/    MAIN130D
        DATA EXPLO(6)/4H0280/                                           MAIN130E
        DATA RHOHE(1), RHOHE(2) /1.72, 1.82/                            MAIN131D
        DATA RHOHE(3) /1.63/, RHOHE(4)/1.84/,RHOHE(5)/1.81/,RHOHE(6)/1.74/MAIN132D
        DATA DV(1), DV(2) ,DV(3),DV(4)/.798,.848,.690,.880/             MAIN133D
        DATA DV(5),DV(6)/.8749,.8477/                                   MAIN134D
C        *************************************************************MAIN135
C       READ IN HEADING ONE TIME FOR EACH PARAMETRIC STUDY              MAIN136
C                                                                       MAIN137
      1 CONTINUE                                                        MAIN138
        READ (5,37) IJOHN,HEAD                                          MAIN139R
        IF(EOF(5))  98765,2                                             MAIN139A
      2 WRITE (6,36) IJOHN,HEAD                                         MAIN140R
C                                                                       MAIN141
C       BEGIN LOOP FOR A PARAMETRIC STUDY                               MAIN142
C                                                                       MAIN143
C                                                                       MAIN145
C       READ IN INPUT  ( 2  CARDS.   BOTH WITH  7E10.3,2I5 FORMAT.)     MAIN146
C                                                                       MAIN147
C                                                                       MAIN148
C       READ IN LINER AND CONFINEMENT INPUTS                            MAIN149
C                                                                       MAIN150
        READ (5,36) ALPHA,EPS,RHOJ,RF,H,COF,RHOCON,NPLT,NFCS            MAIN151R
C                                                                       MAIN152
C       READ IN TARGET AND EXPLOSIVE INPUTS                             MAIN153
C                                                                       MAIN154
        READ (5,36) RHOC,SO,CK,UMIN,T1,DPOINT,RDPT,NEXPL,N              MAIN155R
        SH=H                                                            MAIN156
        CO=.395                                                         MAIN156A
        TMJJ=0.                                                         MAIN156B
        JOHNI=1                                                         MAIN157
        TECUT1=0.                                                       MAIN157A
        TECUT2=0.                                                       MAIN157B
        TECUT3=0.                                                       MAIN157C
        TECUT4=0.                                                       MAIN157D
        TECUT5=0.                                                       MAIN157E
        TMJCUT=0.                                                       MAIN157F
        TMCUT1=0.                                                       MAIN157G
        TMCUT2=0.                                                       MAIN157H
        TMCUT3=0.                                                       MAIN157I
        TMCUT4=0.                                                       MAIN157J
```

```
      TMCUTS=0.
      RVMAX=0.
      NRAD=0
      D=DV(NEXPL)
      ICOF=1
      IF (COF.GT.0.) ICOF=3
      CON=.78
      IS=2
      IF (N.EQ.0) N=69
      IERROR=0
      RAD=FLOAT(NRAD)
      VJO=0.
      TMLL=0.
      TMJ=0
      TEJ=0.
      TKE=0.
      TMN=0.
      TML=0.
      SUMVJ=0.
      VJMAX=0.
      UJKMAX=0.
      TMASS=0.0
      DMASS=0.
      DMJTE=0.
      DO 3 J=1,1400
      Z(J)=0.
    3 AMU(J)=0.
C
C     CONVERT ANGLE ALPHA FROM DEGREES TO RADIANS.
C
      PI=3.14159265389793
      DEGTOR=57.2957795131
      ALRAD=ALPHA/DEGTOR
      TRRF=TAN(.5*ALRAD)
C     COMPUTE THE HEIGHT OF THE LINER IF NO GIVEN IN INPUT.
C
      IF (H.LE.0.) H=RF/TAN(ALRAD)
C
      DZ=H/FLOAT(N)
      DTZ=DZ/D
C     SET UP CONSTANTS TO BE IN LATER EQUATIONS.
      RHOE=CON*RHOJ*EPS
      SA=SIN(ALRAD)
      CA=COS(ALRAD)
      TA=TAN(ALRAD)
      IF (RF.LE.0.) RF=TA*H
      PIPS=PI/3.
      PIP =2.0*PI
      SIGMA=RHOJ*EPS
C
C     DETONATION POINT IS THE HEIGHT OF THE CHARGE - HEIGHT OF THE CONE.
C
C     DPOINT=DP[illegible]NT-H
      IF (DPOINT.[illegible].0.) DPOINT=2.*RF
      IF (COF.GT.0.) CONFTK=COF
      DELCOF=CONFTK/20.
C
```

```
C      COF - CONFINEMENT FACTOR (INCREASE IN EXPLOSIVE THICKNESS).        MAIN209
C                                                                         MAIN210
       COF=1.+.64*RHOCON*CONFTK*8.9*.1778/(7.8*.60198*RHOJ*EPS)*2.4003*RFMAIN211
      1  /(DPOINT*2.0553)                                                 MAIN212
       WRITE (6,28) ALPHA,CON,EPS,RHOJ,CONF(ICOF),CONFTK,RHOCON,COF,H,RF,MAIN213W
      1  DZ,DTZ,N                                                         MAIN214W
       WRITE (6,29) EXPLO(NEXPL),D,RHOHE(NEXPL),DPOINT,RDPT,RHUC,SO,      MAIN215W
      1  VMIN,PLOT(NPLT+1)                                                MAIN216W
       RRF=RF                                                             MAIN217
       PHI(1)=3.0/DEGTOR                                                  MAIN218
C      INITIAL TIME OF COLLAPSE      TW=TAU.                              MAIN219
       TW=.1                                                              MAIN220
C      CONTANT  FOR THE ACCELERATION ROUTINE.                             MAIN221
       C1=2.*CO*EPS*RHOJ/(.392*.269*8.9)                                  MAIN221A
       FTERR=.000001                                                      MAIN222
C                                                                         MAIN223
C      SETUP ROUTINE                                                      MAIN224
C                                                                         MAIN225
C      SETUP INITIAL POSITIONS (R,Z)                                      MAIN226
C                                                                         MAIN227
C      RI- INSIDE RADIUS OF THE CONE.   R - OUTSIDE RADIUS OF THE CONE.   MAIN228
C                                                                         MAIN229
       X=EPS/CA                                                           MAIN230
C                                                                         MAIN231
C      THIS IS A SETUP ROUTINE FOR A SHAPED CHAGE LINER WITH CONSTANT EPSMAIN232
C                                                                         MAIN233
       IF (NPOS.EQ.0) NPOS=1                                              MAIN234
       NPOS=NPOS+1                                                        MAIN235
       WRITE (6,27)                                                       MAIN236W
       IF (NPOS.GE.N) GO TO 5                                             MAIN237
       DO 4 J=NPOS,N                                                      MAIN238
       Z(J)=Z(J-1)+DZ                                                     MAIN239
       IMAT(J)=1                                                          MAIN239A
       R(J)=Z(J)*TA                                                       MAIN240
       RI(J)=R(J)-X                                                       MAIN241
       IF (RI(J).LE.0.) RI(J)=0.                                          MAIN242
       IF (RI(J).LE.0.) IS=J+1                                            MAIN242A
       IF(ABS(RI(J)-0.0).LE..0001) RI(J)=0.0                              MAIN242B
     4 CONTINUE                                                           MAIN243
     5 CONTINUE                                                           MAIN244
       WRITE (6,31)                                                       MAIN245W
       WRITE (6,34) (I,Z(I),I=1,N)                                        MAIN246W
       WRITE (6,32)                                                       MAIN247W
       WRITE (6,34) (I,R(I),I=1,N)                                        MAIN248W
       WRITE (6,33)                                                       MAIN249W
       WRITE (6,34) (I,RI(I),I=1,N)                                       MAIN250W
C                                                                         MAIN251
C                                                                         MAIN252
C      END OF SETUP ROUTINE                                               MAIN253
C                                                                         MAIN254
       TZ(1)=DPOINT/D                                                     MAIN255
       EPSI(1)=EPS                                                        MAIN255A
C                                                                         MAIN256
C      START SPACE + TIME ITERATION.                                      MAIN257
C                                                                         MAIN258
       DO 10 I=2,N                                                        MAIN259
       V(I)=0.                                                            MAIN260
```

```
      VN(I)=0.                                                          MAIN261
      VJ(I)=0.                                                          MAIN262
      UJK(I)=0.                                                         MAIN263
C     FIND HALF APEX ANGLE-ALPHA                                        MAIN266
      DZ=Z(I)-Z(I-1)                                                    MAIN267
      DR=R(I)-R(I-1)                                                    MAIN268
      ALRAD=ATAN2(DR,DZ)                                                MAIN269
      SA=SIN(ALRAD)                                                     MAIN270
      CA=COS(ALRAD)                                                     MAIN271
      TA=TAN(ALRAD)                                                     MAIN272
      IF(IMAT(I).EQ.1) CO=.392                                          MAIN273
      IF(IMAT(I).EQ.1) RHOJ=8.9                                         MAIN273A
      EPS=(R(I)-RI(I))*CA                                               MAIN274
C                                                                       MAIN275
C     GO TO SUBROUTINE CALAI TO CALCULATE INCLINATION ANGLE (AI),       MAIN276
C     (DA)-DETONATION COMPONENT TO VELOCITY, AND (RPHIO)-1./PHIO.       MAIN277
C                                                                       MAIN278
      CALL CALAI (I,Z,R,DPOINT,RDPT,JOHNI,AI)                           MAIN279
      DAI(I)=DA                                                         MAIN280
C                                                                       MAIN281
C     COF IS FACTOR FOR CONFINEMENT.                                    MAIN282
C                                                                       MAIN283
C                                                                       MAIN284
C     IF RAD IS GIVEN NO EQ. 0. CLACULATE CURVED THICKNESS OF EXPLOSIVE.MAIN285
C                                                                       MAIN286
      IF (RAD.GT.0.) E(I)=SQRT(ABS(RAD**2-(H-Z(I))**2))-RAD+(H-Z(I))*TA MAIN287
C                                                                       MAIN288
C     CALCULATE EXPLOSIVE THICKNESS                                     MAIN289
      E(I)=COF*(RF-R(I))+(COF-1.)*RHOCON*CONFTK/7.8                     MAIN290
C     CALCULATE  1./PHI                                                 MAIN291
C                                                                       MAIN292
      TZ(I)=Z(I)/(DA*CA)                                                MAIN293
      TZ(I)=TZ(I)+TZ(1)                                                 MAIN294
      THE90=.5*PI-AI                                                    MAIN295
      THE=ALRAD-THE90                                                   MAIN296
      EPSI(I)=EPS/COS(THE90)                                            MAIN297
      E(I)=E(I)/COS(THE)                                                MAIN298
      RHOE=CON*RHOJ*EPSI(I)                                             MAIN299
      CONE=RHOE*C1                                                      MAIN300
      RPHI(I)=RPHIO+RHOE/E(I)                                           MAIN301
C                                                                       MAIN302
C     SUBROUTINE TO CALCULATE THE ACCELERATION OF THE LINER.            MAIN303
C                                                                       MAIN304
C     ROUTINE WILL ITERATE ON TAU AND PHI.                              MAIN305
C                                                                       MAIN306
      DO 6 J=1,300                                                      MAIN307
      CT=EXP((SQRT(CONE/(E(I)*TW))))                                    MAIN308
      RP(J)=RPHI(I)*CT                                                  MAIN309
      TW=R(I)/(DA*(SIN(ALRAD+1.0/RP(J))-SA))                            MAIN310
      IF (J.EQ.1) GO TO 6                                               MAIN311
      IF (ABS(RP(J)-RP(J-1)).LE.ETERM) GO TO 7                          MAIN312
    6 CONTINUE                                                          MAIN315
C                                                                       MAIN316
C     END ITERATIVE PROCESS                                             MAIN317
C                                                                       MAIN318
      J=J-1                                                             MAIN319
    7 CONTINUE                                                          MAIN320
```

```
C
C     THE END OF THE INVERSE VELOCITY GRADIENT SUBROUTINE.
C
      TAU(I)=TW
      RPHI(I)=RP(J)
C
      PHI(I)=1.0/RPHI(I)
      DPHI(I)=ABS(PHI(I-1)-PHI(I))
      IF(PI(I).LE.0.0) GO TO 10
      SP=SIN(PHI(I))
      TP=TAN(PHI(I))
      SAP=SIN(ALRAD+PHI(I))
C     CALCULATE  TAN(BETA-ALPHA)
C
      TALPHAB=(DZ*(SAP-SA)*TP+R(I)*DPHI(I)*CA)/(DZ*(SAP-SA)-R(I)*DPHI(I)
     1  *CA*TP)
C
C     SOLVE FOR THE ANGLE BETA IN RADIANS.
C
      BETA(I)=ATAN(TALPHAB)+ALRAD
      IF (I.EQ.1) BETA(I)=ALRAD+PHI(I)
C
C     SOLVE FOR THE POINT OF COLLAPSE ON THE AXIS, STAGNATION POINT +SP,
      C(I)=Z(I)*SP/(CA*(SAP-SA))
C     SOLVE FOR COLLAPSE VELOCITY
      V(I)=2.0*DA*SIN(PHI(I)*.5)
      GAMA(I)=.5*PI-(ALRAD+.5*PHI(I))
      VJ(I)=V(I)*COS(ALRAD+.5*PHI(I)-.5*BETA(I))/SIN(.5*BETA(I))
      VN(I)=V(I)*SIN(ALRAD+.5*PHI(I)-.5*BETA(I))/COS(.5*BETA(I))
      DML(I)=PIP *EPS*R(I)*DZ/CA
      DML(I)=DML(I)*RHOJ
      DLMASS=DML(I)
      DMN(I)=.5*(1.+COS(BETA(I)))
      DMJ(I)=.5*(1.-COS(BETA(I)))
      AT=2.*(ALRAD+.5*PHI(I)-.5*BETA(I))
      DEJ(I)=.5*(1.+COS(AT))
      DEN(I)=.5*(1.-COS(AT))
C
C     COMPUTE THE RELATIVE VELOCITY OF THE JET AND SLUG.
C     THIS IS THE FLOW VELOCITY. (VF).
      RV(I)=.5*(VJ(I)-VN(I))
      IF(RV(I).GT.RVMAX) RVMAX=RV(I)
C
      TML=TML+DML(I)
      TMJ=TMJ+DMJ(I)*DML(I)
C     IF THE FLOW VELOCITY IS GREATER THAN 1.23*CO, REMOVE MASS FROM JET
      IF(RV(I)/CO.GT.1.23) TMJ=0.
C     ALSO REMOVE KINETIC ENERGY FOR JET.
      IF(RV(I)/CO.GT.1.23)TEJ=0.
      TMN=TMN+DMN(I)*DML(I)
      DMJK(I)=DMJ(I)*DML(I)
      DEL(I)=.5*DML(I)*V(I)**2
      TKE=TKE+DEL(I)
      TEJ=TEJ+DEJ(I)*DEL(I)
      UJK(I)=VJ(I)
      IF (VJ(I).LE.VJMAX) GO TO 9
      VJMAX=VJ(I)
```

```
      DMJTE=DMJTE+DMJK(I)                                               MAIN370
      SUMVJ=SUMVJ+VJ(I)*DMJK(I)                                         MAIN371
      VJTE=SUMVJ/DMJTE                                                  MAIN372
      MM=I                                                              MAIN373
    9 CONTINUE                                                          MAIN374
   10 CONTINUE                                                          MAIN375
C     END OF TIME AND SPACE INCREMENT ALONG THE HEIGHT OF THE LINER.    MAIN376
C                                                                       MAIN377
C                                                                       MAIN378
C     CALL SUBROUTINE TO COMPRESS THE JET AND CALCULATE NEW JET VELOCITYMAIN379
C                                                                       MAIN380
      CALL VELGR (N,UJK,DMJK,IS)                                        MAIN381
      TEJCUT=0.                                                         MAIN382
      DO 12 I=IS,N                                                      MAIN383
      IF(UJK(I).GE..5) TMCUT1=TMCUT1+DMJK(I)                            MAIN383A
      IF(UJK(I).GE..4) TMCUT2=TMCUT2+DMJK(I)                            MAIN383B
      IF(UJK(I).GE..3) TMCUT3=TMCUT3+DMJK(I)                            MAIN383C
      IF(UJK(I).GE..2) TMCUT4=TMCUT4+DMJK(I)                            MAIN383D
      IF(UJK(I).GE..1) TMCUT5=TMCUT5+DMJK(I)                            MAIN383E
      IF (UJK(I).GE..25) TMJCUT=TMJCUT+DMJK(I)                          MAIN383F
      IF (UJK(I).GE..25) TEJCUT=TEJCUT+DEJ(I)*DEL(I)                    MAIN384
      IF(UJK(I).GE..5) TECUT1=TECUT1+DEJ(I)*DEL(I)                      MAIN384A
      IF(UJK(I).GE..4) TECUT2=TECUT2+DEJ(I)*DEL(I)                      MAIN384B
      IF(UJK(I).GE..3) TECUT3=TECUT3+DEJ(I)*DEL(I)                      MAIN384C
      IF(UJK(I).GE..2) TECUT4=TECUT4+DEJ(I)*DEL(I)                      MAIN384D
      IF(UJK(I).GE..1) TECUT5=TECUT5+DEJ(I)*DEL(I)                      MAIN384E
      IF (UJK(I).LE.UJKMAX) GO TO 11                                    MAIN385
      IF(RV(I)/CO.GT.1.23) TEJCUT=0.                                    MAIN385A
      IF(RV(I)/CO.GT.1.23) TMJCUT=0.                                    MAIN385B
      IF(RV(I)/CO.GT.1.23) TECUT1=0.                                    MAIN385C
      IF(RV(I)/CO.GT.1.23) TECUT2=0.                                    MAIN385D
      IF(RV(I)/CO.GT.1.23) TECUT3=0.                                    MAIN385E
      IF(RV(I)/CO.GT.1.23) TECUT4=0.                                    MAIN385F
      IF(RV(I)/CO.GT.1.23) TECUT5=0.                                    MAIN385G
      IF(RV(I)/CO.GT.1.23) TMCUT5=0.                                    MAIN385H
      IF(RV(I)/CO.GT.1.23) TMCUT4=0.                                    MAIN385I
      IF(RV(I)/CO.GT.1.23) TMCUT3=0.                                    MAIN385J
      IF(RV(I)/CO.GT.1.23) TMCUT2=0.                                    MAIN385K
      IF(RV(I)/CO.GT.1.23) TMCUT1=0.                                    MAIN385L
      TMASS=TMASS+DMJK(I)                                               MAIN386
      UJKMAX=UJK(I)                                                     MAIN387
      MN=I                                                              MAIN388
   11 CONTINUE                                                          MAIN389
      IF(RV(I)/CO.GT.1.23) TMASS=DMJK(I+1)                              MAIN389A
      IF(RV(I)/CO.GT.1.23) UJKMAX=UJK(I+1)                              MAIN389B
      IF(RV(I)/CO.GT.1.23)  MN=I+1                                      MAIN389C
   12 CONTINUE                                                          MAIN390
      N1=1                                                              MAIN391
      N2=N                                                              MAIN392
      IF (N.GE.57) N2=57                                                MAIN393
   13 CONTINUE                                                          MAIN394
      WRITE (6,23)                                                      MAIN395*
      WRITE (6,24)                                                      MAIN396*
      DO 14 I=N1,N2                                                     MAIN397
      PHI(I)=PHI(I)*DEGTOR                                              MAIN398
      BETA(I)=BETA(I)*DEGTOR                                            MAIN399
      GAMA(I)=GAMA(I)*DEGTOR                                            MAIN400
```

```
      DPHI(I)=DPHI(I)*DEGTOR                                            MAIN401
      Z(I)=Z(I)/H                                                       MAIN402
      WRITE (6,23) I,Z(I),TZ(I),EPSI(I),E(I),PHI(I),BETA(I),DPHI(I),   MAIN403W
     1  RPHI(I),V(I),R(I),TAU(I),C(I)                                   MAIN404W
      BETA(I)=BETA(I)/DEGTOR                                            MAIN405
   14 CONTINUE                                                          MAIN406
      IF (N.LE.N2) GO TO 15                                             MAIN407
      N1=N2+1                                                           MAIN408
      N2=N                                                              MAIN409
      GO TO 13                                                          MAIN410
   15 CONTINUE                                                          MAIN411
      TMJ=0.0                                                           MAIN411A
      N1=1                                                              MAIN412
      N2=N                                                              MAIN413
      IF (N.GE.57) N2=57                                                MAIN414
   16 CONTINUE                                                          MAIN415
      WRITE (6,23)                                                      MAIN416W
      WRITE (6,25)                                                      MAIN417W
      DO 17 I=N1,N2                                                     MAIN418
      TMJ=TMJ+DMJK(I)                                                   MAIN418A
      IF(RV(I)/CO.GT.1.23)TMJ=0.                                        MAIN418B
      WRITE (6,23) I,Z(I),VJ(I),VN(I),RV(I),DMJ(I),DMN(I),DEL(I),DML(I),MAIN419W
     1DMJK(I),TMJ                                                       MAIN420W
C                                                                       MAIN421
      Z(I)=Z(I)*H                                                       MAIN421A
   17 CONTINUE                                                          MAIN422
      IF (N.LE.N2) GO TO 18                                             MAIN423
      N1=N2+1                                                           MAIN424
      N2=N                                                              MAIN425
      GO TO 16                                                          MAIN426
   18 CONTINUE                                                          MAIN427
      IF (IERROR.EQ.1) GO TO 20                                         MAIN427A
      IF(RHOC.EQ.0.0) GO TO 20                                          MAIN428
C     CALL PENETRATION SUBROUTINE CALCULATES JET RADIUS,DEPTH OF        MAIN429
C        PENETRATION, HOLE RADIUS.,AND ALSO PENETRATION STANDOFF CURVES.MAIN430
C                                                                       MAIN431
      CALL PENTRAT (N,Z,R,TZ,DMJ,BETA,TAU,C,UJK,RV,VJO,DMASS,MN,HEAD,PSOMAIN432
     1,PPT,NCD,EPSI,DAI)                                                MAIN433
C                                                                       MAIN434
C                                                                       MAIN435
      DO 19 I=1,N                                                       MAIN436
C     CONVERT VELOCITIES TO (MM/MICROSEC) FOR PLOTTING AND REPORTS.     MAIN437
C     ALSO CONVERT DISTANCES TO MM.                                     MAIN438
C                                                                       MAIN439
      BETA(I)=BETA(I)*DEGTOR                                            MAIN440
      VJ(I)=VJ(I)*10.                                                   MAIN441
      V(I)=V(I)*10.                                                     MAIN442
      C(I)=C(I)*10.                                                     MAIN443
      UJK(I)=10.*UJK(I)                                                 MAIN444
      Z(I)=Z(I)/H                                                       MAIN444A
   19 CONTINUE                                                          MAIN445
      IF (NPLT.EQ.0) GO TO 20                                           MAIN446
      CALL PLOTS (N,UJK,DPOINT,RDPT,HEAD,PSO,PPT,NCD,NPLT,IS)           MAIN447
   20 CONTINUE                                                          MAIN448
      UJKMAX=UJKMAX*10.                                                 MAIN449
C     PRINT SUMMARY OF RESULTS                                          MAIN450
C                                                                       MAIN451
```

```
      WRITE (6,39) HEAD                                                  MAIN452W
      WRITE (6,30) TML,TMJ,TMN,TKE,TEJ,TEJCUT,TMJCUT                     MAIN453W
      AMMACH=RVMAX/CO                                                    MAIN453A
      WRITE(6,41) TECUT1,TMCUT1,TECUT2,TMCUT2,TECUT3,TMCUT3,             MAIN454W
     1TECUT4,TMCUT4,TECUT5,TMCUT5,AMMACH                                 MAIN454A
      WRITE (6,35) MN,Z(MN),UJKMAX,TMASS                                 MAIN455W
      NPOS=0                                                             MAIN455A
      IF (IJOHN.GT.1) GO TO 1                                            MAIN456
      GO TO 2                                                            MAIN457
98765 WRITE (6,40)                                                       MAIN459W
      WRITE (6,23) I,TW,RP(J),RPHI(I),CT,BETA(I)                         MAIN460W
      IERROR=1                                                           MAIN461
      STOP                                                               MAIN462
C                                                                        MAIN463
C     FORMATS                                                            MAIN464
C                                                                        MAIN465
   23 FORMAT (I4,2X,1P12E10.3)                                           MAIN466
   24 FORMAT (2H1I,5X,2H Z,8X,2HTZ,8X,3HEPS,7X,2H E,6X,3HPHI,7X,4HBETA,6MAIN467
     1X,4HDPHI,6X,4HRPHI,6X,4H   V,6X,4H  R ,6X,4H TAU,6X,4H   C/)     MAIN468
   25 FORMAT (2H1I,6X,1HZ,8X,3H VJ,8X,2HVN,7X,3H RV,7X,3HDMJ,7X,3HDMN,7XMAIN469
     1,3HDEL,7X,3HDML,7X,4HDMJK,9X,3HTMJ/)                               MAIN470
   26 FORMAT (8E10.4)                                                    MAIN471
   27 FORMAT(1H1/'     INITIAL POSITION'/)                               MAIN472
   28 FORMAT(  ////50X,'INPUT PARAMETERS'//,5X,' ALPHA = ',F6.3,7X,'K COMAIN473
     1NSTANT = ',F6.3,7X,'THICKNESS OF LINER = ',F6.3,7X,' DENSITY = ', MAIN474
     2F6.3//5X,A10,5X,' THICKNESS = ',F6.3,7X,' DENSITY = ',F6.3,5X,'FACMAIN475
     3TOP = ',F6.4//5X,'LINER HEIGHT = ',F10.4,7X,'LINER RADIUS =',F10.4MAIN476
     4,//5X,' INCREMENT OF Z (DZ) = ',F10.4,7X,' INCREMENT OF TIME (DTZ)MAIN477
     5 =',F10.4,7X,'NUMBER OF ELEMENTS (N) = ',I4,//50X,'DETONATION'//) MAIN478
   29 FORMAT(5X,'EXPLOSIVE = ',5X,A10,3X,'DETONATION VELOCITY(D) = ',   MAIN479
     1F10.5,5X,'EXPLOSIVE DENSITY = 'F6.3//5X,'POINT OF DETONATION FROM MAIN480
     2CONE APEX(DPOINT) = ',F10.4,7X,'DET. RADIUS (RDPT) = ',F10.4//50X,MAIN481
     3'TARGET INPUTS'//5X,'TARGET DENSITY = ',F7.3,7X,'STAND-OFF DISTANCMAIN482
     4E = ',F7.3,7X,'CK CONSTANT(BHN) = ',F10.6//50X'MISC. INPUTS'//5X, MAIN483
     5A10,'PLOTS')                                                       MAIN484
   30 FORMAT(///////////,30X,'     SUMMARY OF RESULTS'/////' LINER MASS ='MAIN485
     1,F10.4,' GM    ',5X,'JET MASS = ',F10.4,' GM    ',5X,'SLUG MASS = ',MAIN486
     2F10.4,' GM    '//' TOTAL KINETIC ENERGY = ',F10.4,' ERGS*1.0E12'//'MAIN487
     3 TOTAL JET KINETIC ENERGY = ',F10.4,' ERGS*1.0E12'//' TOTAL JET KIMAIN488
     4NETIC ENERGY ABOVE JET VELOCITY .25 CM/MSEC = ',F10.4,' ERGS*1.0E1MAIN488A
     52'//' TOTAL JET MASS ABOVE JET VELOCITY .25 CM/MSEC = ',F10.4,' GMMAIN488B
     6   '//)                                                            MAIN488C
   31 FORMAT (//7(2H  I,6X,2H Z,7X))                                     MAIN489
   32 FORMAT (//7(3H  I,6X,2H R,7X))                                     MAIN490
   33 FORMAT (//7(3H  I,6X,2HPI,7X))                                     MAIN491
   34 FORMAT (7(I4,4X,F7.4,3X))                                          MAIN492
   35 FORMAT(' JET TIP AT I = ',I5,'    RELATIVE POSITION Z/H = ',F10.8//MAIN493
     1' MEASURED JET TIP VELOCITY = ',F10.8,' MM/MICROSEC'//' MEASURED MMAIN494
     2ASS OF JET TIP = ',F10.4,' GM    '/1H1)                            MAIN494A
   36 FORMAT (7E10.3,2I5)                                                MAIN495
   37 FORMAT (I1,8A10)                                                   MAIN496
   38 FORMAT (I1,30X,8A10)                                               MAIN497
   39 FORMAT (1H1,30X,8A10)                                              MAIN498
   40 FORMAT ('ERROR')                                                   MAIN499
   41 FORMAT(/' KINETIC ENERGY ABOVE .5 CM/MSEC = ',F10.4,                MAIN500
     1'          AND JET MASS = ',F10.4/                                 MAIN501
     2         ' KINETIC ENERGY ABOVE .4 CM/MSEC = ',F10.4,              MAIN502
     3'          AND JET MASS = ',F10.4/                                 MAIN503
     4         ' KINETIC ENERGY ABOVE .3 CM/MSEC = ',F10.4,              MAIN504
     5'          AND JET MASS = ',F10.4/                                 MAIN505
     6         ' KINETIC ENERGY ABOVE .2 CM/MSEC = ',F10.4,              MAIN506
     7'          AND JET MASS = ',F10.4/                                 MAIN507
     8         ' KINETIC ENERGY ABOVE .1 CM/MSEC = ',F10.4,              MAIN508
     9'          AND JET MASS = ',F10.4//                                MAIN509
     A         ' MAXIMUM RELATIVE MACH NUMBER = ',F10.4/)                MAIN510
      END                                                                MAIN511
```

```
      SUBROUTINE PENTRAT (N,Z,R,TZ,DMJ,BETA,TAU,C,VJ,RV,VJO,DMASS,MN,    * 511* 1
     1  HEAD,PSO,PPT,NCD,EPSI,DAI)                                       PENTT 2
C                                                                        PENTT 3
C     COMPUTE PENETRATION,RADIUS OF JET,RADIUS OF THE HOLE.              PENTT 4
C                                                                        PENTT 5
      DIMENSION HEAD(8)                                                  PENTT 6
      DIMENSION EPSI(100), DAI(100)                                      PENTT 7
      DIMENSION PPT(50), PSO(50), PVJT(50)                               PENTT 8
      DIMENSION Z(100), TZ(100), DMJ(100), BETA(100), TAU(100), C(100),  PENTT 9
     1  VJ(100), R(100), RV(100)                                         PENTT10
C                                                                        PENTT11
C     COMMON                                                             PENTT12
C                                                                        PENTT13
      COMMON ALRAD, EPS, RHOJ, RHOC, RF, RPHIO, DTZ, SO, CK, DA, H, D,   PENTT14
     1  PT, DEGTOR                                                       PENTT15
      COMMON AMU(100), THETA(100), F(100), DF(100), T(100), DT(100),     PENTT16
     1  G(100), P(100), A(100), DELA(100), DVJ(100),  ZDOT(100),         PENTT17
     2  RSQ(100), RC(100), T1, UMIN                                      PENTT18
C     PENETRATION PHASE                                                  PENTT19
      VJO=0.0                                                            PENTT19A
      DO 11 I=MN,N                                                       PENTT20
      EPS=EPSI(I)                                                        PENTT21
      DA=DAI(I)                                                          PENTT22
      IF (I.LE.MN) VJ(I)=VJ(MN)                                          PENTT23
      IF (I.EQ.1) RETURN                                                 PENTT24
      IF (VJO.GT.0.0) GO TO 4                                            PENTT25
      VJO=VJ(MN)                                                         PENTT26
      JC1=1                                                              PENTT27
      AKAY=SQRT(RHOJ/RHOC)                                               PENTT28
      AK1=AKAY+1.                                                        PENTT29
      AK3=(3.+AKAY)/(2.*AKAY)                                            PENTT30
      AKOK1=AKAY/AK1                                                     PENTT31
      A1OK=1./AK1                                                        PENTT32
      BHN=320.                                                           PENTT32A
      IF(UMIN.GT.1.0) BHN=UMIN                                           PENTT32B
      IF (CK.EQ.0.) CK=(2250.+4.20*BHN )*1.0E-5                          PENTT33
      IF(UMIN.GT.1.0)UMIN=(CK*1.0E5-1350.)/20400.                        PENTT34
C     T1=T1*(.7511-.28)/(VJO-.28)                                        PENTT35
      M=MN                                                               PENTT36
      A(I)=0.                                                            PENTT37
      DELA(I)=0.                                                         PENTT38
      DF(I)=0.                                                           PENTT39
      F(I)=0.                                                            PENTT40
      DVJ(I)=0.                                                          PENTT41
      SUMMU=0.                                                           PENTT42
      K=I-1                                                              PENTT42A
      TZ(K)=TZ(K)-TZ(1)                                                  PENTT42B
      DMASS=DMJ(K)                                                       PENTT42C
      IF (VJ(K).[illegible]E.0.0) VJ(K)=1.0E-02                          PENTT42D
      AMU(K)=V[illegible]J(K)                                            PENTT42E
      THETA(K)=[illegible]Y[illegible]TAU(K)                             PENTT42F
      F(K)=THETA(K)/AMU(K)-C(K)/VJO                                      PENTT42G
                      DF(K)=F(K)                                         PENTT42H
      SUMMU=AMU(K)**(-AKAY)*DF(K)+SUMMU                                  PENTT42I
      T(K)=AMU(K)**(1.+AKAY)*(TO-(1.+AKAY)*SUMMU)                        PENTT42J
      DT(K)=T(K)-TO                                                      PENTT42K
      G(K)=VJO*(T(K)/AMU(K)-F(K))                                        PENTT42L
```

```
                    A(K)=Z(K)-R(K)*COT(BETA(K)/2.)                       PENTT42M
                    DELA(K)=A(K)                                         PENTT42N
      VJ(K)=VJ(2)                                                        PENTT42O
      NCD=1                                                              PENTT43
      IF (SO.EQ.0.) NCD=25                                               PENTT44
      DO 3 J=1,NCD                                                       PENTT45
      IF (NCD.GT.1) SO=FLOAT(J)*RF*2.                                    PENTT46
      ZO=H+SO                                                            PENTT47
      TO=ZO/VJO                                                          PENTT48
      IF (ZO.GE.VJO*T1) GO TO 1                                          PENTT49
      PT=AK1*(VJO*T1)**AKOK1*ZO**A1OK-SQRT(AKAY*AK1*UMIN*T1*(VJO*T1)*    PENTT50
     1  *AKOK1*ZO**A1OK)-ZO                                              PENTT51
      VJT=(AK1*(VJO*T1)**AKOK1*ZO**A1OK-(ZO+PT))/(AKAY*T1)               PENTT52
      GO TO 2                                                            PENTT53
    1 CONTINUE                                                           PENTT54
      PT=AKAY*(VJO*T1-SQRT(UMIN*T1*(VJO*T1+ZO/AKAY)))                    PENTT55
      VJT=VJO-PT/(AKAY*T1)                                               PENTT56
    2 CONTINUE                                                           PENTT57
      PSO(J)=FLOAT(J)                                                    PENTT58
      PPT(J)=PT                                                          PENTT59
      PPT(J)=PPT(J)*10.                                                  PENTT60
      PVJT(J)=VJT                                                        PENTT61
    3 CONTINUE                                                           PENTT63
C     IF PLOTTING PENATRATION- STANDOFF CURVE USE 2. CD TO PLOT HOLE PROPENTT64
      IF (NCD.GT.1) NCDI=3                                               PENTT64A
      IF(NCD.GT.1) SO=FLOAT(NCDI)*RF*2.                                  PENTT65
      IF (NCD.GT.1) PT=PPT(NCDI)*.1                                      PENTT66
      IF (NCD.GT.1) VJT=PVJT(NCDI)*.1                                    PENTT67
      ZO=SO+H                                                            PENTT68
      TO=ZO/VJO                                                          PENTT69
C     RETURN                                                             PENTT70
    4 CONTINUE                                                           PENTT71
      TZ(I)=TZ(I)-TZ(1)                                                  PENTT72
      DMASS=DMJ(I)                                                       PENTT75
      IF (VJ(I).LE.0.0) VJ(I)=1.0E-02                                    PENTT76
      AMU(I)=VJO/VJ(I)                                                   PENTT77
      IF (AMU(I).LT.0.) RETURN                                           PENTT78
      THETA(I)=TZ(I)+TAU(I)                                              PENTT79
      F(I)=THETA(I)/AMU(I)-C(I)/VJO                                      PENTT79A
                       DF(I)=F(I)-F(I-1)                                 PENTT80
      SUMMU=AMU(I)**(-AKAY)*DF(I)+SUMMU                                  PENTT81
      T(I)=AMU(I)**(1.+AKAY)*(TO+(1.+AKAY)*SUMMU)                        PENTT82
      DT(I)=T(I)-TO                                                      PENTT83
      G(I)=VJO*(T(I)/AMU(I)-F(I))                                        PENTT84
                    A(I)=Z(I)-R(I)*COT(BETA(I)/2.)                       PENTT85
                    DELA(I)=A(I)-A(I-1)                                  PENTT86
                    DVJ(I)=VJ(I)-VJ(I-1)                                 PENTT87
      DZODT(I)=(T(I)-TZ(I))*DVJ(I)/DTZ-VJ(I)+DELA(I)/DTZ                 PENTT88
C     DZODT(I)=VJ(I)-((T(I)-TZ(I))*DVJ(I)/DTZ+DELA(I)/DTZ)               PENTT89
      IF (T(I).GT.T1) GO TO 6                                            PENTT90
      IF (ZO.GE.VJO*T1) GO TO 5                                          PENTT91
C                                                                        PENTT92
C     CALCULATE DEPTH OF PENETRATION                                     PENTT93
C                                                                        PENTT94
      P(I)=ZO*((T(I)/TO)**AKOK1-1.0)                                     PENTT95
      RSQ(I)=2.*R(I)*EPS*DA*DMASS/DZODT(I)                               PENTT96
      RSQ(I)=SQRT(ABS(RSQ(I)))                                           PENTT97
```

```
C
C     CALCULATE RADIUS OF THE JET
C
      RC(I)=SQRT(RHOJ/(2.*AKAY*CK))*SQRT(T1/TO)*VJO*(ZO/(ZO+P(I)))**AK3
     1  *RSQ(I)
      GO TO 9
    5 CONTINUE
      P(I)=VJO*(T(I)-TO)*T1/(T1+T(I)/AKAY)
      VJP=VJO*(T1+TO/AKAY)/(T1+T(I)/AKAY)
      DVJP=VJP-VJPO
      DZODT(I)=(T1-T(I))*DVJP-VJP+DELA(I)
      DZODT(I)=-DZODT(I)
      RSQ(I)=2.*R(I)*EPS*DA*DMASS/DZODT(I)
      RSQ(I)=SQRT(RSQ(I))
      RC(I)=SQRT(RHOJ/(2.*AKAY*CK))*RSQ(I)*VJO*(1.-P(I)/(AKAY*VJO*T1))
      VJPO=VJP
      GO TO 10
    6 CONTINUE
      IF (P(I).LT.PT) GO TO 8
      IF (JC1.NE.1) GO TO 7
      JC1=2
      TP=T(I)
    7 CONTINUE
      IF (T(I).GT.TP) RETURN
    8 CONTINUE
      DZODT(I)=(T1-TZ(I))*DVJ(I)/DTZ-VJ(I)+DELA(I)/DTZ
      P(I)=(AK1*(T1/TO)**AKOK1*T(I)/(T(I)+AKAY*T1)-1.0)*ZO
      RSQ(I)=2.*R(I)*EPS*DA*DMASS/DZODT(I)
      RSQ(I)=SQRT(ABS(RSQ(I)))
      RC(I)=SQRT(RHOJ/(2.*AKAY*CK))*(VJO/AKAY)*(AK1*(ZO/(VJO*T1))**A1OK
     1  -(ZO+P(I))/(VJO*T1))*RSQ(I)
    9 CONTINUE
      VJPO=VJ(I-1)
   10 CONTINUE
   11 CONTINUE
      WRITE (6,31) HEAD
      WRITE (6,22)
      WRITE (6,29) T1,TO,ZO,PT,VJT,VJO,AKAY,UMIN,CK
      N1=1
      N2=N
      IF (N.GE.57) N2=55
      WRITE (6,30)
   12 CONTINUE
      WRITE (6,23)
      WRITE (6,27)
      II=0
      DO 13 I=N1,N2
      WRITE (6,23) I,AMU(I),THETA(I),F(I),DF(I),T(I),DT(I),G(I),RSQ(I),
     1  A(I),DELA(I),DVJ(I),DZODT(I)
   13 CONTINUE
      IF (N.LE.N2) GO TO 14
      N1=N2+1
      N2=N
      GO TO 12
   14 CONTINUE
      DO 15 I=MN,N
   15 CONTINUE
```

```
      N1=1                                                              PENT155
      N2=N                                                              PENT156
      IF (N.GE.50) N2=50                                                PENT157
      WRITE (6,31) HEAD                                                 PENT158W
      SO=SO/(2.*RF)                                                     PENT159
      WRITE (6,28) SO                                                   PENT160W
      WRITE (6,23)                                                      PENT161W
      WRITE (6,25)                                                      PENT162W
   16 CONTINUE                                                          PENT163
      IF (N1.GT.25) WRITE (6,26)                                        PENT164W
      DO 19 I=N1,N2                                                     PENT165
      IF (P(I).GT.PT) GO TO 20                                          PENT166
      IF (P(I).EQ.0.0) II=II+1                                          PENT167
      IF (I.GT.25) GO TO 17                                             PENT168
      WRITE (6,24) I,P(I),RC(I),PPT(I),PSO(I)                           PENT169W
      GO TO 18                                                          PENT170
   17 CONTINUE                                                          PENT171
      WRITE (6,24) I,P(I),RC(I)                                         PENT172W
   18 CONTINUE                                                          PENT173
   19 CONTINUE                                                          PENT174
      IF (N.LE.N2) GO TO 20                                             PENT175
      N1=N2+1                                                           PENT176
      N2=N                                                              PENT177
      GO TO 16                                                          PENT178
   20 CONTINUE                                                          PENT179
      II=II+1                                                           PENT180
      DO 21 I=1,II                                                      PENT181
      RC(I)=RC(II)                                                      PENT182
   21 CONTINUE                                                          PENT183
      RETURN                                                            PENT184
C                                                                       PENT185
C     PENETRATION FORMATS                                               PENT186
C                                                                       PENT187
   22 FORMAT(40X,'INITIAL CONDITIONS FOR PENETRATION'//)                PENT188
   23 FORMAT (I4,2X,1P12E10.3)                                          PENT189
   24 FORMAT (I3,7X,2(F10.5,10X,F10.5,20X))                             PENT190
   25 FORMAT (3H  I,12X,'P(CM)',15X,'RC(CM)',23X,'PT(MM)',15X,'SO(CD)'/)PENT191
   26 FORMAT (1H1,3H  I,13X,'P',18X,'RC')                               PENT192
   27 FORMAT (2H I,6X,2HMU,8X,5HTHETA,5X,2H F,FX,3H DF,7X,2H T,8X,2HDT,8PENT193
     1X,2H G,8X,3HRSQ,8X,1HA,8X,4HDELA,7X,2HDV,6X,4HDZDT/)              PENT194
   28 FORMAT(10X,'HOLE PROFILE    SO = ',F6.2,3H CD,25X,'PENTRATION STANPENT195
     1DOFF'/)                                                           PENT195A
   29 FORMAT(5X,'T1 = ',F10.4,5X,'TO = ',F10.4,5X,' ZO = ',F10.4,//4X,  PENT196
     1' PT =',F10.4,5X,'VJT =',F10.4,5X,' VJO =',F10.4//4X,' AKAY = '   PENT197
     2,F10.6,5X,' UMIN = ',F10.5,5X,' CK = ',F10.5//)                   PENT198
   30 FORMAT(1H1,' PENETRATION PHASE'/)                                 PENT199
   31 FORMAT (1H1,30X,8A10///)                                          PENT200
      END                                                               PENT201-
```

```
      SUBROUTINE CALAI (I,Z,R,DPOINT,RDPT,JOHNI,AI)                    * 701* 2
C                                                                       CALAI 2
C     SUBROUTINE WILL CALCULATE INCLINATION ANGLE (AI), DETONATION      CALAI 3
C     COMPONENT OF THE COLLAPSE VELOCITY (DA), AND WILL CALL CALPHI     CALAI 4
C     SUBROUTINE WHICH WILL CALCULATE 1./PHIO (RPHIO) GIVEN (AI).      CALAI 5
C                                                                       CALAI 6
      DIMENSION Z(100), R(100)                                          CALAI 7
      COMMON ALRAD, EPS, RHOJ, RHOC, RF, RPHIO, DTZ, SO, CK, DA, H, D,  CALAI 8
     1  PT, DEGTOR                                                      CALAI 9
      ALPHA=ALRAD*DEGTOR                                                CALAI10
      THETA=ATAN((R(I)-RDPT)/(DPOINT+Z(I)))                             CALAI11
      THETA=THETA*DEGTOR                                                CALAI12
      AI=90.-(ALPHA-THETA)                                              CALAI13
      IF (AI.LT.0.) AI=180.-(ALPHA-THETA)                               CALAI14
      CALL CALPHI (AI)                                                  CALAI15
      AI=AI/DEGTOR                                                      CALAI16
      DA=D/SIN(AI)                                                      CALAI17
      RETURN                                                            CALAI18
      END                                                               CALAI19-
```

```
      SUBROUTINE CALPHI (AI)                                            * 720* 3
C                                                                       CALPI 2
C     GIVEN AN INCLINATION ANGLE (AI) INTERPOLATE INTO TABLES AND FIND  CALPI 3
C     AN ANGLE PHIO. THEN CALCULATE 1./PHIO (RPHIO) AND RETURN.         CALPI 4
C                                                                       CALPI 5
      DIMENSION TPHI(37), TAI(37)                                       CALPI 6
      COMMON ALRAD, EPS, RHOJ, RHOC, RF, RPHIO, DTZ, SO, CK, DA, H, D,  CALPI 7
     1  PT, DEGTOR                                                      CALPI 8
      DATA TPHI /0.0, .08, .25, .59, 1.02, 1.43, 1.76, 2.03, 2.47, 2.86,CALPI 9D
     1 3.30, 3.70, 4.14, 4.51, 5.08, 5.65, 5.98, 6.37, 6.70, 7.01, 7.22,CALPI10D
     2 7.42, 7.58, 7.73, 7.90, 8.04, 8.17, 8.23, 8.26, 8.30, 8.26, 8.16,CALPI11D
     3 8.06, 7.99, 7.85, 7.75, 7.56/                                    CALPI12D
      DATA TAI /0.0, .02, .05, .15, .23, .32, .42, .48, .60, .72, .84, .CALPI13D
     194, 1.06, 1.14, 1.29, 1.44, 1.54, 1.67, 1.79, 1.92, 2.03, 2.16, 2.CALPI14D
     228, 2.41, 2.61, 2.79, 3.01, 3.14, 3.25, 3.38, 3.57, 3.72, 3.88, 4.CALPI15D
     3300, 4.16, 4.29, 4.47/                                            CALPI16D
C     TAI SCALE FACTOR  100 DEG = 5.01 COUNTS  (SFI=5.01/100.)          CALPI17
C     TPHI SCALE FACTOR  40 DEG = 8.08 COUNTS (SFPHI=8.08/40.)          CALPI18
      SFI=.0501                                                         CALPI19
      SFPHI=.202                                                        CALPI20
      X=SFI*AI                                                          CALPI21
      DO 1 J=1,37                                                       CALPI22
      IF (TAI(J).GT.X) GO TO 2                                          CALPI23
    1 CONTINUE                                                          CALPI24
    2 CONTINUE                                                          CALPI25
      DXI=X-TAI(J-1)                                                    CALPI26
      RDX=DXI/(TAI(J)-TAI(J-1))                                         CALPI27
      Y=RDX*(TPHI(J)-TPHI(J-1))+TPHI(J-1)                               CALPI28
      IF (PHIO.LE..0001) PHIO=0.                                        CALPI29
      PHIO=Y/SFPHI                                                      CALPI30
      RPHIO=1.0/PHIO                                                    CALPI31
      RPHIO=RPHIO*DEGTOR                                                CALPI32
      RETURN                                                            CALPI33
      END                                                               CALPI34-
```

```
      SUBROUTINE VELGR (IK,UJK,DMJK,IS)                               * 754* 4
      DIMENSION UJK(200), DMJK(200)                                   VELGR 2
      E=0.                                                            VELGR 3
      IJK=IK-1                                                        VELGR 4
    1 KP=1                                                            VELGR 5
C         COMPRESSION OF THE JET                                      VELGR 6
      DO 2 M=IS,IJK                                                   VELGR 7
      IF (UJK(M).GE.UJK(M+1)) GO TO 2                                 VELGR 8
      IF (ABS(UJK(M)-UJK(M+1)).LE.1.E-5) GO TO 2                      VELGR 9
      T1=DMJK(M)*UJK(M)+DMJK(M+1)*UJK(M+1)                            VELGR10
      T2=2*DMJK(M+1)*(UJK(M)-UJK(M+1))                                VELGR11
      DEM=1.0/(DMJK(M)+DMJK(M+1))                                     VELGR12
      UJK(M)=(T1-T2)*DEM                                              VELGR13
      UJK(M+1)=(T1+T2)*DEM                                            VELGR14
      KP=0                                                            VELGR15
    2 CONTINUE                                                        VELGR16
      IF (KP.EQ.0) GO TO 1                                            VELGR17
      RETURN                                                          VELGR18
      END                                                             VELGR19-
```

```
      SUBROUTINE PLOTS (N,UJK,DPOINT,RDPT,HEAD,PSO,PPT,NCD,NPLT,ISTART) * 772* 5
      DIMENSION PSO(50), PPT(50), S(50)                                 PLOTS 2
      DIMENSION B(5000), HEAD(8)                                        PLOTS 3
      DIMENSION UJK(200), DMJK(200)                                     PLOTS 4
      DIMENSION RD(4), CV(4), AB(4), TC(4), PC(4), DMNJ(4), VVC(4)      PLOTS 5
      DIMENSION Z(100), TZ(100), TAU(100), E(100), PHI(100), DPHI(100), PLOTS 6
     1  BETA(100), GAMA(100), R(100), C(100), VJ(100), VN(100), DMJ(100)PLOTS 7
     2  , DMN(100), DEJ(100), DEN(100), RPHI(100), V(100)               PLOTS 8
      DIMENSION F(4), G(4)                                              PLOTS 9
      COMMON ALRAD, EPS, RHOJ, RHOC, RF, RPHIO, DTZ, SO, CK, DA, H, D,  PLOTS10
     1  PT, DEGTOR                                                      PLOTS11
      COMMON /LPLOT/ Z, TZ, TAU, E, PHI, DPHI, BETA, GAMA, R, C, VJ, VN,PLOTS12
     1  DMJ, DMN, DEJ, DEN, RPHI, V                                     PLOTS13
      DATA DMNJ(1), DMNJ(2) /10HRELATIVE M, 4HASS>/                     PLOTS14D
      DATA RD(1), RD(2), RD(3) /10HRELATIVE D, 10HISTANCE FR, 10HOM CONEPLOTS15D
     1 AP/                                                              PLOTS16D
      DATA RD(4) /3HEX>/                                                PLOTS17D
      DATA CV(1), CV(2), CV(3) /10HCOLLAPSE V, 10HELOCITY IN, 10H CM/MICPLOTS18D
     1ROS/                                                              PLOTS19D
      DATA CV(4) /3HEC>/                                                PLOTS20D
      DATA AB(1), AB(2), AB(3) /10HANGLE BETA, 10H (DEGREES), 1H>/      PLOTS21D
      DATA TC(1), TC(2), TC(3) /10HTIME OF CO, 10HLLAPSE (MI, 10HCRO SECPLOTS22D
     1)> /                                                              PLOTS23D
      DATA PC(1), PC(2), PC(3) /10HPOINT OF C, 10HOLLAPSE (M, 3HM)>/    PLOTS24D
      DATA VVC(1), VVC(2), VVC(3) /10H V, VJ (MM, 10H/MICROSEC), 1H>/   PLOTS25D
      DATA TJET /4HJET>/                                                PLOTS26D
      DATA TSLUG /5HSLUG>/                                              PLOTS27D
      XPAGE=14                                                          PLOTS28
      CALL PLTCCR (XPAGE,1,B(1),B(5000))                                PLOTS29
      II=N-ISTART                                                       PLOTS30
      YMAX=12.                                                          PLOTS31
      CALL PLOTS1 (3.0,3.0,1.0,YMAX,.1,.50,RD,VVC,16,10,4)              PLOTS32
      CALL PLTCCD (1,0,Z(ISTART),V(ISTART),II)                          PLOTS33
      CALL PLTCCD (1,0,Z(ISTART),VJ(ISTART),II)                         PLOTS34
      CALL PLTCCD (4,0,Z(ISTART),UJK(ISTART),II)                        PLOTS35
      CALL PLCCSP (XS,YS,UFAC)                                          PLOTS36
      XX=.25                                                            PLOTS37
      YY=VJ(35)+.04*.5                                                  PLOTS38
      YY=V(35)+.04*.5                                                   PLOTS39
C                                                                       PLOTS40
C     DO EXPERMINTAL DATA POINTS FOR THE 105MM UNCONFINED SHAPED CHARGE.PLOTS41
C                                                                       PLOTS42
C     CALL PLTEXP(N)                                                    PLOTS43
C                                                                       PLOTS44
      DPOINT=DPOINT*10.                                                 PLOTS45
      ENCODE (21,2,S(1) )DPOINT                                         PLOTS46*
      RDPT=RDPT*10.                                                     PLOTS47
      ENCODE (17,3,S(4) )RDPT                                           PLOTS48*
      ALPHA=ALRAD*DEGTOR                                                PLOTS49
      ENCODE (20,4,S(8) )ALPHA                                          PLOTS50*
      RF=RF*10.                                                         PLOTS51
      ENCODE (18,5,S(12) )RF                                            PLOTS52*
      EPS=EPS*10.                                                       PLOTS53
      ENCODE (19,6,S(16) )EPS                                           PLOTS54*
      YY=YMAX+.2*YS                                                     PLOTS54A
      XMAX=1.0                                                          PLOTS54B
      XX=.5*XMAX-.2*XS*7.                                               PLOTS54C
```

```
      XX=0.0
      CALL PLTCCT(.2,HEAD(1),0.,1.,XX,YY)
      YY=.85*YMAX
      XX=.6
      CALL PLTCCT (.1,S(1),0.,1.,XX,YY)
      YY=.80*YMAX
      CALL PLTCCT (.1,S(4),0.,1.,XX,YY)
      XA=.5-.1*XS*10.
      YA=-1.1*YS
      CALL PLTCCT (.1,S(8),0.,1.,XA,YA)
      XA=.5-.1*XS*9.
      YA=-1.3*YS
      CALL PLTCCT (.1,S(12),0.,1.,XA,YA)
      YA=-1.5*YS
      CALL PLTCCT (.1,S(16),0.,1.,XA,YA)
C     THIS NEXT STATEMENT BYPASSES SOME PLOTTINHG ROUTINES
C     IF (NPLT.GT.0) GO TO 1
      CALL PLOTS1 (3.,16.,1.,160.,.1,20.,RD,PC,16,11,4)
      CALL PLTCCD (1,0,Z(ISTART),C(ISTART),II)
      CALL PLTCCP
      CALL PLOTS1 (3.0,3.0,1.0,1.0,.1,.1,RD,DMNJ,16,10,4)
      XX=.35
      YY=DMN(35)-.1
      CALL PLTCCT (.2,TSLUG,0.,1.,XX,YY)
      YY=DMJ(35)-.1
      CALL PLTCCT (.2,TJET,0.,1.,XX,YY)
      CALL PLTCCD (1,0,Z(ISTART),DMJ(ISTART),II)
      CALL PLTCCD (1,0,Z(ISTART),DMN(ISTART),II)
      CALL PLOTS1 (3.0,16.,1.0,180.,.1,20.,RD,AB,16,10,4)
      CALL PLTCCD (1,0,Z(ISTART),HETA(ISTART),II)
    1 CONTINUE
      CALL PLTCCP
C     THIS NEXT STATMENT PART OF PLOTTING BYPASS
C
C     DO PENETRATION PLOTS( HOLE PROFILES).
C
      CALL PLOTPEN (N,S,PS0,PFT,NCD,HEAD)
      RETURN
C
    2 FORMAT (9H (L-H) = ,F8.4,4H MM>)
    3 FORMAT (5H RD =,F8.4,4H MM>)
    4 FORMAT (9H ALPHA = ,F6.2,5H DEG>)
    5 FORMAT (6H RF = ,F8.4,4H MM>)
    6 FORMAT (7H EPS = ,F8.5,4H MM>)
      END
```

```
      SUBROUTINE PLOTS1 (XBAR,YBAR,XMAX,YMAX,DX,DY,PTX,PTY,NNCX,NNCY,
     1  NCD)
      DIMENSION PTX(4), PTY(4)
      CNY=NNCY
      CNX=NNCX
      YS=YMAX/5.
      XS=XMAX/7.
      CALL PLTCCS (XBAR,YBAR,XMIN,YMIN,XS,YS)
      HT=.15
      YY=-.8*YS
      XX=.5*XMAX-HT*CNX*XS
      CALL PLTCCT (HT,PTX(1),0.,1.,XX,YY)
      XX=-.8*XS
      YY=.5*YMAX-HT*CNY*YS
      CALL PLTCCT (HT,PTY(1),1.,0.,XX,YY)
      CALL PLTCCA (DX,DY,XMIN,XMAX,YMIN,YMAX,4)
      CALL LABELA (DX,DY,XMIN,XMAX,YMIN,YMAX,1.0,1.0)
      RETURN
      END
```

```
      SUBROUTINE PLOTPEN (N,S,PSO,PPT,NCD,HEAD)
      DIMENSION TSO(4), TPT(4),HEAD(8)
      DIMENSION S(50), PSO(50), PPT(50)
      DIMENSION HOL(2), RCN(100), PEN(3), PENT(3), RAD(2)
      COMMON ALRAD, EPS, RHOJ, RHOC, RF, RPHIO, DTZ, SO, CK, DA, H, D,
     1  PT, DEGTOR
      COMMON AMU(100), THETA(100), F(100), DF(100), T(100), DT(100),
     1  G(100), P(100), A(100), DELA(100), DVJ(100), DZODT(100),
     2  RSQ(100), RC(100), T1, UMIN
      DATA HOL(1), HOL(2) /10HHOLE PROFI, 3HLE>/
      DATA PEN(1), PEN(2), PEN(3) /10HRADIUS-VS-, 10HDEPTH OF P, 6HEN.(M
     1M)>/
      DATA PENT(1), PENT(2), PENT(3) /10HTIME-VS-DE, 10HPTH OF PEN, 6H.(
     1CM)>/
      DATA RAD(1), RAD(2) /10HRADIUS (MM, 2H)>/
      DATA TSO(1), TSO(2) /10HSTANDOFF -, 5H(CD)>/
      DATA TPT(1), TPT(2) /10HPENETRATIO, 7HN (MM)>/
      RM=0.
      DO 1 I=1,N
      IF (P(I).GE.PT) GO TO 2
      P(I)=-P(I)
      RCN(I)=-RC(I)
      IF (RC(I).GT.RM) RM=RC(I)
    1 CONTINUE
      P(N)=-P(N)
    2 CONTINUE
      N=I
      PM=-P(N)
      XMAX=10.
      XMIN=-XMAX
      YMIN=-PM
      IF (PM.LT.100.) YMIN=-100.
      IF (PM.LT.60.) YMIN=-60.
      YMAX=0.
      YS=(YMAX-YMIN)/8.
      XS=YS
      XBAR=3.0
      YBAR=15.0
      CALL PLTCCS (XBAR,YBAR,XMIN,YMIN,XS,YS)
      XA=-.2*XS*.5*12.
      YA=YMAX+.3*YS
      CALL PLTCCT (.20,HOL(1),0.,1.,XA,YA)
      XA=-.1*XS*5.
      YA=YMIN-.5*YS
      CALL PLTCCT (.1,RAD(1),0.,1.,XA,YA)
      XA=-.1*XS*9.
      YA=YMIN-.75*YS
      CALL PLTCCT (.1,S(1),0.,1.,XA,YA)
      XA=-.1*XS*7.
      YA=YMIN-YS
      CALL PLTCCT (.1,S(4),0.,1.,XA,YA)
      ENCODE (16,5,T(1) )SO
      XA=-.1*XS*8.
      YA=YS*1.2
      CALL PLTCCT (.1,T(1),0.,1.,XA,YA)
      XA=XMIN-.8*XS
      YA=.5*YMIN-.1*YS*.5*18.
```

```
      CALL PLTCCT (.1,PEN(2),1.,0.,XA,YA)                                PLOTN58
      XA=-.2*XS*15.                                                      PLOTN58A
      YA=YS*1.4                                                          PLOTN58B
      CALL PLTCCT(.2,HEAD(1),0.,1.,XA,YA)                                PLOTN58C
      DX=1.                                                              PLOTN59
      DY=1.                                                              PLOTN60
      CALL PLTCCA (DX,DY,XMIN,XMAX,YMIN,YMAX,4)                          PLOTN61
      DY=2.*DY                                                           PLOTN62
      DX=5.0                                                             PLOTN63
      XMIN=-XMAX                                                         PLOTN64
      XMAX=0.                                                            PLOTN65
      CALL LABELA (DX,DY,XMIN,XMAX,YMIN,YMAX,-10.0,-10.0)                PLOTN66
      DY=0.                                                              PLOTN67
      XMAX=-XMIN                                                         PLOTN68
      XMIN=0.                                                            PLOTN69
      CALL LABELA (DX,DY,XMIN,XMAX,YMIN,YMAX,10.0,0.0)                   PLOTN70
      RC(N)=0.                                                           PLOTN71
      P(N)=PM                                                            PLOTN72
      CALL PLTCCD (1.0,RC(1),P(1),N)                                     PLOTN73
      RCN(N)=0.                                                          PLOTN74
      CALL PLTCCD (1.0,RCN(1),P(1),N)                                    PLOTN75
      XA=-.1*XS*10.                                                      PLOTN76
      YA=.8*YS                                                           PLOTN77
      CALL PLTCCT (.1,S(8),0.,1.,XA,YA)                                  PLOTN78
      XA=-.1*XS*9.                                                       PLOTN79
      YA=YS                                                              PLOTN80
      CALL PLTCCT (.1,S(12),0.,1.,XA,YA)                                 PLOTN81
      YA=.6*YS                                                           PLOTN82
      CALL PLTCCT (.1,S(16),0.,1.,XA,YA)                                 PLOTN83
      IF (NCD.GT.1) GO TO 3                                              PLOTN84
      CALL PLTCCP                                                        PLOTN85
      RETURN                                                             PLOTN86
    3 CONTINUE                                                           PLOTN87
      XMAX=PSO(NCD)                                                      PLOTN88
      YMAX=0.                                                            PLOTN89
      DO 4 I=1,NCD                                                       PLOTN90
      IF (PPT(I).GT.YMAX) YMAX=PPT(I)                                    PLOTN91
    4 CONTINUE                                                           PLOTN92
      YMAX=.01*YMAX                                                      PLOTN93
      YMAX=AINT(YMAX)+1.0                                                PLOTN94
      YMAX=YMAX*100.                                                     PLOTN95
      DY=.2*YMAX                                                         PLOTN96
      CALL PLOTS1 (3.0,3.0,XMAX,YMAX,1.,DY,TSO,TPT,7,8,2)                PLOTN97
      CALL PLCCSP (XS,YS,UFAC)                                           PLOTN98
      XA=.5*XMAX-.2*XS*7.                                                PLOTN98A
      XA=0.                                                              PLOTN98B
      YA=YMAX+.2*YS                                                      PLOTN98C
      CALL PLTCCT(.2,HEAD(1),0.,1.,XA,YA)                                PLOTN98D
      YA=-1.1*YS                                                         PLOTN99
      XA=.5*XMAX-.1*XS*10.                                               PLOT100
      CALL PLTCCT (.1,S(8),0.,1.,XA,YA)                                  PLOT101
      XA=.5*XMAX-.1*XS*9.                                                PLOT102
      YA=-1.3*YS                                                         PLOT103
      CALL PLTCCT (.1,S(12),0.,1.,XA,YA)                                 PLOT104
      YA=-1.5*YS                                                         PLOT105
      CALL PLTCCT (.1,S(16),0.,1.,XA,YA)                                 PLOT106
      CALL PLTCCD (1.0,PSO(1),PPT(1),NCD)                                PLOT107
      CALL PLTCCP                                                        PLOT108
      RETURN                                                             PLOT109
C                                                                        PLOT110
    5 FORMAT (6H SO = ,F6.2,4H CD>)                                      PLOT111
      END                                                                PLOT112-
```

```
      SUBROUTINE PLTEXP (N)                                             *1002* 8
      DIMENSION PEXX(60), PEXVJ(60), PEXVO(60), PEXV(4), TEXP(3),       PLTEP 2
     1  PEXPX(4)                                                        PLTEP 3
      DIMENSION BASC(3)                                                 PLTEP 4
      COMMON ALRAD, EPS, RHOJ, RHOC, RF, RPHIO, DTZ, SO, CK, DA, H, D   PLTEP 5
      DATA TEXP(1), TEXP(2), TEXP(3) /10HEXPERIMENT, 10HAL DATA    , 2H,>PLTEP 6D
     1/                                                                 PLTEP 7D
      DATA (PEXX(I),I=1,9) /4.0, 4.5, 5.0, 5.5, 6.0, 6.5, 7.0, 7.5, 8.0/PLTEP 8D
      DATA (PEXVJ(I),I=1,9) /7.01, 6.68, 6.35, 6.03, 5.62, 5.01, 4.17, 3PLTEP 9D
     1.19, 2.25/                                                        PLTEP10D
      DATA (PEXVO(I),I=1,9) /2.050, 2.069, 2.065, 2.046, 2.013, 1.956, 1PLTEP11D
     1.870, 1.729, 1.509/                                               PLTEP12D
      DATA (PEXPX(I),I=1,3) /5.68, 6.94, 8.21/                          PLTEP13D
      DATA (PEXV(I),I=1,3) /2.1, 1.78, 1.42/                            PLTEP14D
      M=10                                                              PLTEP15
      ICOUNT=ICOUNT+1                                                   PLTEP16
      IF (ICOUNT.LE.1) GO TO 1                                          PLTEP17
      READ (5,5) M,(PEXX(I),PEXVJ(I),I=1,M)                             PLTEP18R
      M=M+1                                                             PLTEP19
      PEXX(M)=.875                                                      PLTEP20
      PEXVJ(M)=9.13                                                     PLTEP21
      GO TO 4                                                           PLTEP22
    1 CONTINUE                                                          PLTEP23
      PEXX(10)=.875                                                     PLTEP24
      PEXVJ(10)=9.13                                                    PLTEP25
      PEXPX(4)=.910                                                     PLTEP26
      PEXV(4)=9.13                                                      PLTEP27
      FAC=.5*.7506                                                      PLTEP28
      DO 2 I=1,9                                                        PLTEP29
      PEXX(I)=PEXX(I)+FAC                                               PLTEP30
      PEXX(I)=PEXX(I)/H                                                 PLTEP31
    2 CONTINUE                                                          PLTEP32
      DO 3 I=1,3                                                        PLTEP33
      PEXPX(I)=PEXPX(I)+FAC                                             PLTEP34
      PEXPX(I)=PEXPX(I)/H                                               PLTEP35
    3 CONTINUE                                                          PLTEP36
      CALL PLTCCD (2,5,PEXX(1),PEXVO(1),9)                              PLTEP37
      CALL PLTCCD (2,4,PEXPX(1),PEXV(1),4)                              PLTEP38
    4 CONTINUE                                                          PLTEP39
      YY=9.                                                             PLTEP40
      XX=.6                                                             PLTEP41
      CALL PLTCCT (.1,TEXP(1),0.,1.,XX,YY)                              PLTEP42
      YY=8.                                                             PLTEP43
C                  CALL PLTCCT(.1,BASC(1),0.,1.,XX,YY)                  PLTEP44
      CALL PLTCCD (2,5,PEXX(1),PEXVJ(1),M)                              PLTEP45
      RETURN                                                            PLTEP46
C                                                                       PLTEP47
    5 FORMAT (I5/(8E10.1))                                              PLTEP48
      END                                                               PLTEP49-
```

SAMPLE INPUT

CARD NO. 1

HEADING CARD

1 105-MM SHAPED CHARGE SAMPLE CASE

CARD NO. 2

LINER PARAMETERS

ALPHA	EPS	RHOJ	RF	H	CONF TKS	RHO CONF.	NPLT	NPOS
21.	.269	8.9	4.3185	0.	0.	0.	0	0

CARD NO. 3

TARGET PARAMETERS

RHOC	SO	CK	BHN	T1	DPOINT	HDPT	NEXP	N
7.8	0.	0.	300.	112.	3.9899	0.	1	100

105-MM SHAPED CHAGE SAMPLE CASE

INPUT PARAMETERS

ALPHA = 21.000   K CONSTANT = .780   THICKNESS OF LINER = .269   DENSITY = 8.900

UNCONFINED   THICKNESS = 0.000   DENSITY = 0.000   FACTOR = 1.0000

LINER HEIGHT = 11.2561   LINER RADIUS = 4.3185

INCREMENT OF Z (DZ) = .1125   INCREMENT OF TIME (DTZ) = .1410   NUMBER OF ELEMENTS (N) = 100

DETONATION

EXPLOSIVE = COMP B   DETONATION VELOCITY(D) = .79800   EXPLOSIVE DENSITY = 1.720

POINT OF DETONATION FROM CONE APEX(DPOINT) = 3.9809   DET. RADIUS (RDPT) = 0.0000

TARGET INPUTS

TARGET DENSITY = 7.800   STAND-OFF DISTANCE = 9.000   CK CONSTANT(BHN) = 300.000000

MISC. INPUTS

SKIP   PLOTS

INITIAL POSITION

I	Z	I	Z	I	Z	I	Z	I	Z	I	Z	I	Z
1	0.0000	2	.1125	3	.2250	4	.3375	5	.4500	6	.5625	7	.6750
8	.7875	9	.9000	10	1.0125	11	1.1250	12	1.2375	13	1.3500	14	1.4625
15	1.5750	16	1.6875	17	1.8000	18	1.9125	19	2.0250	20	2.1375	21	2.2500
22	2.3625	23	2.4750	24	2.5875	25	2.7000	26	2.8125	27	2.9250	28	3.0375
29	3.1500	30	3.2625	31	3.3750	32	3.4875	33	3.6000	34	3.7125	35	3.8250
36	3.9375	37	4.0500	38	4.1625	39	4.2750	40	4.3875	41	4.5000	42	4.6125
43	4.7250	44	4.8375	45	4.9500	46	5.0625	47	5.1750	48	5.2875	49	5.4000
50	5.5125	51	5.6250	52	5.7375	53	5.8500	54	5.9625	55	6.0750	56	6.1875
57	6.3000	58	6.4125	59	6.5250	60	6.6375	61	6.7500	62	6.8625	63	6.9750
64	7.0875	65	7.2000	66	7.3126	67	7.4251	68	7.5376	69	7.6501	70	7.7626
71	7.8751	72	7.9876	73	8.1001	74	8.2126	75	8.3251	76	8.4376	77	8.5501
	8.6626	79	8.7751	80	8.8876	81	9.0001	82	9.1126	83	9.2251	84	9.3376
85	9.4501	86	9.5626	87	9.6751	88	9.7876	89	9.9001	90	10.0126	91	10.1251
92	10.2376	93	10.3501	94	10.4626	95	10.5751	96	10.6876	97	10.8001	98	10.9126
99	11.0251	100	11.1376										

I	R	I	R	I	R	I	R	I	R	I	R	I	R
1	0.0000	2	.0432	3	.0864	4	.1296	5	.1727	6	.2159	7	.2591
8	.3023	9	.3455	10	.3887	11	.4319	12	.4750	13	.5182	14	.5614
15	.6046	16	.6478	17	.6910	18	.7342	19	.7773	20	.8205	21	.8637
22	.9069	23	.9501	24	.9933	25	1.0364	26	1.0796	27	1.1228	28	1.1660
29	1.2092	30	1.2524	31	1.2956	32	1.3387	33	1.3819	34	1.4251	35	1.4683
36	1.5115	37	1.5547	38	1.5978	39	1.6410	40	1.6842	41	1.7274	42	1.7706
43	1.8138	44	1.8570	45	1.9001	46	1.9433	47	1.9865	48	2.0297	49	2.0729
50	2.1161	51	2.1593	52	2.2024	53	2.2456	54	2.2888	55	2.3320	56	2.3752
57	2.4184	58	2.4615	59	2.5047	60	2.5479	61	2.5911	62	2.6343	63	2.6775
64	2.7207	65	2.7638	66	2.8070	67	2.8502	68	2.8934	69	2.9366	70	2.9798
71	3.0230	72	3.0661	73	3.1093	74	3.1525	75	3.1957	76	3.2389	77	3.2821
78	3.3252	79	3.3684	80	3.4116	81	3.4548	82	3.4980	83	3.5412	84	3.5844
85	3.6275	86	3.6707	87	3.7139	88	3.7571	89	3.8003	90	3.8435	91	3.8867
92	3.9298	93	3.9730	94	4.0162	95	4.0594	96	4.1026	97	4.1458	98	4.1889
99	4.2321	100	4.2753										

I	RI	I	RI	I	RI	I	RI	I	RI	I	RI	I	RI
1	0.0000	2	0.0000	3	0.0000	4	0.0000	5	0.0000	6	0.0000	7	0.0000
8	.0142	9	.0573	10	.1005	11	.1437	12	.1869	13	.2301	14	.2733
15	.3165	16	.3596	17	.4028	18	.4460	19	.4892	20	.5324	21	.5756
22	.6187	23	.6619	24	.7051	25	.7483	26	.7915	27	.8347	28	.8779
29	.9210	30	.9642	31	1.0074	32	1.0506	33	1.0938	34	1.1370	35	1.1802
36	1.2233	37	1.2665	38	1.3097	39	1.3529	40	1.3961	41	1.4393	42	1.4824
43	1.5256	44	1.5688	45	1.6120	46	1.6552	47	1.6984	48	1.7416	49	1.7847
50	1.8279	51	1.8711	52	1.9143	53	1.9575	54	2.0007	55	2.0439	56	2.0870
57	2.1302	58	2.1734	59	2.2166	60	2.2598	61	2.3030	62	2.3461	63	2.3893
64	2.4325	65	2.4757	66	2.5189	67	2.5621	68	2.6053	69	2.6484	70	2.6916
71	2.7348	72	2.7780	73	2.8212	74	2.8644	75	2.9076	76	2.9507	77	2.9939
78	3.0371	79	3.0803	80	3.1235	81	3.1667	82	3.2098	83	3.2530	84	3.2962
85	3.3394	86	3.3826	87	3.4258	88	3.4690	89	3.5121	90	3.5553	91	3.5985
92	3.6417	93	3.6849	94	3.7281	95	3.7713	96	3.8144	97	3.8576	98	3.9008
99	3.9440	100	3.9872										

	Z	TZ	EPS	E	PHI	BETA	DPHI	RPHI	V	R	TAU	C
1	0.	5.000E+00	2.690E-01	0.	3.000E+00	0.	0.	0.	0.	0.	0.	0.
2	1.000E-02	5.141E+00	4.301E-02	4.276E+00	1.683E+01	0.	1.383E+01	3.404E+00	0.	4.319E-02	1.989E-01	0.
3	2.000E-02	5.284E+00	8.571E-02	4.233E+00	1.625E+01	0.	5.849E-01	3.527E+00	0.	8.637E-02	4.124E-01	0.
4	3.000E-02	5.427E+00	1.281E-01	4.191E+00	1.569E+01	0.	5.505E-01	3.651E+00	0.	1.296E-01	6.407E-01	0.
5	4.000E-02	5.572E+00	1.703E-01	4.149E+00	1.516E+01	0.	5.196E-01	3.776E+00	0.	1.727E-01	8.838E-01	0.
6	5.000E-02	5.717E+00	2.123E-01	4.107E+00	1.468E+01	0.	4.994E-01	3.904E+00	0.	2.159E-01	1.143E+00	0.
7	6.000E-02	5.862E+00	2.541E-01	4.066E+00	1.420E+01	0.	4.731E-01	4.034E+00	0.	2.591E-01	1.417E+00	0.
8	7.000E-02	6.009E+00	2.819E-01	4.024E+00	1.407E+01	3.659E+01	1.312E-01	4.072E+00	2.048E-01	3.023E-01	1.672E+00	9.485E-01
9	8.000E-02	6.155E+00	2.812E-01	3.983E+00	1.455E+01	4.162E+01	4.743E-01	3.939E+00	2.112E-01	3.455E-01	1.857E+00	1.086E+00
10	9.000E-02	6.303E+00	2.806E-01	3.942E+00	1.495E+01	4.167E+01	4.071E-01	3.832E+00	2.167E-01	3.887E-01	2.041E+00	1.223E+00
11	1.000E-01	6.450E+00	2.801E-01	3.900E+00	1.531E+01	4.170E+01	3.529E-01	3.743E+00	2.213E-01	4.319E-01	2.224E+00	1.361E+00
12	1.100E-01	6.598E+00	2.796E-01	3.859E+00	1.561E+01	4.171E+01	3.083E-01	3.669E+00	2.253E-01	4.750E-01	2.406E+00	1.499E+00
13	1.200E-01	6.746E+00	2.791E-01	3.818E+00	1.588E+01	4.166E+01	2.694E-01	3.607E+00	2.288E-01	5.182E-01	2.588E+00	1.637E+00
14	1.300E-01	6.895E+00	2.786E-01	3.777E+00	1.612E+01	4.162E+01	2.372E-01	3.554E+00	2.316E-01	5.614E-01	2.771E+00	1.774E+00
15	1.400E-01	7.044E+00	2.782E-01	3.736E+00	1.633E+01	4.157E+01	2.098E-01	3.508E+00	2.345E-01	6.046E-01	2.953E+00	1.912E+00
16	1.500E-01	7.193E+00	2.778E-01	3.695E+00	1.652E+01	4.150E+01	1.858E-01	3.469E+00	2.368E-01	6.478E-01	3.136E+00	2.050E+00
17	1.600E-01	7.342E+00	2.775E-01	3.653E+00	1.668E+01	4.141E+01	1.647E-01	3.435E+00	2.388E-01	6.910E-01	3.319E+00	2.188E+00
18	1.700E-01	7.492E+00	2.771E-01	3.612E+00	1.683E+01	4.131E+01	1.460E-01	3.405E+00	2.406E-01	7.341E-01	3.503E+00	2.326E+00
19	1.800E-01	7.641E+00	2.768E-01	3.571E+00	1.696E+01	4.120E+01	1.292E-01	3.379E+00	2.421E-01	7.773E-01	3.688E+00	2.464E+00
20	1.900E-01	7.791E+00	2.765E-01	3.529E+00	1.707E+01	4.107E+01	1.141E-01	3.356E+00	2.435E-01	8.205E-01	3.873E+00	2.602E+00
21	2.000E-01	7.941E+00	2.762E-01	3.488E+00	1.717E+01	4.094E+01	1.003E-01	3.337E+00	2.446E-01	8.637E-01	4.060E+00	2.740E+00
22	2.100E-01	8.091E+00	2.759E-01	3.446E+00	1.726E+01	4.079E+01	8.777E-02	3.320E+00	2.456E-01	9.069E-01	4.247E+00	2.878E+00
23	2.200E-01	8.242E+00	2.757E-01	3.405E+00	1.733E+01	4.063E+01	7.624E-02	3.305E+00	2.465E-01	9.501E-01	4.436E+00	3.016E+00
24	2.300E-01	8.392E+00	2.754E-01	3.363E+00	1.740E+01	4.042E+01	6.447E-02	3.293E+00	2.472E-01	9.933E-01	4.626E+00	3.154E+00
25	2.400E-01	8.542E+00	2.752E-01	3.321E+00	1.745E+01	4.021E+01	5.397E-02	3.283E+00	2.477E-01	1.036E+00	4.814E+00	3.292E+00
26	2.500E-01	8.693E+00	2.750E-01	3.279E+00	1.750E+01	4.002E+01	4.461E-02	3.274E+00	2.482E-01	1.080E+00	5.011E+00	3.430E+00
27	2.600E-01	8.843E+00	2.748E-01	3.238E+00	1.753E+01	3.981E+01	3.623E-02	3.268E+00	2.485E-01	1.123E+00	5.205E+00	3.567E+00
28	2.700E-01	8.994E+00	2.746E-01	3.196E+00	1.756E+01	3.959E+01	2.817E-02	3.262E+00	2.487E-01	1.166E+00	5.402E+00	3.705E+00
29	2.800E-01	9.145E+00	2.744E-01	3.154E+00	1.758E+01	3.936E+01	2.055E-02	3.259E+00	2.488E-01	1.209E+00	5.599E+00	3.842E+00
30	2.900E-01	9.296E+00	2.742E-01	3.112E+00	1.760E+01	3.912E+01	1.333E-02	3.256E+00	2.489E-01	1.252E+00	5.799E+00	3.980E+00
31	3.000E-01	9.447E+00	2.741E-01	3.069E+00	1.760E+01	3.886E+01	6.459E-03	3.255E+00	2.488E-01	1.296E+00	6.001E+00	4.117E+00
32	3.100E-01	9.597E+00	2.739E-01	3.027E+00	1.760E+01	3.861E+01	1.058E-04	3.255E+00	2.486E-01	1.339E+00	6.205E+00	4.254E+00
33	3.200E-01	9.748E+00	2.737E-01	2.985E+00	1.760E+01	3.887E+01	6.400E-03	3.256E+00	2.484E-01	1.382E+00	6.410E+00	4.391E+00
34	3.300E-01	9.899E+00	2.736E-01	2.943E+00	1.758E+01	3.914E+01	1.246E-02	3.258E+00	2.481E-01	1.425E+00	6.619E+00	4.528E+00
35	3.400E-01	1.005E+01	2.735E-01	2.900E+00	1.757E+01	3.941E+01	1.830E-02	3.262E+00	2.477E-01	1.468E+00	6.829E+00	4.665E+00
36	3.500E-01	1.020E+01	2.733E-01	2.858E+00	1.754E+01	3.968E+01	2.396E-02	3.266E+00	2.473E-01	1.511E+00	7.042E+00	4.802E+00
37	3.600E-01	1.035E+01	2.732E-01	2.815E+00	1.751E+01	3.999E+01	3.028E-02	3.272E+00	2.467E-01	1.555E+00	7.258E+00	4.939E+00
38	3.700E-01	1.050E+01	2.731E-01	2.772E+00	1.748E+01	4.028E+01	3.596E-02	3.279E+00	2.461E-01	1.598E+00	7.477E+00	5.075E+00
39	3.800E-01	1.065E+01	2.730E-01	2.730E+00	1.743E+01	4.056E+01	4.116E-02	3.286E+00	2.454E-01	1.641E+00	7.698E+00	5.212E+00
40	3.900E-01	1.081E+01	2.728E-01	2.687E+00	1.739E+01	4.085E+01	4.626E-02	3.295E+00	2.447E-01	1.684E+00	7.923E+00	5.348E+00
41	4.000E-01	1.096E+01	2.727E-01	2.644E+00	1.734E+01	4.114E+01	5.127E-02	3.305E+00	2.439E-01	1.727E+00	8.151E+00	5.484E+00
42	4.100E-01	1.111E+01	2.726E-01	2.601E+00	1.728E+01	4.144E+01	5.621E-02	3.316E+00	2.430E-01	1.771E+00	8.383E+00	5.620E+00
43	4.200E-01	1.126E+01	2.725E-01	2.558E+00	1.722E+01	4.175E+01	6.110E-02	3.327E+00	2.421E-01	1.814E+00	8.618E+00	5.756E+00
44	4.300E-01	1.141E+01	2.724E-01	2.515E+00	1.715E+01	4.206E+01	6.594E-02	3.340E+00	2.411E-01	1.857E+00	8.857E+00	5.891E+00
45	4.400E-01	1.156E+01	2.724E-01	2.472E+00	1.708E+01	4.239E+01	7.075E-02	3.354E+00	2.400E-01	1.900E+00	9.100E+00	6.027E+00
46	4.500E-01	1.171E+01	2.723E-01	2.429E+00	1.701E+01	4.273E+01	7.555E-02	3.369E+00	2.389E-01	1.943E+00	9.348E+00	6.162E+00
47	4.600E-01	1.187E+01	2.722E-01	2.386E+00	1.693E+01	4.308E+01	8.033E-02	3.385E+00	2.377E-01	1.987E+00	9.600E+00	6.297E+00
48	4.700E-01	1.202E+01	2.721E-01	2.343E+00	1.684E+01	4.344E+01	8.512E-02	3.402E+00	2.364E-01	2.030E+00	9.856E+00	6.432E+00
49	4.800E-01	1.217E+01	2.720E-01	2.300E+00	1.675E+01	4.382E+01	8.993E-02	3.420E+00	2.351E-01	2.073E+00	1.012E+01	6.567E+00
50	4.900E-01	1.232E+01	2.719E-01	2.256E+00	1.666E+01	4.422E+01	9.476E-02	3.440E+00	2.337E-01	2.116E+00	1.039E+01	6.701E+00
51	5.000E-01	1.247E+01	2.719E-01	2.213E+00	1.656E+01	4.463E+01	9.963E-02	3.460E+00	2.323E-01	2.159E+00	1.066E+01	6.836E+00
52	5.100E-01	1.262E+01	2.718E-01	2.170E+00	1.645E+01	4.506E+01	1.045E-01	3.482E+00	2.307E-01	2.202E+00	1.094E+01	6.970E+00
53	5.200E-01	1.277E+01	2.717E-01	2.126E+00	1.634E+01	4.551E+01	1.095E-01	3.506E+00	2.292E-01	2.246E+00	1.122E+01	7.104E+00
54	5.300E-01	1.292E+01	2.717E-01	2.083E+00	1.623E+01	4.598E+01	1.145E-01	3.531E+00	2.275E-01	2.289E+00	1.151E+01	7.237E+00
55	5.400E-01	1.308E+01	2.716E-01	2.039E+00	1.611E+01	4.648E+01	1.196E-01	3.557E+00	2.258E-01	2.332E+00	1.181E+01	7.371E+00
56	5.500E-01	1.323E+01	2.716E-01	1.996E+00	1.598E+01	4.700E+01	1.248E-01	3.585E+00	2.240E-01	2.375E+00	1.212E+01	7.504E+00
57	5.600E-01	1.338E+01	2.715E-01	1.952E+00	1.585E+01	4.755E+01	1.301E-01	3.614E+00	2.222E-01	2.418E+00	1.244E+01	7.637E+00

	Z	TZ	EPS	E	PHI	BETA	DPHI	HPHI	V	R	TAU	C
58	5.700E-01	1.353E+01	2.714E-01	1.908E+00	1.572E+01	4.812E+01	1.355E-01	3.645E+00	2.202E-01	2.462E+00	1.276E+01	7.769E+00
59	5.800E-01	1.368E+01	2.714E-01	1.865E+00	1.558E+01	4.873E+01	1.410E-01	3.678E+00	2.182E-01	2.505E+00	1.310E+01	7.901E+00
60	5.900E-01	1.383E+01	2.713E-01	1.821E+00	1.543E+01	4.937E+01	1.467E-01	3.713E+00	2.161E-01	2.548E+00	1.344E+01	8.033E+00
61	6.000E-01	1.398E+01	2.713E-01	1.777E+00	1.528E+01	5.005E+01	1.524E-01	3.750E+00	2.140E-01	2.591E+00	1.380E+01	8.165E+00
62	6.100E-01	1.414E+01	2.712E-01	1.733E+00	1.512E+01	5.077E+01	1.584E-01	3.789E+00	2.117E-01	2.634E+00	1.417E+01	8.296E+00
63	6.200E-01	1.429E+01	2.712E-01	1.689E+00	1.496E+01	5.153E+01	1.645E-01	3.831E+00	2.094E-01	2.677E+00	1.455E+01	8.427E+00
64	6.300E-01	1.444E+01	2.711E-01	1.645E+00	1.478E+01	5.234E+01	1.707E-01	3.875E+00	2.070E-01	2.721E+00	1.494E+01	8.558E+00
65	6.400E-01	1.459E+01	2.711E-01	1.601E+00	1.461E+01	5.319E+01	1.772E-01	3.922E+00	2.045E-01	2.764E+00	1.535E+01	8.688E+00
66	6.500E-01	1.474E+01	2.711E-01	1.557E+00	1.442E+01	5.409E+01	1.839E-01	3.972E+00	2.019E-01	2.807E+00	1.578E+01	8.818E+00
67	6.600E-01	1.489E+01	2.710E-01	1.513E+00	1.423E+01	5.505E+01	1.908E-01	4.026E+00	1.992E-01	2.850E+00	1.622E+01	8.948E+00
68	6.700E-01	1.504E+01	2.710E-01	1.469E+00	1.404E+01	5.604E+01	1.976E-01	4.082E+00	1.964E-01	2.893E+00	1.669E+01	9.077E+00
69	6.800E-01	1.520E+01	2.709E-01	1.425E+00	1.383E+01	5.711E+01	2.050E-01	4.143E+00	1.935E-01	2.937E+00	1.717E+01	9.206E+00
70	6.900E-01	1.535E+01	2.709E-01	1.381E+00	1.362E+01	5.825E+01	2.127E-01	4.207E+00	1.905E-01	2.980E+00	1.768E+01	9.334E+00
71	7.000E-01	1.550E+01	2.709E-01	1.337E+00	1.340E+01	5.946E+01	2.206E-01	4.277E+00	1.874E-01	3.023E+00	1.821E+01	9.462E+00
72	7.100E-01	1.565E+01	2.708E-01	1.293E+00	1.317E+01	6.074E+01	2.289E-01	4.351E+00	1.842E-01	3.066E+00	1.878E+01	9.589E+00
73	7.200E-01	1.580E+01	2.708E-01	1.249E+00	1.293E+01	6.210E+01	2.376E-01	4.431E+00	1.809E-01	3.109E+00	1.937E+01	9.716E+00
74	7.300E-01	1.595E+01	2.707E-01	1.204E+00	1.268E+01	6.353E+01	2.466E-01	4.517E+00	1.774E-01	3.153E+00	2.000E+01	9.843E+00
75	7.400E-01	1.610E+01	2.707E-01	1.160E+00	1.243E+01	6.503E+01	2.559E-01	4.610E+00	1.739E-01	3.196E+00	2.067E+01	9.968E+00
76	7.500E-01	1.626E+01	2.707E-01	1.116E+00	1.216E+01	6.662E+01	2.657E-01	4.711E+00	1.701E-01	3.239E+00	2.138E+01	1.009E+01
77	7.600E-01	1.641E+01	2.707E-01	1.071E+00	1.189E+01	6.829E+01	2.760E-01	4.820E+00	1.663E-01	3.282E+00	2.214E+01	1.022E+01
78	7.700E-01	1.656E+01	2.706E-01	1.027E+00	1.160E+01	7.003E+01	2.867E-01	4.939E+00	1.623E-01	3.325E+00	2.296E+01	1.034E+01
79	7.800E-01	1.671E+01	2.706E-01	9.826E-01	1.130E+01	7.186E+01	2.980E-01	5.070E+00	1.581E-01	3.368E+00	2.384E+01	1.047E+01
80	7.900E-01	1.686E+01	2.706E-01	9.382E-01	1.099E+01	7.376E+01	3.098E-01	5.213E+00	1.537E-01	3.412E+00	2.479E+01	1.059E+01
81	8.000E-01	1.701E+01	2.705E-01	8.937E-01	1.067E+01	7.572E+01	3.222E-01	5.370E+00	1.492E-01	3.455E+00	2.583E+01	1.071E+01
82	8.100E-01	1.716E+01	2.705E-01	8.493E-01	1.033E+01	7.775E+01	3.353E-01	5.544E+00	1.445E-01	3.498E+00	2.696E+01	1.083E+01
83	8.200E-01	1.731E+01	2.705E-01	8.048E-01	9.985E+00	7.984E+01	3.491E-01	5.738E+00	1.397E-01	3.541E+00	2.821E+01	1.095E+01
84	8.300E-01	1.747E+01	2.705E-01	7.602E-01	9.622E+00	8.197E+01	3.637E-01	5.955E+00	1.346E-01	3.584E+00	2.959E+01	1.107E+01
85	8.400E-01	1.762E+01	2.704E-01	7.157E-01	9.242E+00	8.413E+01	3.791E-01	6.199E+00	1.293E-01	3.628E+00	3.112E+01	1.119E+01
86	8.500E-01	1.777E+01	2.704E-01	6.711E-01	8.847E+00	8.631E+01	3.953E-01	6.476E+00	1.237E-01	3.671E+00	3.285E+01	1.131E+01
87	8.600E-01	1.792E+01	2.704E-01	6.265E-01	8.435E+00	8.849E+01	4.126E-01	6.793E+00	1.180E-01	3.714E+00	3.480E+01	1.142E+01
88	8.700E-01	1.807E+01	2.704E-01	5.819E-01	8.004E+00	9.066E+01	4.310E-01	7.159E+00	1.119E-01	3.757E+00	3.703E+01	1.154E+01
89	8.800E-01	1.822E+01	2.703E-01	5.373E-01	7.553E+00	9.280E+01	4.505E-01	7.586E+00	1.056E-01	3.800E+00	3.962E+01	1.165E+01
90	8.900E-01	1.837E+01	2.703E-01	4.926E-01	7.082E+00	9.489E+01	4.712E-01	8.090E+00	9.905E-02	3.843E+00	4.266E+01	1.177E+01
91	9.000E-01	1.853E+01	2.703E-01	4.479E-01	6.588E+00	9.693E+01	4.934E-01	8.696E+00	9.215E-02	3.887E+00	4.627E+01	1.188E+01
92	9.100E-01	1.868E+01	2.703E-01	4.032E-01	6.071E+00	9.888E+01	5.171E-01	9.437E+00	8.492E-02	3.930E+00	5.067E+01	1.199E+01
93	9.200E-01	1.883E+01	2.703E-01	3.585E-01	5.529E+00	1.007E+02	5.425E-01	1.036E+01	7.733E-02	3.973E+00	5.614E+01	1.210E+01
94	9.300E-01	1.898E+01	2.702E-01	3.138E-01	4.959E+00	1.025E+02	5.698E-01	1.155E+01	6.936E-02	4.016E+00	6.313E+01	1.221E+01
95	9.400E-01	1.913E+01	2.702E-01	2.690E-01	4.360E+00	1.041E+02	5.992E-01	1.314E+01	6.098E-02	4.059E+00	7.241E+01	1.231E+01
96	9.500E-01	1.928E+01	2.702E-01	2.242E-01	3.729E+00	1.056E+02	6.308E-01	1.536E+01	5.216E-02	4.103E+00	8.536E+01	1.242E+01
97	9.600E-01	1.943E+01	2.702E-01	1.794E-01	3.064E+00	1.070E+02	6.650E-01	1.870E+01	4.286E-02	4.146E+00	1.047E+02	1.252E+01
98	9.700E-01	1.959E+01	2.702E-01	1.346E-01	2.362E+00	1.082E+02	7.020E-01	2.426E+01	3.304E-02	4.189E+00	1.369E+02	1.262E+01
99	9.800E-01	1.974E+01	2.701E-01	8.974E-02	1.620E+00	1.093E+02	7.422E-01	3.537E+01	2.266E-02	4.232E+00	2.012E+02	1.272E+01
100	9.900E-01	1.989E+01	2.701E-01	4.486E-02	8.338E-01	1.102E+02	7.860E-01	6.871E+01	1.166E-02	4.275E+00	3.938E+02	1.281E+01

I	Z	VZ	VR	RV	DMJ	DMN	DEL	DML	DMJK	TMJ
1	0.	0.	0.	0.	0.	0.	0.	0.	0.	0.
2	1.000E-02	0.	0.	0.	0.	0.	0.	0.	0.	0.
3	2.000E-02	0.	0.	0.	0.	0.	0.	0.	0.	0.
4	3.000E-02	0.	0.	0.	0.	0.	0.	0.	0.	0.
5	4.000E-02	0.	0.	0.	0.	0.	0.	0.	0.	0.
6	5.000E-02	0.	0.	0.	0.	0.	0.	0.	0.	0.
7	6.000E-02	0.	0.	0.	0.	0.	0.	0.	0.	0.
8	7.000E-02	6.431E-01	3.650E-02	3.033E-01	9.856E-02	9.014E-01	1.150E-02	5.480E-01	5.401E-02	5.401E-02
9	8.000E-02	5.895E-01	2.935E-02	2.801E-01	1.262E-01	8.738E-01	1.397E-02	6.263E-01	7.905E-02	1.331E-01
10	9.000E-02	6.037E-01	3.082E-02	2.864E-0	.265E-01	8.735E-01	1.654E-02	7.045E-01	8.914E-02	2.222E-01
11	1.000E-01	6.160E-01	3.215E-02	2.919E-	.267E-01	8.733E-01	1.917E-02	7.828E-01	9.917E-02	3.214E-01
12	1.100E-01	6.269E-01	3.336E-02	2.968E-0.	.267E-01	8.733E-01	2.186E-02	8.611E-01	1.091E-01	4.305E-01
13	1.200E-01	6.369E-01	3.453E-02	3.012E-01	1.265E-01	8.735E-01	2.459E-02	9.394E-01	1.188E-01	5.493E-01
14	1.300E-01	6.457E-01	3.559E-02	3.051E-01	1.262E-01	8.738E-01	2.734E-02	1.018E+00	1.284E-01	6.777E-01
15	1.400E-01	6.537E-01	3.656E-02	3.086E-01	1.259E-01	8.741E-01	3.012E-02	1.096E+00	1.380E-01	8.157E-01
16	1.500E-01	6.610E-01	3.747E-02	3.118E-01	1.255E-01	8.745E-01	3.291E-02	1.174E+00	1.474E-01	9.631E-01
17	1.600E-01	6.678E-01	3.833E-02	3.147E-01	1.250E-01	8.750E-01	3.571E-02	1.253E+00	1.566E-01	1.120E+00
18	1.700E-01	6.741E-01	3.915E-02	3.175E-01	1.244E-01	8.756E-01	3.851E-02	1.331E+00	1.656E-01	1.285E+00
19	1.800E-01	6.799E-01	3.992E-02	3.200E-01	1.238E-01	8.762E-01	4.130E-02	1.409E+00	1.744E-01	1.460E+00
20	1.900E-01	6.855E-01	4.066E-02	3.224E-01	1.231E-01	8.769E-01	4.409E-02	1.487E+00	1.831E-01	1.643E+00
21	2.000E-01	6.907E-01	4.137E-02	3.247E-01	1.223E-01	8.777E-01	4.685E-02	1.566E+00	1.915E-01	1.834E+00
22	2.100E-01	6.958E-01	4.206E-02	3.268E-01	1.214E-01	8.786E-01	4.960E-02	1.644E+00	1.996E-01	2.034E+00
23	2.200E-01	7.006E-01	4.272E-02	3.289E-01	1.205E-01	8.795E-01	5.232E-02	1.722E+00	2.076E-01	2.241E+00
24	2.300E-01	7.057E-01	4.342E-02	3.311E-01	1.193E-01	8.807E-01	5.500E-02	1.800E+00	2.149E-01	2.456E+00
25	2.400E-01	7.105E-01	4.408E-02	3.332E-01	1.182E-01	8.818E-01	5.765E-02	1.879E+00	2.220E-01	2.678E+00
26	2.500E-01	7.148E-01	4.468E-02	3.351E-01	1.171E-01	8.829E-01	6.026E-02	1.957E+00	2.291E-01	2.907E+00
27	2.600E-01	7.191E-01	4.527E-02	3.369E-01	1.159E-01	8.841E-01	6.284E-02	2.035E+00	2.359E-01	3.143E+00
28	2.700E-01	7.235E-01	4.584E-02	3.387E-01	1.147E-01	8.853E-01	6.537E-02	2.114E+00	2.424E-01	3.386E+00
29	2.800E-01	7.274E-01	4.640E-02	3.405E-01	1.134E-01	8.866E-01	6.786E-02	2.192E+00	2.486E-01	3.634E+00
30	2.900E-01	7.315E-01	4.694E-02	3.423E-01	1.121E-01	8.879E-01	7.030E-02	2.270E+00	2.544E-01	3.889E+00
31	3.000E-01	7.356E-01	4.749E-02	3.441E-01	1.107E-01	8.893E-01	7.268E-02	2.348E+00	2.599E-01	4.149E+00
32	3.100E-01	7.396E-01	4.800E-02	3.458E-01	1.093E-01	8.907E-01	7.502E-02	2.427E+00	2.652E-01	4.414E+00
33	3.200E-01	7.344E-01	4.738E-02	3.435E-01	1.107E-01	8.893E-01	7.729E-02	2.505E+00	2.774E-01	4.691E+00
34	3.300E-01	7.290E-01	4.673E-02	3.411E-01	1.122E-01	8.878E-01	7.951E-02	2.583E+00	2.898E-01	4.981E+00
35	3.400E-01	7.234E-01	4.605E-02	3.387E-01	1.137E-01	8.863E-01	8.167E-02	2.662E+00	3.025E-01	5.284E+00
36	3.500E-01	7.177E-01	4.534E-02	3.362E-01	1.152E-01	8.848E-01	8.376E-02	2.740E+00	3.156E-01	5.599E+00
37	3.600E-01	7.111E-01	4.451E-02	3.333E-01	1.169E-01	8.831E-01	8.578E-02	2.818E+00	3.295E-01	5.929E+00
38	3.700E-01	7.048E-01	4.370E-02	3.305E-01	1.186E-01	8.814E-01	8.773E-02	2.896E+00	3.434E-01	6.272E+00
39	3.800E-01	6.985E-01	4.290E-02	3.278E-01	1.202E-01	8.798E-01	6.960E-02	2.975E+00	3.574E-01	6.630E+00
40	3.900E-01	6.920E-01	4.206E-02	3.250E-01	1.218E-01	8.782E-01	9.140E-02	3.053E+00	3.718E-01	7.001E+00
41	4.000E-01	6.854E-01	4.119E-02	3.221E-01	1.234E-01	8.766E-01	9.312E-02	3.131E+00	3.866E-01	7.388E+00
42	4.100E-01	6.785E-01	4.029E-02	3.191E-01	1.252E-01	8.748E-01	9.477E-02	3.210E+00	4.018E-01	7.790E+00
43	4.200E-01	6.715E-01	3.935E-02	3.161E-01	1.270E-01	8.730E-01	9.633E-02	3.288E+00	4.174E-01	8.207E+00
44	4.300E-01	6.642E-01	3.837E-02	3.129E-01	1.288E-01	8.712E-01	9.781E-02	3.366E+00	4.336E-01	8.641E+00
45	4.400E-01	6.568E-01	3.736E-02	3.097E-01	1.307E-01	8.693E-01	9.920E-02	3.444E+00	4.503E-01	9.091E+00
46	4.500E-01	6.491E-01	3.631E-02	3.064E-01	1.327E-01	8.673E-01	1.005E-01	3.523E+00	4.675E-01	9.558E+00
47	4.600E-01	6.412E-01	3.522E-02	3.030E-01	1.348E-01	8.652E-01	1.017E-01	3.601E+00	4.854E-01	1.004E+01
48	4.700E-01	6.330E-01	3.409E-02	2.995E-01	1.370E-01	8.630E-01	1.028E-01	3.679E+00	5.040E-01	1.055E+01
49	4.800E-01	6.247E-01	3.292E-02	2.959E-01	1.393E-01	8.607E-01	1.038E-01	3.758E+00	5.233E-01	1.107E+01
50	4.900E-01	6.161E-01	3.170E-02	2.922E-01	1.416E-01	8.584E-01	1.048E-01	3.836E+00	5.433E-01	1.161E+01
51	5.000E-01	6.072E-01	3.044E-02	2.884E-01	1.442E-01	8.558E-01	1.056E-01	3.914E+00	5.642E-01	1.218E+01
52	5.100E-01	5.981E-01	2.913E-02	2.845E-01	1.468E-01	8.532E-01	1.063E-01	3.992E+00	5.861E-01	1.276E+01
53	5.200E-01	5.888E-01	2.778E-02	2.805E-01	1.496E-01	8.504E-01	1.069E-01	4.071E+00	6.090E-01	1.337E+01
54	5.300E-01	5.792E-01	2.637E-02	2.764E-01	1.525E-01	8.475E-01	1.074E-01	4.149E+00	6.329E-01	1.401E+01
55	5.400E-01	5.693E-01	2.490E-02	2.722E-01	1.557E-01	8.443E-01	1.078E-01	4.227E+00	6.581E-01	1.466E+01
56	5.500E-01	5.592E-01	2.338E-02	2.679E-01	1.590E-01	8.410E-01	1.080E-01	4.305E+00	6.845E-01	1.535E+01
57	5.600E-01	5.489E-01	2.181E-02	2.635E-01	1.625E-01	8.375E-01	1.082E-01	4.384E+00	7.123E-01	1.606E+01

	Z	VJ	VN	HV	DMJ	DMN	DEL	DML	DMJK	TMJ
58	5.700E-01	5.382E-01	2.017E-02	2.590E-01	1.662E-01	8.338E-01	1.082E-01	4.462E+00	7.417E-01	1.680E+01
59	5.800E-01	5.273E-01	1.847E-02	2.544E-01	1.702E-01	8.298E-01	1.081E-01	4.540E+00	7.728E-01	1.758E+01
60	5.900E-01	5.162E-01	1.671E-02	2.497E-01	1.744E-01	8.256E-01	1.079E-01	4.619E+00	8.057E-01	1.836E+01
61	6.000E-01	5.048E-01	1.488E-02	2.449E-01	1.790E-01	8.210E-01	1.075E-01	4.697E+00	8.406E-01	1.922E+01
62	6.100E-01	4.931E-01	1.298E-02	2.401E-01	1.838E-01	8.162E-01	1.070E-01	4.775E+00	8.777E-01	2.010E+01
63	6.200E-01	4.812E-01	1.100E-02	2.351E-01	1.890E-01	8.110E-01	1.064E-01	4.853E+00	9.171E-01	2.102E+01
64	6.300E-01	4.690E-01	8.950E-03	2.300E-01	1.945E-01	8.055E-01	1.056E-01	4.932E+00	9.592E-01	2.198E+01
65	6.400E-01	4.566E-01	6.821E-03	2.249E-01	2.004E-01	7.996E-01	1.047E-01	5.010E+00	1.004E+00	2.298E+01
66	6.500E-01	4.439E-01	4.612E-03	2.196E-01	2.068E-01	7.932E-01	1.037E-01	5.088E+00	1.052E+00	2.403E+01
67	6.600E-01	4.310E-01	2.320E-03	2.144E-01	2.136E-01	7.864E-01	1.025E-01	5.167E+00	1.103E+00	2.514E+01
68	6.700E-01	4.181E-01	-9.977E-06	2.091E-01	2.207E-01	7.793E-01	1.012E-01	5.245E+00	1.158E+00	2.629E+01
69	6.800E-01	4.049E-01	-2.464E-03	2.037E-01	2.285E-01	7.715E-01	9.969E-02	5.323E+00	1.216E+00	2.751E+01
70	6.900E-01	3.914E-01	-5.016E-03	1.982E-01	2.369E-01	7.631E-01	9.806E-02	5.401E+00	1.280E+00	2.879E+01
71	7.000E-01	3.777E-01	-7.656E-03	1.927E-01	2.459E-01	7.541E-01	9.627E-02	5.480E+00	1.348E+00	3.014E+01
72	7.100E-01	3.640E-01	-1.038E-02	1.872E-01	2.556E-01	7.444E-01	9.433E-02	5.558E+00	1.421E+00	3.156E+01
73	7.200E-01	3.501E-01	-1.319E-02	1.816E-01	2.660E-01	7.340E-01	9.223E-02	5.636E+00	1.499E+00	3.306E+01
74	7.300E-01	3.361E-01	-1.609E-02	1.761E-01	2.771E-01	7.229E-01	8.997E-02	5.715E+00	1.583E+00	3.464E+01
75	7.400E-01	3.220E-01	-1.905E-02	1.706E-01	2.890E-01	7.110E-01	8.755E-02	5.793E+00	1.674E+00	3.631E+01
76	7.500E-0	3.080E-01	-2.209E-02	1.650E-01	3.016E-01	6.984E-01	8.497E-02	5.871E+00	1.771E+00	3.809E+01
77	7.600E-01	2.939E-01	-2.518E-02	1.595E-01	3.150E-01	6.850E-01	8.224E-02	5.949E+00	1.874E+00	3.996E+01
78	7.700E-01	2.799E-01	-2.831E-02	1.541E-01	3.293E-01	6.707E-01	7.934E-02	6.028E+00	1.985E+00	4.194E+01
79	7.800E-01	2.659E-01	-3.147E-02	1.487E-01	3.443E-01	6.557E-01	7.629E-02	6.106E+00	2.102E+00	4.405E+01
80	7.900E-01	2.520E-01	-3.464E-02	1.433E-01	3.601E-01	6.399E-01	7.309E-02	6.184E+00	2.227E+00	4.627E+01
81	8.000E-01	2.382E-01	-3.777E-02	1.380E-01	3.767E-01	6.233E-01	6.974E-02	6.263E+00	2.359E+00	4.863E+01
82	8.100E-01	2.246E-01	-4.085E-02	1.328E-01	3.939E-01	6.061E-01	6.624E-02	6.341E+00	2.498E+00	5.113E+01
83	8.200E-01	2.112E-01	-4.383E-02	1.275E-01	4.116E-01	5.882E-01	6.260E-02	6.419E+00	2.643E+00	5.377E+01
84	8.300E-01	1.980E-01	-4.666E-02	1.223E-01	4.301E-01	5.699E-01	5.883E-02	6.497E+00	2.795E+00	5.657E+01
85	8.400E-01	1.851E-01	-4.929E-02	1.172E-01	4.489E-01	5.511E-01	5.494E-02	6.576E+00	2.952E+00	5.952E+01
86	8.500E-01	1.723E-01	-5.166E-02	1.120E-01	4.678E-01	5.322E-01	5.094E-02	6.654E+00	3.113E+00	6.263E+01
87	8.600E-01	1.598E-01	-5.369E-02	1.066E-01	4.868E-01	5.132E-01	4.685E-02	6.732E+00	3.277E+00	6.591E+01
88	8.700E-01	1.476E-01	-5.532E-02	1.015E-01	5.058E-01	4.942E-01	4.267E-02	6.810E+00	3.444E+00	6.935E+01
89	8.800E-01	1.356E-01	-5.645E-02	9.603E-02	5.244E-01	4.756E-01	3.844E-02	6.889E+00	3.613E+00	7.297E+01
90	8.900E-01	1.239E-01	-5.701E-02	9.044E-02	5.427E-01	4.573E-01	3.418E-02	6.967E+00	3.781E+00	7.675E+01
91	9.000E-01	1.123E-01	-5.690E-02	8.461E-02	5.603E-01	4.397E-01	2.991E-02	7.045E+00	3.947E+00	8.070E+01
92	9.100E-01	1.010E-01	-5.602E-02	7.850E-02	5.772E-01	4.228E-01	2.569E-02	7.124E+00	4.112E+00	8.481E+01
93	9.200E-01	8.978E-02	-5.430E-02	7.204E-02	5.932E-01	4.068E-01	2.153E-02	7.202E+00	4.272E+00	8.908E+01
94	9.300E-01	7.870E-02	-5.162E-02	6.516E-02	6.082E-01	3.918E-01	1.751E-02	7.280E+00	4.428E+00	9.351E+01
95	9.600E-01	6.770E-02	-4.792E-02	5.781E-02	6.221E-01	3.779E-01	1.368E-02	7.358E+00	4.577E+00	9.808E+01
96	9.500E-01	5.672E-02	-4.310E-02	4.991E-02	6.348E-01	3.652E-01	1.012E-02	7.437E+00	4.721E+00	1.028E+02
97	9.600E-01	4.571E-02	-3.709E-02	4.140E-02	6.463E-01	3.537E-01	6.901E-03	7.515E+00	4.857E+00	1.077E+02
98	9.700E-01	3.460E-02	-2.982E-02	3.221E-02	6.565E-01	3.435E-01	4.144E-03	7.593E+00	4.985E+00	1.126E+02
99	9.800E-01	2.333E-02	-2.124E-02	2.229E-02	6.654E-01	3.346E-01	1.969E-03	7.672E+00	5.105E+00	1.178E+02
100	9.900E-01	1.183E-02	-1.132E-02	1.157E-02	6.730E-01	3.270E-01	5.270E-04	7.750E+00	5.215E+00	1.230E+02

105-MM SHAPED CHAGE SAMPLE CASE

INITIAL CONDITIONS FOR PENETRATION

T1 =	112.0000	T0 =	53.0039	Z0 =	37.1611
FT =	36.0439	VJT =	.0316	VJ0 =	.7011
ARAY =	1.062188	UMIN =	.10588	CK =	.03510

PENETRATION PHASE

	MU	THETA	F	DF	T	DT	G	RSQ	A	DELA	DV	D/DT
1	0.	0.	0.	0.	0.	0.	0.	0.	0.	0.	0.	0.
2	0.	0.	0.	0.	0.	0.	0.	0.	0.	0.	0.	0.
3	0.	0.	0.	0.	0.	0.	0.	0.	0.	0.	0.	0.
4	0.	0.	0.	0.	0.	0.	0.	0.	0.	0.	0.	0.
5	0.	0.	0.	0.	0.	0.	0.	0.	0.	0.	0.	0.
6	0.	0.	0.	0.	0.	0.	0.	0.	0.	0.	0.	0.
7	0.	0.	0.	0.	0.	0.	0.	0.	0.	0.	0.	0.
8	0.	0.	0.	0.	0.	0.	0.	0.	0.	0.	0.	0.
9	0.	0.	0.	0.	0.	0.	0.	0.	0.	0.	0.	0.
10	0.	0.	0.	0.	0.	0.	0.	0.	0.	0.	0.	0.
11	0.	0.	0.	0.	0.	0.	0.	0.	0.	0.	0.	0.
12	0.	0.	0.	0.	0.	0.	0.	0.	0.	0.	0.	0.
13	0.	0.	0.	0.	0.	0.	0.	0.	0.	0.	0.	0.
14	0.	0.	0.	0.	0.	0.	0.	0.	0.	0.	0.	0.
15	0.	0.	0.	0.	0.	0.	0.	0.	0.	0.	0.	0.
16	0.	0.	0.	0.	0.	0.	0.	0.	0.	0.	0.	0.
17	0.	0.	0.	0.	0.	0.	0.	0.	0.	0.	0.	0.
18	0.	0.	0.	0.	0.	0.	0.	0.	0.	0.	0.	0.
19	0.	0.	0.	0.	0.	0.	0.	0.	0.	0.	0.	0.
20	0.	0.	0.	0.	0.	0.	0.	0.	0.	0.	0.	0.
21	0.	0.	0.	0.	0.	0.	0.	0.	0.	0.	0.	0.
22	0.	0.	0.	0.	0.	0.	0.	0.	0.	0.	0.	0.
23	0.	0.	0.	0.	0.	0.	0.	0.	0.	0.	0.	0.
24	0.	0.	0.	0.	0.	0.	0.	0.	0.	0.	0.	0.
25	0.	0.	0.	0.	0.	0.	0.	0.	0.	0.	0.	0.
26	0.	0.	0.	0.	0.	0.	0.	0.	0.	0.	0.	0.
27	0.	0.	0.	0.	0.	0.	0.	0.	0.	0.	0.	0.
28	0.	0.	0.	0.	0.	0.	0.	0.	0.	0.	0.	0.
29	0.	0.	0.	0.	0.	0.	0.	0.	0.	0.	0.	0.
30	0.	0.	0.	0.	0.	0.	0.	0.	0.	0.	0.	0.
31	0.	0.	0.	0.	0.	0.	0.	0.	0.	0.	0.	0.
32	0.	0.	0.	0.	0.	0.	0.	0.	0.	0.	0.	0.
33	0.	0.	0.	0.	0.	0.	0.	0.	0.	0.	0.	0.
34	0.	0.	0.	0.	0.	0.	0.	0.	0.	0.	0.	0.
35	0.	0.	0.	0.	0.	0.	0.	0.	0.	0.	0.	0.
36	0.	0.	0.	0.	0.	0.	0.	0.	0.	0.	0.	0.
37	0.	0.	0.	0.	0.	0.	0.	0.	0.	0.	0.	0.
38	0.	0.	0.	0.	0.	0.	0.	0.	0.	0.	0.	0.
39	0.	0.	0.	0.	0.	0.	0.	0.	0.	0.	0.	0.
40	0.	0.	0.	0.	0.	0.	0.	0.	0.	0.	0.	0.
41	0.	0.	0.	0.	0.	0.	0.	0.	0.	0.	0.	0.
42	0.	0.	0.	0.	0.	0.	0.	0.	0.	0.	0.	0.
43	0.	0.	0.	0.	0.	0.	0.	0.	0.	0.	0.	0.
44	0.	0.	0.	0.	0.	0.	0.	0.	0.	0.	0.	0.
45	0.	0.	0.	0.	0.	0.	0.	0.	0.	0.	0.	0.
46	0.	0.	0.	0.	0.	0.	0.	0.	0.	0.	0.	0.
47	1.000E+00	1.261E+01	5.566E+00	5.566E+00	1.151E+01	1.151E+01	4.169E+00	0.	-2.226E-01	-2.226E-01	0.	0.
48	1.000E+00	1.298E+01	5.742E+00	1.754E-01	6.488E+01	1.187E+01	4.146E+01	1.686E-02	-1.941E-01	2.852E-02	7.011E-01	2.948E+02
49	1.004E+00	1.335E+01	5.871E+00	1.290E-01	6.565E+01	1.264E+01	4.174E+01	2.333E-01	-1.657E-01	2.838E-02	-2.594E-03	-1.601E+00
50	1.013E+00	1.373E+01	5.924E+00	5.382E-02	6.703E+01	1.403E+01	4.224E+01	1.661E-01	-1.354E-01	3.037E-02	-6.460E-03	-3.282E+00
51	1.023E+00	1.411E+01	5.971E+00	4.644E-02	6.848E+01	1.548E+01	4.275E+01	1.662E-01	-1.029E-01	3.246E-02	-6.653E-03	-3.406E+00
52	1.033E+00	1.449E+01	6.010E+00	3.874E-02	7.000E+01	1.700E+01	4.329E+01	1.662E-01	-6.826E-02	3.466E-02	-6.850E-03	-3.537E+00
53	1.044E+00	1.488E+01	6.040E+00	3.069E-02	7.160E+01	1.859E+01	4.384E+01	1.661E-01	-3.129E-02	3.647E-02	-7.052E-03	-3.677E+00
54	1.056E+00	1.527E+01	6.063E+00	2.231E-02	7.327E+01	2.027E+01	4.442E+01	1.659E-01	8.112E-03	3.940E-02	-7.258E-03	-3.827E+00
55	1.068E+00	1.566E+01	6.076E+00	1.351E-02	7.504E+01	2.203E+01	4.502E+01	1.656E-01	5.010E-02	4.198E-02	-7.471E-03	-3.988E+00
56	1.080E+00	1.606E+01	6.080E+00	4.389E-03	7.690E+01	2.389E+01	4.565E+01	1.651E-01	9.478E-02	4.468E-02	-7.687E-03	-4.159E+00
57	1.093E+00	1.646E+01	6.075E+00	-5.149E-03	7.886E+01	2.586E+01	4.630E+01	1.646E-01	1.423E-01	4.752E-02	-7.909E-03	-4.343E+00
58	1.106E+00	1.687E+01	6.060E+00	-1.509E-02	8.094E+01	2.793E+01	4.699E+01	1.640E-01	1.928E-01	5.052E-02	-8.136E-03	-4.541E+00
59	1.122E+00	1.729E+01	6.035E+00	-2.546E-02	8.314E+01	3.013E+01	4.770E+01	1.633E-01	2.465E-01	5.367E-02	-8.368E-03	-4.753E+00
60	1.138E+00	1.770E+01	5.999E+00	-3.625E-02	8.547E+01	3.247E+01	4.845E+01	1.625E-01	3.035E-01	5.698E-02	-8.604E-03	-4.982E+00
61	1.155E+00	1.813E+01	5.951E+00	-4.749E-02	8.795E+01	3.495E+01	4.923E+01	1.616E-01	3.639E-01	6.046E-02	-8.845E-03	-5.228E+00
62	1.172E+00	1.856E+01	5.892E+00	-5.918E-02	9.060E+01	3.759E+01	5.006E+01	1.606E-01	4.280E-01	6.411E-02	-9.091E-03	-5.494E+00
63	1.191E+00	1.900E+01	5.821E+00	-7.133E-02	9.342E+01	4.041E+01	5.092E+01	1.596E-01	4.960E-01	6.794E-02	-9.340E-03	-5.781E+00
64	1.210E+00	1.944E+01	5.737E+00	-8.394E-02	9.644E+01	4.343E+01	5.183E+01	1.584E-01	5.679E-01	7.196E-02	-9.593E-03	-6.092E+00
65	1.231E+00	1.989E+01	5.640E+00	-9.703E-02	9.967E+01	4.667E+01	5.279E+01	1.572E-01	6.441E-01	7.616E-02	-9.849E-03	-6.428E+00

56	1.254E+00	2.035E+01	5.529E+00	-1.108E-01	1.031E+02	5.014E+01	5.381E+01	1.559E-01	7.246E-01	8.056E-02	-1.011E-02	-6.703E+00
57	1.277E+00	2.082E+01	5.404E+00	-1.246E-01	1.069E+02	5.388E+01	5.488E+01	1.546E-01	8.098E-01	8.515E-02	-1.037E-02	-7.190E+00
58	1.303E+00	2.129E+01	5.265E+00	-1.391E-01	1.109E+02	5.792E+01	5.601E+01	1.532E-01	8.997E-01	8.994E-02	-1.063E-02	-7.622E+00
59	1.330E+00	2.178E+01	5.111E+00	-1.541E-01	1.153E+02	6.229E+01	5.722E+01	1.542E-01	9.947E-01	9.493E-02	-1.089E-02	-7.838E+00
60	1.358E+00	2.228E+01	4.942E+00	-1.695E-01	1.200E+02	6.703E+01	5.849E+01	1.561E-01	1.095E+00	1.001E-01	-1.116E-02	-7.970E+00
61	1.389E+00	2.278E+01	4.756E+00	-1.853E-01	1.252E+02	7.218E+01	5.985E+01	1.531E-01	1.200E+00	1.055E-01	-1.142E-02	-8.009E+00
62	1.422E+00	2.330E+01	4.555E+00	-2.015E-01	1.308E+02	7.779E+01	6.130E+01	1.603E-01	1.311E+00	1.110E-01	-1.168E-02	-8.224E+00
63	1.457E+00	2.383E+01	4.337E+00	-2.181E-01	1.369E+02	8.393E+01	6.285E+01	1.626E-01	1.428E+00	1.168E-01	-1.193E-02	-8.345E+00
64	1.495E+00	2.438E+01	4.102E+00	-2.350E-01	1.437E+02	9.066E+01	6.450E+01	1.652E-01	1.551E+00	1.227E-01	-1.218E-02	-8.459E+00
65	1.536E+00	2.494E+01	3.850E+00	-2.522E-01	1.511E+02	9.806E+01	6.627E+01	1.679E-01	1.679E+00	1.287E-01	-1.242E-02	-8.567E+00
66	1.579E+00	2.552E+01	3.580E+00	-2.697E-01	1.592E+02	1.062E+02	6.817E+01	1.709E-01	1.814E+00	1.349E-01	-1.265E-02	-8.666E+00
67	1.627E+00	2.612E+01	3.293E+00	-2.873E-01	1.683E+02	1.153E+02	7.021E+01	1.740E-01	1.956E+00	1.412E-01	-1.288E-02	-8.757E+00
68	1.677E+00	2.673E+01	2.994E+00	-2.987E-01	1.782E+02	1.251E+02	7.239E+01	1.785E-01	2.101E+00	1.449E-01	-1.292E-02	-8.735E+00
69	1.732E+00	2.737E+01	2.672E+00	-3.215E-01	1.893E+02	1.363E+02	7.475E+01	1.813E-01	2.254E+00	1.536E-01	-1.326E-02	-8.888E+00
70	1.791E+00	2.803E+01	2.332E+00	-3.407E-01	2.017E+02	1.487E+02	7.732E+01	1.851E-01	2.415E+00	1.607E-01	-1.348E-02	-8.969E+00
71	1.856E+00	2.871E+01	1.974E+00	-3.581E-01	2.157E+02	1.627E+02	8.010E+01	1.895E-01	2.582E+00	1.671E-01	-1.364E-02	-9.011E+00
72	1.926E+00	2.943E+01	1.598E+00	-3.751E-01	2.315E+02	1.784E+02	8.312E+01	1.943E-01	2.755E+00	1.735E-01	-1.378E-02	-9.037E+00
73	2.003E+00	3.017E+01	1.207E+00	-3.916E-01	2.492E+02	1.962E+02	8.640E+01	1.994E-01	2.935E+00	1.796E-01	-1.389E-02	-9.047E+00
74	2.086E+00	3.095E+01	7.992E-01	-4.076E-01	2.694E+02	2.164E+02	8.998E+01	2.050E-01	3.121E+00	1.856E-01	-1.398E-02	-9.040E+00
75	2.177E+00	3.177E+01	3.765E-01	-4.227E-01	2.923E+02	2.393E+02	9.388E+01	2.110E-01	3.312E+00	1.913E-01	-1.404E-02	-9.014E+00
76	2.276E+00	3.264E+01	-6.065E-02	-4.370E-01	3.186E+02	2.656E+02	9.816E+01	2.176E-01	3.509E+00	1.967E-01	-1.407E-02	-8.969E+00
77	2.385E+00	3.355E+01	-5.106E-01	-4.501E-01	3.487E+02	2.957E+02	1.028E+02	2.246E-01	3.710E+00	2.017E-01	-1.407E-02	-8.905E+00
78	2.505E+00	3.452E+01	-9.727E-01	-4.621E-01	3.835E+02	3.305E+02	1.080E+02	2.322E-01	3.917E+00	2.062E-01	-1.404E-02	-8.822E+00
79	2.637E+00	3.555E+01	-1.445E+00	-4.727E-01	4.238E+02	3.708E+02	1.137E+02	2.404E-01	4.127E+00	2.101E-01	-1.398E-02	-8.719E+00
80	2.782E+00	3.666E+01	-1.927E+00	-4.818E-01	4.707E+02	4.177E+02	1.200E+02	2.491E-01	4.340E+00	2.134E-01	-1.388E-02	-8.599E+00
81	2.943E+00	3.784E+01	-2.417E+00	-4.893E-01	5.257E+02	4.727E+02	1.269E+02	2.584E-01	4.556E+00	2.160E-01	-1.375E-02	-8.461E+00
82	3.121E+00	3.913E+01	-2.912E+00	-4.952E-01	5.904E+02	5.374E+02	1.347E+02	2.684E-01	4.774E+00	2.179E-01	-1.360E-02	-8.308E+00
83	3.319E+00	4.052E+01	-3.411E+00	-4.993E-01	6.671E+02	6.141E+02	1.433E+02	2.788E-01	4.993E+00	2.189E-01	-1.341E-02	-8.142E+00
84	3.540E+00	4.205E+01	-3.913E+00	-5.017E-01	7.587E+02	7.057E+02	1.530E+02	2.898E-01	5.212E+00	2.191E-01	-1.320E-02	-7.966E+00
85	3.789E+00	4.374E+01	-4.415E+00	-5.024E-01	8.690E+02	8.160E+02	1.639E+02	3.013E-01	5.430E+00	2.185E-01	-1.298E-02	-7.783E+00
86	4.068E+00	4.561E+01	-4.917E+00	-5.015E-01	1.003E+03	9.498E+02	1.763E+02	3.131E-01	5.647E+00	2.170E-01	-1.273E-02	-7.597E+00
87	4.386E+00	4.772E+01	-5.416E+00	-4.990E-01	1.167E+03	1.114E+03	1.903E+02	3.253E-01	5.862E+00	2.146E-01	-1.249E-02	-7.412E+00
88	4.750E+00	5.010E+01	-5.911E+00	-4.953E-01	1.371E+03	1.318E+03	2.065E+02	3.375E-01	6.074E+00	2.115E-01	-1.223E-02	-7.233E+00
89	5.170E+00	5.284E+01	-6.401E+00	-4.904E-01	1.628E+03	1.575E+03	2.253E+02	3.498E-01	6.281E+00	2.076E-01	-1.199E-02	-7.063E+00
90	5.660E+00	5.602E+01	-6.886E+00	-4.845E-01	1.959E+03	1.906E+03	2.474E+02	3.618E-01	6.484E+00	2.030E-01	-1.175E-02	-6.907E+00
91	6.242E+00	5.980E+01	-7.364E+00	-4.780E-01	2.392E+03	2.339E+03	2.738E+02	3.734E-01	6.682E+00	1.978E-01	-1.154E-02	-6.770E+00
92	6.944E+00	6.435E+01	-7.835E+00	-4.711E-01	2.974E+03	2.921E+03	3.058E+02	3.843E-01	6.874E+00	1.920E-01	-1.135E-02	-6.655E+00
93	7.810E+00	6.996E+01	-8.299E+00	-4.640E-01	3.785E+03	3.732E+03	3.456E+02	3.943E-01	7.060E+00	1.858E-01	-1.119E-02	-6.567E+00
94	8.909E+00	7.711E+01	-8.756E+00	-4.570E-01	4.961E+03	4.908E+03	3.966E+02	4.032E-01	7.239E+00	1.791E-01	-1.108E-02	-6.509E+00
95	1.036E+01	8.655E+01	-9.206E+00	-4.503E-01	6.765E+03	6.712E+03	4.644E+02	4.107E-01	7.411E+00	1.721E-01	-1.100E-02	-6.485E+00
96	1.236E+01	9.965E+01	-9.650E+00	-4.441E-01	9.743E+03	9.690E+03	5.593E+02	4.167E-01	7.576E+00	1.648E-01	-1.098E-02	-6.497E+00
97	1.534E+01	1.192E+02	-1.009E+01	-4.387E-01	1.521E+04	1.516E+04	7.023E+02	4.209E-01	7.733E+00	1.573E-01	-1.101E-02	-6.551E+00
98	2.026E+01	1.515E+02	-1.052E+01	-4.344E-01	2.703E+04	2.698E+04	9.427E+02	4.232E-01	7.883E+00	1.495E-01	-1.111E-02	-6.649E+00
99	3.005E+01	2.159E+02	-1.095E+01	-4.312E-01	6.104E+04	6.099E+04	1.432E+03	4.236E-01	8.024E+00	1.415E-01	-1.127E-02	-6.794E+00
100	5.928E+01	4.087E+02	-1.139E+01	-4.294E-01	2.488E+05	2.488E+05	2.951E+03	4.220E-01	8.157E+00	1.332E-01	-1.151E-02	-6.993E+00

105-MM SHAPED CHAGE SAMPLE CASE

HOLE PROFILE SO = 3.00 CM

I	P(CM)	HC(CM)
1	0.00000	0.00000
2	0.00000	0.00000
3	0.00000	0.00000
4	0.00000	0.00000
5	0.00000	0.00000
6	0.00000	0.00000
7	0.00000	0.00000
8	0.00000	0.00000
9	0.00000	0.00000
10	0.00000	0.00000
11	0.00000	0.00000
12	0.00000	0.00000
13	0.00000	0.00000
14	0.00000	0.00000
15	0.00000	0.00000
16	0.00000	0.00000
17	0.00000	0.00000
18	0.00000	0.00000
19	0.00000	0.00000
0	0.00000	0.00000
1	0.00000	0.00000
2	0.00000	0.00000
3	0.00000	0.00000
4	0.00000	0.00000
5	0.00000	0.00000
6	0.00000	0.00000
7	0.00000	0.00000
8	0.00000	0.00000
9	0.00000	0.00000
0	0.00000	0.00000
1	0.00000	0.00000
2	0.00000	0.00000
3	0.00000	0.00000
4	0.00000	0.00000
5	0.00000	0.00000
6	0.00000	0.00000
7	0.00000	0.00000
8	4.08966	.15347
9	4.34083	2.09919
0	4.79126	1.46420
1	5.25781	1.43460
2	5.74158	1.40390
3	6.24376	1.37219
4	6.76563	1.33959
5	7.30875	1.30593
6	7.87454	1.27163
7	8.46474	1.23655
8	9.08121	1.20080
9	9.72599	1.16446
0	10.40131	1.12760

PENTRATION STANDOFF

PT(MM)	SO(CM)
311.70736	1.00000
354.96580	2.00000
380.93877	3.00000
395.21635	4.00000
400.88556	5.00000
399.86846	6.00000
393.45955	7.00000
382.67360	8.00000
370.83340	9.00000
359.28549	10.00000
348.00923	11.00000
336.98630	12.00000
326.20037	13.00000
315.63678	14.00000
305.28231	15.00000
295.12501	16.00000
285.15404	17.00000
275.35950	18.00000
265.73235	19.00000
256.26429	20.00000
246.94767	21.00000
237.77546	22.00000
228.74115	23.00000
219.83869	24.00000
211.06247	25.00000

I	P	RC
51	11.10963	1.09029
52	11.85363	1.05261
53	12.63628	1.01462
54	13.46083	.97641
55	14.33090	.93804
56	15.25045	.89958
57	16.22389	.86112
58	17.25609	.82272
59	18.34664	.80865
60	19.48506	.80245
61	20.67288	.79583
62	21.91220	.78874
63	23.20498	.78115
64	24.55304	.77303
65	25.95794	.76432
66	27.42096	.75498
67	28.94292	.74494
68	30.50486	.73845
69	32.14110	.72330
70	33.84023	.70978
71	35.59544	.69633
72	37.40375	.68182

105-MM SHAPED CHAGE SAMPLE CASE

SUMMARY OF RESULTS

LINER MASS = 385.8492 GM   JET MASS = 122.9672 GM   SLUG MASS = 262.8820 GM

TOTAL KINETIC ENERGY = 6.3894 ERGS*1.0E12

TOTAL JET KINETIC ENERGY = 6.2273 ERGS*1.0E12

TOTAL JET KINETIC ENERGY ABOVE JET VELOCITY .25 CM/MSEC = 5.6405 ERGS*1.0E12

TOTAL JET MASS ABOVE JET VELOCITY .25 CM/MSEC = 46.2734 GM

KINETIC ENERGY ABOVE .5 CM/MSEC = 3.8664   AND JET MASS = 19.2223
KINETIC ENERGY ABOVE .4 CM/MSEC = 4.6964   AND JET MASS = 27.5096
KINETIC ENERGY ABOVE .3 CM/MSEC = 5.3368   AND JET MASS = 38.0850
KINETIC ENERGY ABOVE .2 CM/MSEC = 5.8294   AND JET MASS = 53.7738
KINETIC ENERGY ABOVE .1 CM/MSEC = 6.1685   AND JET MASS = 84.8073

MAXIMUN RELATIVE MACH NUMBER = .8821

JET TIP AT I = 38 RELATIVE POSITION Z/H = .37000000

MEASURED JET TIP VELOCITY = 7.01100675 MM/MICROSEC

MEASURED MASS OF JET TIP = 6.1533 GM

DISTRIBUTION LIST

No. of Copies	Organization
12	Commander Defense Technical Info Center ATTN: DDC-DDA Cameron Station Alexandria, VA 22314
1	Assistant Secretary of the Army (R&D) ATTN: Asst for Research Washington, DC 20310
2	HQDA (DAMA-ZA; DAMA-AR) Washington, DC 20310
1	Commander US Army Materiel Development and Readiness Command ATTN: DRCDMD-ST 5001 Eisenhower Avenue Alexandria, VA 22333
2	Commander US Army Armament Research and Development Command ATTN: DRDAR-TSS Dover, NJ 07801
4	Commander US Army Armament Research and Development Command ATTN: DARPA-FR-E Mr. T. Stevens Mr. G. Randers-Pehrson Mr. J. Hershkowitz Mr. J. Pearson Dover, NJ 07801
1	Commander US Army Armament Materiel Readiness Command ATTN: DRSAR-LEP-L, Tech Lib Rock Island, IL 61299
1	Director US Army ARRADCOM Benet Weapons Laboratory ATTN: DRDAR-LCB-TL Watervliet, NY 12189
1	Iowa Army Ammo Plant ATTN: J. Polson Burlington, IA 52601
1	Commander US Army Aviation Research and Development Command ATTN: DRSAV-E P. O. Box 209 St. Louis, MO 63166
1	Director US Army Air Mobility Research and Development Laboratory Ames Research Center Moffett Field, CA 94035
1	Commander US Army Communications Rsch and Development Command ATTN: DRDCO-PPA-SA Fort Monmouth, NJ 07703
1	Commander US Army Electronics Rsch and Development Command Technical Support Activity ATTN: DELSD-L Fort Monmouth, NJ 07703
1	Commander US Army Missile Command ATTN: DRSMI-R Redstone Arsenal, AL 35809
1	Commander US Army Missile Command ATTN: DRSMI-YDL Redstone Arsenal, AL 35809

DISTRIBUTION LIST

No. of Copies	Organization
1	Commander US Army Missile Command ATTN: Mr. W. Zecher Redstone Arsenal, AL 35809
1	Commander US Army Missile Command ATTN: Mr. B. Cobb Redstone Arsenal, AL 35809
1	Commander US Army Tank Automotive Research & Development Cmd ATTN: DRDTA-UL Warren, MI 48090
2	Commander US Army Materials and Mechanics Research Center ATTN: DRXMR-RF, J. Mescall Tech Lib Watertown, MA 02172
1	Director US Army TRADOC Systems Analysis Activity ATTN: ATAA-SL, Tech Lib White Sands Missile Range NM 88002
2	Chief of Naval Research Department of the Navy ATTN: Code 427 Code 470 Washington, DC 20325
2	Commander Naval Air Systems Command ATTN: Code AIR-310 Code AIR-350 Washington, DC 20360
1	Commander Naval Ordnance Systems Command ATTN: Code ORD-0332 Washington, DC 20360

No. of Copies	Organization
3	Commander Naval Surface Weapons Center ATTN: DG-50 Mr. S. Griscavage DX-21, Lib Br. Dahlgren, VA 22448
2	Commander Naval Surface Weapons Center ATTN: Code 730, Lib Silver Spring, MD 20910
1	Commander Naval Weapons Center ATTN: Code 3835 China Lake, CA 93555
2	Commander Naval Weapons Center ATTN: Code 3431, Tech Lib Code 3835, R. Sewell China Lake, CA 93555
1	Commander Naval Research Laboratory Washington, DC 20375
1	USAF/AFRDDA Washington, DC 20311
1	AFSC/SDW Andrews AFB Washington, DC 20311
1	US Air Force Academy ATTN: Code FJS-41 (NC) Tech Lib Colorado Springs, CO 80840
1	AFATL/DLJW (J. Foster) Eglin AFB, FL 32542
1	AFWL (SUL, LT Tennant) Kirtland AFB, NM 87116

DISTRIBUTION LIST

No. of Copies	Organization
1	Director Lawrence Livermore Laboratory ATTN: Dr. J. Kury P. O. Box 808 Livermore, CA 94550
1	Director Lawrence Livermore Laboratory ATTN: Dr. M. Wilkins P. O. Box 808 Livermore, CA 94550
1	Director Lawrence Livermore Laboratory ATTN: Dr. E. Lee P. O. Box 808 Livermore, CA 94550
1	Director Lawrence Livermore Laboratory ATTN: Dr. H. Hornig P. O. Box 808 Livermore, CA 94550
1	Director Lawrence Livermore Laboratory ATTN: Tech Lib P. O. Box 808 Livermore, CA 94550
1	Battelle Columbus Labs ATTN: Mr. Joseph E. Backofen 505 King Avenue Columbus, OH 43201
2	Dyna East Corporation ATTN: P. C. Chou J. Carleone 227 Hemlock Road Wynnewood, PA 19096

No. of Copies	Organization
2	Firestone Tire & Rubber Defense Rsch & Products Div. ATTN: Mr. E. Clark Mr. R. Berus 1200 Firestone Parkway Akron, OH 44317
1	General Dynamic Pomona Div ATTN: J. Cuadros Mail Zone 4-75 P. O. Box 2507 Pomona, CA 91766
1	Honeywell, Inc. Government and Aeronautical Products Division ATTN: C. R. Hargreaves 600 Second Street Hopkins, MN 55343
2	Physics International Corp. ATTN: Dr. L. Behrmann Dr. R. Brown 2700 Merced Street San Leandro, CA 94577
2	Rockwell International Missile Systems Division ATTN: O. Kiphart H. Cox 4300 East 5th Avenue P. O. Box 1259 Columbus, OH 43216
1	Sandia Laboratories ATTN: Dr. W. Herrmann Albuquerque, NM 87115
1	Shock Hydrodynamics ATTN: Dr. L. Zernow 4710-4716 Vineland Avenue North Hollywood, CA 91602

DISTRIBUTION LIST

No. of Copies	Organization
1	Systems, Science & Software ATTN: Dr. R. Sedgwick P. O. Box 1620 La Jolla, CA 92037
1	Drexel Institute of Technology Wave Propagation Rsch Center ATTN: Prof. P. Chou Philadelphia, PA 19104
4	University of California Los Alamos Scientific Lab ATTN: Dr. J. Walsh Dr. R. Karpp Dr. B. Craig P. O. Box 1663 Los Alamos, NM 87544
1	University of Denver Denver Research Institute ATTN: Mr. R. F. Recht 2390 S. University Boulevard Denver, CO 80210

Aberdeen Proving Ground

	Dir, USAMSAA ATTN: DRXSY-D DRXSY-MP, H. Cohen J. Kramar B. Oehrli R. Bell, RAMD Cdr, USATECOM ATTN: DRSTE-TO-F Dir, USACSL, Bldg. E3516 ATTN: DRDAR-CLB-PA

USER EVALUATION OF REPORT

Please take a few minutes to answer the questions below; tear out this sheet, fold as indicated, staple or tape closed, and place in the mail. Your comments will provide us with information for improving future reports.

1. BRL Report Number ____________________

2. Does this report satisfy a need? (Comment on purpose, related project, or other area of interest for which report will be used.)

____

____

____

3. How, specifically, is the report being used? (Information source, design data or procedure, management procedure, source of ideas, etc.) ____________________

____

____

4. Has the information in this report led to any quantitative savings as far as man-hours/contract dollars saved, operating costs avoided, efficiencies achieved, etc.? If so, please elaborate.

____

____

5. General Comments (Indicate what you think should be changed to make this report and future reports of this type more responsive to your needs, more usable, improve readability, etc.) ____________________

____

____

____

6. If you would like to be contacted by the personnel who prepared this report to raise specific questions or discuss the topic, please fill in the following information.

Name: ____________________

Telephone Number: ____________________

Organization Address: ____________________

____

____